ROLE OF INTEGRIN-PROXIMAL COMPLEXES IN CANCER CELL BEHAVIOR AND NORMAL LIVER FUNCTION

by

Vasiliki Gkretsi

B.S. in Biology, National and Capodistrian University of Athens, Greece, 2001

Submitted to the Graduate Faculty of the

University of Pittsburgh School of Medicine,

Department of Cellular and Molecular Pathology,

in partial fulfillment of the requirements for the degree of

Doctor of Philosophy

University of Pittsburgh

2006

UNIVERSITY OF PITTSBURGH

SCHOOL OF MEDICINE

This dissertation was presented

by

Vasiliki Gkretsi

It was defended on

October 2nd, 2006

and approved by

George K. Michalopoulos, M.D., Ph.D,

Chairperson, Professor and Chairman, Department of Pathology

Donna Beer Stolz, Ph.D., Assistant Professor, Department of Cell Biology and Physiology

Alan Wells, MD, DMS, Professor, Department of Pathology

Satdarshan P. Singh Monga, MD, Assistant Professor, Department of Pathology

Dissertation Advisor: Chuanyue Wu, Ph.D, Professor, Department of Pathology

ROLE OF INTEGRIN-PROXIMAL COMPLEXES IN CANCER CELL BEHAVIOR AND NORMAL LIVER FUNCTION

Vasiliki Gkretsi, Ph.D

University of Pittsburgh, 2006

Cell-matrix and cell-cell adhesion proteins are of great significance for many fundamental cellular processes such as survival, differentiation, spreading, adhesion, migration as well as oncogenic transformation. In the present dissertation study, the role of different integrin-proximal protein complexes was investigated *in vitro* in cancer cells and in primary rat hepatocytes and *in vivo* in whole animals.

First it was shown that migfilin, a newly identified cell-matrix adhesion protein, is also an important component of cell-cell junctions critical for the organization and strengthening of the adherens junctions. Next, Ras-Suppressor-1 (RSU-1), which interacts with the focal adhesion protein PINCH, was shown to regulate cell spreading and adhesion, although the exact mechanism is yet unclear.

Furthermore, the role of Integrin-Linked Kinase (ILK) was investigated *in vitro* in the model system of matrix-induced hepatocyte differentiation. It was shown that ILK along with its binding partners PINCH and α-parvin are dramatically down-regulated during the matrix-induced re-differentiation of hepatocytes. Thus, ILK and its binding partners likely play an important role in matrix-induced-hepatocyte differentiation.

Finally, the role of ILK was examined *in vivo* by removing the protein from the whole animal or specifically from the liver. First ILK was removed from ILK-floxed mice following Cre-recombinase-adenoviral injections giving rise to animals with fulminant hepatitis characterized by massive apoptosis, abnormal mitoses, fatty change and necrosis in the liver. Then, ILK-floxed animals were crossbred with alpha-fetoprotein(AFP)-albumin, albumin, or Foxa3-Cre transgenic mice and thus ILK was genetically removed specifically from the liver. In all cases, the livers of the animals had disorganized liver architecture, absence of hepatocyte plates, increased fibrosis, absence of microvilli in the canaliculi, different degrees of malformations in the biliary system, apoptosis and compensatory proliferation. The present findings therefore, clearly show that ILK is critical for hepatocyte differentiation and survival

and more importantly, this holds true *in vivo* where ILK is crucial for the maintainance of normal liver architecture and function.

Thus, the present dissertation work highlights the importance of cell-matrix adhesion proteins *in vitro* and *in vivo* and enhances the scientific knowledge in the field of molecular, cellular, hepatocyte and liver biology.

TABLE OF CONTENTS

LIST OF TABLES

LIST OF FIGURES

LIST OF ABBREVIATIONS

AFP: alpha-fetoprotein

CH-ILK-BP: Calponin Homology-ILK-binding protein

CH-domain: Calponin Homology domain

ECM: extracellular matrix

EGF: epidermal growth factor

EHS: Engelbreth-Holm-Swarm

ERK: extracellular signal regulated kinase

FAK: focal adhesion kinase

FBS: fetal bovine serum

GFP: green fluorescent protein

GSK-3b: glycogen synthase kinase 3 beta

GST: glutathione-S-transferase

HGF: hepatocyte growth factor

HGM: hepatocyte growth medium

HIF: hypoxia inducible factor

ILK: Integrin-linked kinase

ILK-AP: ILK-associated phosphatase

LEF-1: lymphoid enhancer factor

MAPK: mitogen activated protein kinase

Mig-2: Mitogen-inducible-2

MMP-9: metalloproteinase-9

NES: nuclear export signal

NHEK: newborn human embryonic keratinocytes

Pfu: plaque-forming units

PI3K: phosphatidylinositol-3 kinase

PKB/Akt: protein kinase B/Akt

RSU-1: Ras suppressor-1

TGFβ1: Transforming Growth Factorβ1

TUNEL: terminal deoxynucleotidyl-transferase-mediated dUTP-biotin nick end labeling

PREFACE

One of the first few people I met when I came to Pittsburgh for my graduate training was Dr. George Michalopoulos. I did my first rotation in his lab and in one of our discussions I remember him saying that "research is like going into a dark room where you cannot see anything around you but you are searching for something. Once you find a tail of a mouse you are going to be all right. The tail may be thin and long but you may eventually pull out a really big mouse". This is what happened with me as well, and thank God I finally found a mouse inside the dark room of research!

Of course, I did not achieve anything just by myself. During my training here **I was blessed to receive a lot of help from a lot of people.**

First and foremost, I would like to thank my advisor, **<u>Dr. Chuanyue (Cary) Wu</u>**. He taught me basic techniques and principles and offered me an exceptional scientific training. More specifically, he taught me how to start a project from zero and bring it to a certain level, how to ask scientific questions and how to answer them using multiple approaches, and how to always count on the data and formulate a hypothesis based on them. All in all, he guided me in my research efforts, he encouraged me to practice in writing grants and papers and overall did his best to provide me with a solid scientific training. I would like to especially thank him for keeping his door always open for me and my questions as well as for our many long scientific discussions, and for all the time that he invested in me. I certainly hope that I will prove to be a good investment.

I am **equally** grateful to **<u>Dr. George Michalopoulos</u>**, who served as my co-advisor and chairperson of my Thesis committee. I would like to thank him for guiding me in my liver-related research, for taking the time to patiently explain things, take pictures with me under the microscope and discuss hypotheses and ideas. He was always enthousiastic about science and that was an extra motivation for me as well. I really appreciate all his support that came in various forms; encouragement, advice, guidance, as well as financial support to attend scientific meetings and present my work. Finally, I would like to thank him for being so patient, kind, understanding and humble and for being the wonderful person that he is. I really believe that he taught me a lot by means of discussions but mainly by setting an example of excellence as a scientist and a human being.

I would also like to acknowledge the support and help I received from all the members of Dr.Wu's and Dr.Michalopoulos' lab. I would like to thank **Dr.Yongjun Zhang, Yizeng Tu,** and **Ka Chen** from Dr.Wu's lab for all their helpful suggestions and their many pieces of advice.

1.0   PART I: INTRODUCTION TO CELL MATRIX ADHESIONS

One of the major prerequisites for the proper function of cells within a tissue is the formation of contacts with the surrounding extracellular matrix (ECM) and the neighboring cells. The interaction between cells and various components of the ECM is of vital importance for a number of cellular processes such as cell survival, proliferation, differentiation, cell shape modulation, actin organization, migration, and gene expression. Over the last two decades, exciting progress has been made in understanding the general molecular organization, assembly and functions of the cell-ECM adhesions. Meanwhile, the complexity of cell-ECM adhesion structures in different developmental stages as well as various tissues and organs has been well appreciated.

Integrins are heterodimeric, transmembrane glycoprotein receptors that are primarily responsible for mediating cell-ECM interactions (Hynes, 2002). They interact with specific components of the ECM (collagen, fibronectin, vitronectin, laminin, etc.) via the extracellular domains and link them to the intracellular cytoskeletal and signaling complexes via the interactions of their cytoplasmic domains and multiple receptor-proximal cytoplasmic proteins. Apart from mediating the physical connection between ECM components and the actin cytoskeleton, integrins mediate bi-directional transduction of signals between the ECM and the intracellular compartment. Integrins can therefore be activated in two ways; either as a result of their detection of changes in the microenvironment of the cell (outside-in signaling) or in response to signals that originate from the inner compartment of the cell (inside-out signaling) (Geiger et al., 2001; (Hynes, 2002). The "outside-in signaling" of integrins begins with the binding of the ECM ligands to integrins and it is followed by clustering of integrins and the recruitment of actin filaments and signaling complexes to the cytoplasmic domain of integrins (Hynes, 2002). These initial complexes, which in cultured cells were often referred as "focal

complexes", will in turn give rise to mature structures (often referred as focal adhesions (FAs) in cultured cells) that consist of larger and more complicated protein assemblies.

The connection of many of the integrin-associated proteins with the actin cytoskeleton is of great significance for the fate of the cell. It allows the cells to adhere properly to the ECM, modulate their shape via the connections to the cytoskeleton and acquire certain morphology. Additionally, this connection facilitates the transduction of extracellular signals to the interior of the cell, enabling it to respond appropriately by moving, changing morphology, differentiating or coordinating several other functions.

At the molecular level, most of the integrin-associated molecules in FAs are multifunctional (Brakebusch and Fassler, 2003); Burridge and Chrzanowska-Wodnicka, 1996; Calderwood et al., 2000; Geiger et al., 2001; Zamir and Geiger, 2001). They associate with integrins and actin cytoskeleton. In addition, they serve as scaffolds for the attachment of enzymes such as kinases and phosphatases that modify and regulate these complex interactions. Currently, more than sixty FA proteins including talin, α-actinin, filamin, paxillin, focal adhesion kinase (FAK), Integrin-Linked Kinase (ILK), PINCH, and parvins have been identified (Niederreiter, 1994; Zamir and Geiger, 2001). The number of different proteins that are involved in the assembly of FAs, along with the interactions that they mediate, indicates a high level of molecular complexity (Niederreiter, 1994; Zamir and Geiger, 2001), which in turn underlines the importance of those proteins for cellular functions.

The significance of such protein associations is particularly obvious in development. During normal embryonic development, cells are attached to or migrate on ECM, and in both cases they interact with several components of the matrix via integrins and other associated FA proteins. These interactions are very dynamic and are continually modified until the developmental process has been successfully completed. In fact, lack of certain components of FAs, as well as proteins that comprise the cell-cell junctions has been shown to hinder normal development and lead to embryonic lethality or other developmental defects. Vinculin null mice, for example, are embryonic lethal with great defects in heart and brain development (Xu et al., 1998), E-cadherin knockout embryos are unable to form trophectoderm epithelium(Larue et al.,

1994), while **ILK knockout mice die at the pre-implantation stage** (Sakai et al., 2003). This demonstrates the absolute requirement of certain interactions between cells and the ECM for the normal development, morphogenesis and life in general.

1.1 THE PINCH-ILK-PARVIN COMPLEXES

1.1.1 Molecular activities of ILK, PINCH and parvins

One protein that is emerging as a key component of the FAs is **Integrin-Linked Kinase (ILK).** ILK was identified and cloned in 1996 based on its interaction with the β1-subunit of integrin (Hannigan et al., 1996b) and it was shown to localize to cell-ECM adhesions (Li et al., 1999a). It plays a crucial role in integrin-mediated cell adhesion and signaling (Brakebusch and Fassler, 2003; Dedhar, 2000; Grashoff, 2004; Wu, 2001b; Wu, 2004c; Yoganathan et al., 2000). ILK consists of three structurally distinct regions; four ANK repeats in the N-terminal region, followed by a pleckstrin homology (PH)-like domain and a C-terminal domain, which exhibits significant homology to Ser/Thr kinase catalytic domains (Grashoff, 2004; Hannigan et al., 1996b; Wu and Dedhar, 2001a). ILK can phosphorylate several proteins including protein kinase B PKB/Akt (Delcommenne et al., 1998a), Gsk-3β (Delcommenne et al., 1998a), and myosin light chain (Deng et al., 2001) and thereby regulates intracellular signaling (Hannigan et al., 2005). ILK also mediates multiple protein-protein interactions (Figure 1) (Mackinnon et al., 2002b; Wu, 2001b; Wu and Dedhar, 2001a). It binds to **PINCH** via its N-terminal ANK domain (Li et al., 1999a; Tu et al., 1999; Velyvis et al., 2001) and **α- or β-parvin**, members of the CH-ILKBP/α-parvin/actopaxin/affixin protein family (Fukuda et al., 2003a; Fukuda et al., 2003b; Nikolopoulos, 2000; Tu et al., 2001a; Wu, 2001b; Wu and Dedhar, 2001a; Zhang et al., 2002a; Zhang et al., 2002b; Zhang et al., 2002), via its C-terminal domain, resulting in the formation of a ternary complex within cells. PINCH consists of five LIM domains, each of which contains two Zn^{2+} fingers that mediate protein-protein interactions (Dawid et al., 1998; Jurata and Gill, 1998; Schmeichel and Beckerle, 1994). The N-terminal-most LIM1 domain mediates the interaction with ILK (Tu et al., 1999; Velyvis et al., 2001), whereas the C-terminal LIM domains

mediate interactions with several other proteins including Nck-2 (Tu et al., 1998; Velyvis et al., 2003), thymosin β4 (Bock-Marquette et al., 2004), and RSU-1 (Kadrmas et al., 2004). Parvins contain one N-terminal region and two C-terminal Calponin-Homology (CH) domains (Nikolopoulos and Turner, 2000; Olski et al., 2001; Tu et al., 2001; Yamaji et al., 2001). In addition to ILK, other proteins including paxillin (Nikolopoulos and Turner, 2000), α-actinin (Yamaji et al., 2004) and actin (Nikolopoulos and Turner, 2000; Olski et al., 2001) have been shown to interact with α-parvin and/or β-parvin. Thus, the PINCH-ILK-parvin complex likely functions as a molecular platform at cell-ECM adhesions mediating multiple interactions and hence regulates cell-ECM adhesion and signaling (Figure 1).
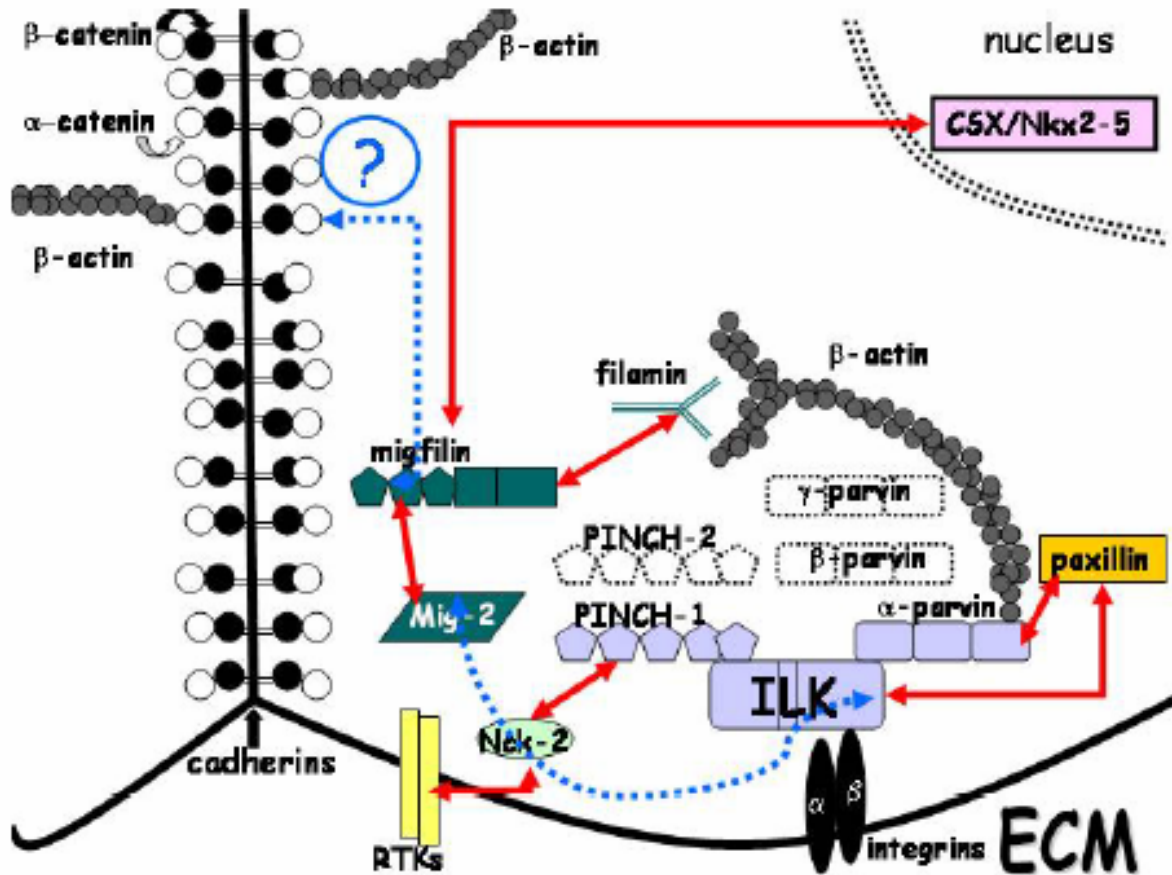
Figure 1. Schematic representation of the protein-protein interactions mediated by ILK and proteins associated with it. In the schematic diagram of this figure, the stable PINCH-ILK-parvin complex is shown in blue and the alternative partners for ILK are enclosed in dashed boxes. All the reported bindings are shown with solid red arrows while other potential protein-protein interactions are shown with blue dashed arrows. RTKs:receptor tyrosine kinases.

4

PINCH, ILK and parvins are widely expressed in the human tissues and well-conserved among different species (Clark, 2003; Mackinnon et al., 2002b; Zervas and Brown, 2002; Zervas, 2001). Genetic studies in *Drosophila, C.elegans* and mouse have demonstrated their essential roles for embryonic development and normal cell function *in vivo* (Zervas et al., 2001; Clark et al., 2003; Hobert et al., 1999; Mackinnon et al., 2002; (Lin et al., 2003). For example, loss of ILK leads to peri-implantation lethality in the mouse (Brakebusch and Fassler, 2003), embryonic lethality in *C.elegans* (Mackinnon et al., 2002b) and *Drosophila* (Brakebusch and Fassler, 2003; Zervas, 2001), characterized by muscle detachment, and severe actin-related defects (Brakebusch and Fassler, 2003; Zervas, 2001). Similarly, PINCH depletion seems to also lead to embryonic lethality during the phase of implantation (Grashoff, 2004). Interestingly enough, the interactions between PINCH, ILK and parvins are well conserved in *C.elegans* and *Drosophila* (Clark et al., 2003; Kadrmas et al., 2004; Lin et al., 2003; Mackinnon et al., 2002). They work together in a multi-protein complex in the invertebrate organisms as well. Thus, the formation of the PINCH-ILK-parvin complex is likely crucial for the functions of these proteins. Indeed, the phenotypes resulting from loss of ILK or PINCH bear significant similarity to the ones observed when the complex formation is disrupted (Zhang et al., 2002).

1.1.2 Assembly and regulation of the PINCH-ILK-parvin complexes

Recent work has shown that ILK, PINCH and parvin are recruited to cell-ECM sites as a pre-assembled complex (Zhang et al., 2002), indicating that the formation of the complex precedes the integrin-mediated cell adhesion and spreading. The assembly of the PINCH-ILK-parvin complex is known to be regulated by two main signaling pathways, although other levels of regulation may be also involved. First, the complex formation is regulated by the protein kinase C (PKC) signaling pathway (Zhang et al., 2002). Inhibition of PKC leads to down-regulation of the assembled complex suggesting that the PINCH-ILK-parvin complex is an important downstream target of PKC pathway through which many cellular processes such as cell migration, spreading, and proliferation are regulated. Second, the formation of the PINCH-ILK-parvin complex is regulated by the phosphatidylinositol-3 (PI-3) kinase pathway, since inhibition of PI3K pathway by small compound inhibitors or by overexpressing PTEN also results in the inhibition of the complex assembly (Attwell et al., 2003).

In mammalian cells, two structurally related PINCH proteins (termed as PINCH-1 and PINCH-2), which are encoded by two different genes, have been identified to date. PINCH-1 and PINCH-2 are co-expressed in a number of cell types and tissues (Braun et al., 2003; Wu, 2004c; Zhang et al., 2002a). Both PINCH-1 and PINCH-2 can bind to ILK (Zhang et al., 2002a). Furthermore, the binding of PINCH-1 and PINCH-2 to ILK is mutually exclusive (Zhang et al., 2002a). As mentioned above, both α- and β-parvins are capable of binding to ILK (via their CH2 domain). Thus, in many types of cells, there exist multiple PINCH-ILK-parvin complexes. It is worth noting though, that the different PINCH-ILK-parvin complexes, although sharing certain common functions, they are not redundant or interchangeable but rather each one plays its own distinct role within the cell (Fukuda et al., 2003a).

1.1.3 Signaling through the PINCH-ILK-parvin complexes

Activation of ILK, either by integrin clustering, or by growth factors, affects multiple cell signaling pathways that regulate cell survival, proliferation and differentiation. As shown in Figure 2, ILK activation results in the phosphorylation and subsequent activation of PKB/Akt (Persad et al., 2000b; Troussard et al., 2003a; Wu and Dedhar, 2001a), as well as Extracellular signal-Regulated Kinase/Mitogen Activated Protein Kinase (Erk/MAPK) (Wu and Dedhar, 2001a). In addition, α-parvin, one of the partners of ILK in the PINCH-ILK-parvin ternary complexes, was shown to regulate cell survival signaling by affecting the membrane translocation of PKB/Akt (Fukuda et al., 2003b). Thus, the components of the ILK complexes appear to function in concert to mediate cellular signaling.
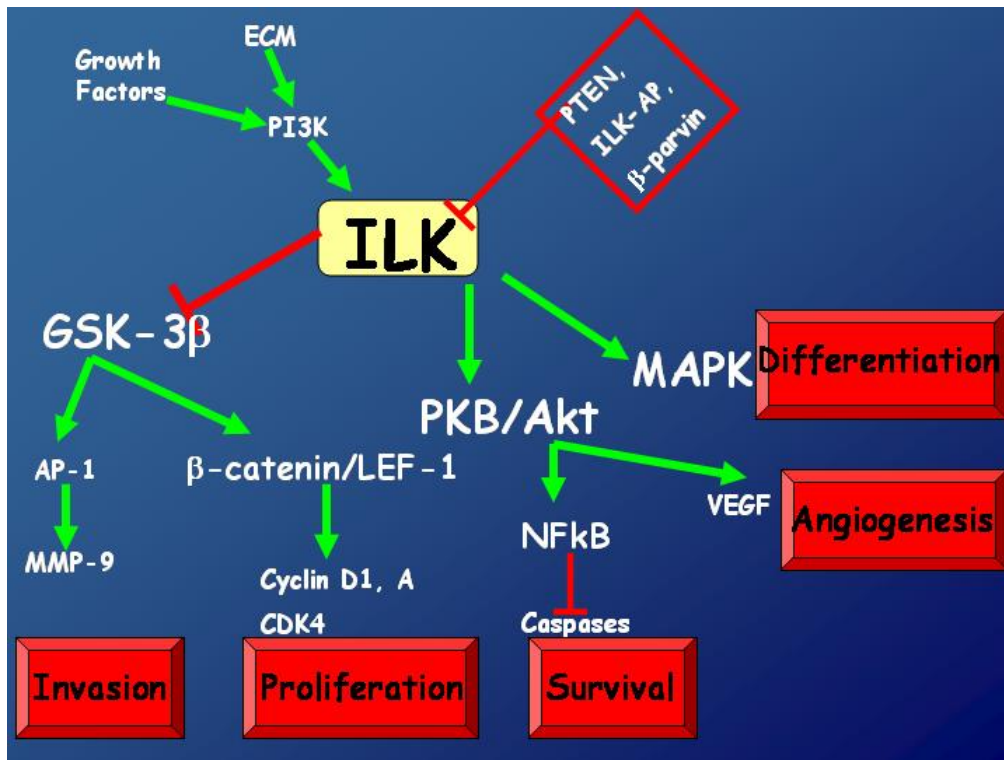
Figure 2. Schematic representation of the signaling mediated by ILK.

The activation of PKB/Akt, for instance, results in a cascade of signaling events leading to protection of cells from apoptosis (Downward, 2004; Franke et al., 2003; Hemmings, 1997). ILK can also phosphorylate and subsequently inhibit Glycogen Synthase Kinase 3-beta (GSK3-β) in a PI3K-dependent manner (Delcommenne et al., 1998a; Mhashilkar et al., 2003; Tan et al., 2001b; Wu and Dedhar, 2001a). This leads to the induction of the transcriptional activities of AP-1 transcription factor as well as the β-catenin/Lymphoid Enhancer Factor-1(LEF1) transcription complex (Novak and Dedhar, 1999; Novak et al., 1998)(Figure 2). This in turn up-regulates the expression of Matrix-metalloproteinase-9 (MMP-9) (Troussard, 2000), c-myc (Novak and Dedhar, 1999), and cyclin D1 respectively (D'Amico et al., 2000), resulting in degradation of the ECM, invasion and cell cycle progression. Activation of PKB/Akt also leads to induction of the expression of hypoxia inducible factor 1α (HIF-1α), which in turn stimulates the expression of vascular endothelial growth factor (VEGF), and thus affecting angiogenesis (Figure 2) (Tan et al., 2004b).

Recent studies have identified several upstream regulators of ILK (Figure 2). For example, ILK activity can be negatively regulated by PTEN (Persad et al., 2000b; Wu and Dedhar, 2001a) and ILK-associated phosphatase (ILK-AP)(Kumar et al., 2004) (Leung-Hagesteijn et al., 2001). Recently it was shown that β-parvin, one of its binding partners, is also capable of inhibiting it (Mongroo et al., 2004). Taking into account the fact that α-parvin promotes cell survival through ILK signaling (Attwell et al., 2003; Fukuda et al., 2003b), it seems that α- and β-parvin, two binding partners of ILK, exert antagonistic effects on ILK signaling. In fact, the binding of α- and β-parvin to ILK is mutually exclusive (Zhang et al., 2004). Thus, ILK signaling, apart from PI3K and growth factors, is also regulated by its binding partners.

Consistent with the fact that ILK regulates major signaling pathways, it has been implicated in many physiologic or pathological processes such as cell **differentiation**, **proliferation**, **migration, platelet aggregation**, and **angiogenesis** (Friedrich et al., 2004b; Huang, 2000; Kaneko et al., 2004; Tan et al., 2004b; Terpstra, 2003; Wu et al., 1998; Yamaji, 2002). ILK was shown to be an important regulator of **myogenic differentiation**, affecting the initial stages of this process by regulating MAPK activation (Huang, 2000). In addition to myogenic differentiation, ILK was shown to be involved in **chondrocyte proliferation and differentiation** (Terpstra, 2003) and platelet aggregation (Yamaji, 2002). Furthermore, it was shown to **regulate tumor angiogenesis** (Tan et al., 2004b) by stimulating the expression of VEGF. In that case, inhibition of ILK leads to the inhibition of VEGF-mediated endothelial cell migration and angiogenesis (Tan et al., 2004b). Finally, recent work by Friedrich et.al., done in mice using the Cre-Lox system and in the developing zebra fish using the antisense technology, has shown that ILK plays a fundamental role in vascular development and endothelial cell survival in vertebrates (Friedrich et al., 2004b).

There is compelling evidence suggesting that ILK plays a role in **oncogenic transformation.** First, overexpression of ILK promotes anchorage-independent growth, and cell cycle progression (Hannigan et al., 1996; Radeva et al., 1997(White et al., 2001; Wu et al., 1998). Second, ILK overexpression in epithelial cells leads to down-regulation of E-cadherin and disruption of cell-cell adhesions (Hannigan et al., 1996b; Wu et al., 1998), as well as

8

inhibition of suspension-induced apoptosis (anoikis), all of which are important traits of cancer cells (Avizienyte, 2002; Cairns, 2003; Cavallaro, 2001; Conacci-Sorrell, 2002; Hajra, 2002; Hanahan, 2000; Popov, 2000). Third, modest overexpression of ILK in intestinal and mammary epithelial cells promotes invasion, and is accompanied by translocation of β-catenin to the nucleus, complex formation between β-catenin and the LEF1 transcription factor and subsequent transcriptional activation of pro-survival genes such as MMP-9, cyclins, and cMYC (Ben-Ze'ev, 1999; Novak and Dedhar, 1999; Novak et al., 1998). Finally, clinic studies have shown that ILK expression level increases in a number of malignancies and there is often a correlation between ILK expression levels and the tumor grade. For instance, the ILK level is increased in highest grade prostate adenocarcinoma as compared to lower grade or to benign prostate hyperplasia (Graff, 2001; Yoganathan et al., 2002b). It is also correlated with the ovarian tumor grade (Ahmed, 2003) and melanoma progression and poor prognosis (Dai et al., 2003). Both ILK activity and expression level are also increased in polyps from Familial Adenomatous Polyposis patients (Marotta et al., 2003; Marotta et al., 2001). This combined with all the above-described evidence indicates that ILK may comprise a useful biological marker for certain types of cancer (Ahmed, 2004) or even a potent target for anti-cancer therapy (Attwell et al., 2000b; Mhashilkar et al., 2003; Yoganathan et al., 2000) (Hannigan et al., 2005).

1.1.4   Proteins interacting with the PINCH-ILK-parvin complexes

The interactions of ILK with PINCH and α-parvin are necessary but not sufficient for ILK localization to cell-ECM adhesion sites (Zhang et al., 2002). This suggests that there are other proteins that interact with the components of the PINCH-ILK-parvin complex and mediate its localization to cell-ECM sites. Indeed, each of the proteins forming the ternary complex of PINCH-ILK-parvin interacts with multiple proteins within the cell. For example, ILK can interact with β1 and β3 integrin cytoplasmic domains (Hannigan et al., 1996b), paxillin (Nikolopoulos, 2001), ILK-AP (Kumar et al., 2004) and **<u>Mitogen inducible gene-2 (Mig-2)</u>**, a mammalian homologue of *C.elegans* UNC-112 (Tu et al., 2003a). Studies in *C.elegans* have shown that UNC-112 binds to PAT4/ILK and is essential for the recruitment of PAT4/ILK to attachment sites (Mackinnon et al., 2002b), thus making UNC-112 a possible candidate for recruiting ILK to cell-ECM sites. Mammalian Mig-2 also interacts with ILK. In addition, it

interacts with **migfilin**, a recently identified LIM domain-containing protein (Tu et al., 2003a). Migfilin, in turn, binds to filamin A and C (hence the name migfilin) (Tu et al., 2003a). These interactions are important for actin cytoskeleton organization and processes that require extensive shape modulation such as cell migration (Stossel and Hartwig, 2003; Tu et al., 2003a).

Migfilin consists of five distinct domains; an N-terminal domain, a proline-rich domain in the center, and three LIM domains in the C-terminal region. Three splice variants of migfilin have been identified to date; the long form migfilin with all the above-described domains, a short form lacking the proline-rich domain (Tu et al., 2003a), and FBLP-1, which lacks the last LIM domain (Takafuta, 2003). The C-terminal region of migfilin is responsible for the binding to Mig-2, the N-terminal accounts for the interaction with filamin (Tu et al., 2003a), while the central proline-rich domain mediates the interaction with VASP (Y. Zhang and C. Wu, manuscript submitted), another actin-regulatory protein (Krause et al., 2002; Krause et al., 2003). Interestingly, Cal, the mouse homologue of migfilin, is capable of interacting with the cardiac homeobox transcription factor CSX/Nkx2-5 via the C-terminal LIM domains (Akazawa, 2004). Taking into consideration the fact that the LIM domain motif with the tandem zinc fingers is known to mediate multiple protein-protein interactions (Jurata and Gill, 1998; Schmeichel and Beckerle, 1994(Bach, 2000; Dawid, 1998; Khurana, 2002), it is anticipated that other binding partners of migfilin exist as well.

In a wide variety of fibroblasts, epithelial and endothelial cells, migfilin is present at the cell-ECM adhesion sites where it is being recruited by Mig-2, and it is also associated with actin filaments as a result of its interaction with filamin (Tu et al., 2003a). Consistent with its association with the CSX/Nkx2-5 transcription factor, the mouse homologue of migfilin was also detected in the nucleus (Akazawa, 2004). The nuclear trafficking of migfilin has not been studied extensively, but existing evidence indicates that migfilin enters the nucleus in response to high intracellular calcium levels, since treatment of the cells with a calcium ionophore promotes the nuclear accumulation of the protein (Akazawa, 2004). As for the nuclear export of migfilin, the nuclear export signal (NES) within the proline-rich domain, was shown to be responsible (Akazawa, 2004).

Studies in *C.elegans* reveal that UNC-112, the invertebrate homologue of Mig2, is essential for the localization of integrins in the muscle cell membrane, indicating that Mig-2 itself is important for integrin-related cell functions (Rogalski, 2000). Depletion of Mig2 from mammalian cells impairs cell spreading showing that Mig-2 is important for cell shape modulation (Tu et al., 2003a). Migfilin, the binding partner of Mig-2, is also critical for cell shape modulation. Depletion of migfilin impairs cell spreading and reduces the level of filamentous actin (F-actin) as compared to the level of free G-actin, thus playing an important role in actin remodeling (Tu et al., 2003a). Intriguingly, a recent study demonstrated that Mig-2 was transcriptionally elevated in uterine leiomyomas as compared to normal myometrium (Kato, 2004). This suggests a putative role for Mig-2 in the hormone-mediated growth of benign smooth muscle tumor cells of uterine leiomyomas.

New insight into the functional role of migfilin in cells is gained from a recent study where Cal, the mouse homologue of migfilin, is shown to be important for cardiac differentiation (Akazawa, 2004). Interestingly, this study shows that the mouse homologue of migfilin possesses itself a transcription-promoting activity and by association with the CSX/Nkx2-5 transcription factor it is capable of transactivating certain genes such as the atrial natriuretic peptide (ANP) promoter, and the transcription factor GATA-4 (Akazawa, 2004). Thus, migfilin seems to play a very significant part in the regulation of transcription of cardiac genes and cardiac development in general.

2.0 PHYSICAL AND FUNCTIONAL ASSOCIATION OF MIGFILIN WITH CELL-CELL ADHESIONS

2.1 INTRODUCTION

As mentioned above, cell-cell and cell-extracellular matrix (ECM) adhesions are constituently and functionally distinct subcellular structures that are essential for the assembly of cells into tissues, and for communication between neighboring cells and between cells and the ECM. Identification of the molecular constituents of cell-cell and cell-ECM adhesions and the structural determinants that control their localization to these two distinct subcellular adhesion structures are therefore of fundamental importance. Migfilin is a recently identified and cloned protein that is a component of cell-ECM adhesions, where it links the cell-ECM adhesions to the actin cytoskeleton and functions in actin cytoskeleton remodeling and cell shape modulation (Tu et al., 2003).

In the present study, we show that migfilin not only localizes to cell-ECM adhesions but also is recruited to cell-cell junctions in epithelial and endothelial cells. Using a combination of biochemical, cell biological, immunofluorescence and immunoelectron microscopic approaches, we have characterized the ultrastructure of the migfilin-containing structures at cell-cell junctions. In addition, we have identified the determinants that control migfilin localization to cell-cell and cell-ECM adhesions. Finally, we have investigated the function of migfilin in cell-cell junctions by RNA interference.

Our results identify a new component of adherens junctions and suggest an important role of migfilin in the organization of the cell-cell adhesion structure.

2.2 MATERIALS AND METHODS

Cell lines and antibodies

Primary newborn human embryonic keratinocytes (NHEK) (Clonetics) were cultured in KBM-2 medium containing the supplements recommended by the company. Primary human microvascular endothelial cells (HMVEC) were purchased from Clonetics and cultured in EGM-MV medium (Clonetics). HaCat and MCF-7 cells were cultured in DMEM medium containing 10% Fetal Bovine Serum (FBS), 1% Glutamax, and 1% penicillin/streptomycin. Human fibrosarcoma HT-1080 cells were cultured in Eagle's MEM medium supplemented with L-glutamine, 10% FBS, and non-essential amino acids. Mouse monoclonal antibodies recognizing migfilin and Mig-2 were generated as described previously (Tu et al., 2003). Rabbit polyclonal antibodies against β-catenin and α-catenin were purchased from Sigma. Mouse monoclonal anti-E-cadherin antibody (SHE78-7) was from Calbiochem. Rhodamine Red™-conjugated anti–mouse IgG antibody, Rhodamine Red™-conjugated anti-rabbit IgG antibody, and FITC-conjugated anti-mouse IgG antibody were purchased from Jackson ImmunoResearch Laboratories. For the immunofluorescent staining in Figure 3, a goat anti-mouse Alexa 488 antibody from Molecular Probes, Eugene OR, and a goat anti-rabbit Cy3 from Jackson Immunolabs were used as secondary antibodies.

Migfilin expression vectors, site-directed mutagenesis and DNA transfection

The expression vectors encoding GFP-tagged migfilin, the short form splicing variant of migfilin that lacks the proline-rich domain (migfilin(s)), and the deletion mutants of migfilin (as specified in each experiment) were generated by inserting the corresponding cDNA fragments into pEGFP-C2 vector (Clontech). Point mutations were generated by PCR using the Pfu DNA polymerase from Invitrogen, and the QuickChange™ site-directed mutagenesis system from Stratagene. All mutations were confirmed by DNA sequencing. HaCat cells were transfected with expression vectors encoding GFP-tagged wild type and mutant forms of migfilin with LipofectAmine PLUS (Life Technologies) following the manufacturer's protocol.

Immunofluorescent staining and Confocal microscopy

Immunofluorescent staining was performed as described (Tu et al., 2003; Zhang et al., 2002). Briefly, cells were plated on fibronectin-coated cover slips, fixed with 4% paraformaldehyde, and incubated at room temperature with appropriate primary and secondary antibodies or Rhodamine-conjugated phalloidin as specified in each experiment. In experiments in which cells were transfected with GFP-migfilin expression vectors, Rhodamine Red[TM]-conjugated secondary anti–mouse or anti-rabbit IgG antibodies were used. In double staining experiments with mouse anti-migfilin antibody and rabbit anti-β-catenin antibody, FITC-conjugated anti-mouse IgG and Rhodamine Red[TM]-conjugated anti-rabbit IgG secondary antibodies were used. The cells were observed either under a Leica DM R fluorescence microscope or an Olympus Fluoview BX61 confocal microscope.

Cytoskeletal Extraction

Cytoskeletal extractions of cells were performed essentially as described previously (Heuser and Kirschner, 1980). Briefly, with all solutions at 37°C, cells on 12 mm round glass coverslips, were washed with Cytoskeletal Buffer (100 mM PIPES, pH 6.9, 0.1 mM EDTA, 0.5mM MgCl$_2$, 4 M glycerol, 1:100 dilution mammalian protease inhibitor cocktail, Sigma), and then extracted with Cytoskeletal Buffer supplemented with 0.75% Triton X-100 for 3 minutes with one change of the extraction buffer during this time period. Extracted cells were washed once with Cytoskeletal Buffer, and then fixed in Cytokeletal Buffer supplemented with 2% paraformaldehyde for 1 hour. Cells were stored in PBS at 4°C until use.

Cationic Colloidal Silica Unroofing of Cells*

Cells were unroofed as described previously (Stolz and Jacobson, 1992). All isolation solutions were maintained at 4°C. Briefly, cells were washed in MES-Buffered Saline (MBS: 20 mM morpholinoethane sulfonic acid, 135 mM NaCl, 0.5 mM CaCl$_2$, 1 mM MgCl$_2$), and were then overcoated with a 1% solution of cationic colliodal silica, which was prepared as a 30% stock colloid as described (Chaney and Jacobson, 1983). Cells were subsequently washed with MBS, overcoated with 1% polyacrylic acid in MBS (stock 25% aqueous polyacrylic acid solution, ave. mol. wt. 100,000, Aldrich, St. Louis, MO). Then, cells were washed with MBS and they were allowed to swell in hypotonic lysis buffer for 10 min [lysis buffer: 2.5mM imidizole, pH 7.0,

supplemented with protease inhibitors (1:100 dilution mammalian protease inhibitor cocktail, Sigma)]. Cells were then unroofed by squirting the monolayers with lysis buffer through a 5 ml syringe fitted with a blunted, flattened 18 gauge needle. The degree of lysis was monitored by observing cells on an inverted microscope. Footprints were washed once with MBS and fixed in 2% paraformaldehyde in PBS for 1 hr and stored in PBS at 4°C until use. (*Cationic colloidal silica can be obtained by written request from Dr. Donna Beer Stolz, University of Pittsburgh, Pittsburgh, PA 15261, E-mail: dstolz@pitt.edu.)

Immunoelectron microscopy

HaCat cells were fixed in cryofix (2% paraformaldehyde, 0.01% glutaraldehyde in 0.1 M PBS) and stored at 4°C for 1 hour. Cells were pelleted and resuspended in a small amount of 3% gelatin in PBS, solidified at 4°C then fixed for an additional 15 minutes in cryofix. Gelatin-cell block was cryoprotected in PVP cryoprotectant overnight at 4°C [25% poly(vinylpyrrolidone), 2.3 M sucrose, 0.055 M Na2CO3, pH 7.4 (Tokuyasu, 1989)]. Cell blocks were frozen on ultracryotome stubs under liquid nitrogen and stored in liquid nitrogen until use. Ultrathin sections (70-100 nm) were cut using a Reichert Ultracut U ultramicrotome with a FC4S cryo-attachment, lifted on a small drop of 2.3 M sucrose and mounted on Formvar-coated copper grids. Sections were washed three times with PBS, then three times with PBS containing 0.5% bovine serum albumin and 0.15% glycine (PBG buffer); this was followed by a 30 minute blocking incubation with 5% normal goat serum in PBG. Sections were labeled with a rabbit anti-â-catenin antiserum (1:100) and the ascites fluid of the mouse monoclonal anti-migfilin antibody (clone 43) (1:100) in PBG for 1 hour. Sections were washed four times in PBG and labeled with goat anti-rabbit (10 nm) or goat anti-mouse (5 nm) gold conjugated secondary antibodies (Amersham), each at a dilution of 1:25 for 1 hour. Sections were washed three times in PBG, three times in PBS then fixed in 2.5% glutaraldehyde in PBS for 5 minutes, washed twice in PBS then washed six times in ddH2O. Sections were post-stained in 2% neutral uranyl acetate for 7 minutes, washed three times in ddH2O, stained for 2 minutes in 4% uranyl acetate then embedded in 1.25% methyl cellulose. Labeling was observed on a JEOL JEM 1210 electron microscope (Peabody, MA) at 80 kV.

Pre-embedding immuno-transmission microscopy

HaCat cells were grown on 35 mm tissue culture plates, the cytoskeleton was extracted as described above and cells were fixed with 2% paraformaldehyde in PBS for 1 hr. Cells were then washed 3 times with PBS, and 3 times with PBS supplemented with 0.5% BSA and 0.15% glycine (PBG). Following this washing step, cells were blocked in 20% normal goat serum in PBG for 40 min and were then washed once with PBG. Primary antibodies were added to cells in PBG at designated dilutions and incubated at room temperature for 4 hr. Cells were washed 4 times in PBG and secondary antibodies conjugated to gold (goat anti-rabbit, 5 nm, goat anti-mouse, 10 nm, Amersham) were added to the cells overnight at 4°C. Cells were then washed 3 times in PBG, and 3 times in PBS and they were fixed in 2.5% glutaraldehyde for 1 hr. Another wash step in PBS followed and cells were then post-fixed in 1% aqueous osmium tetroxide for 1 hr. They were subsequently washed in PBS and were dehydrated through a 30-100% ethanol series and several changes of Polybed 812 embedding resin (Polysciences, Warrington, PA). Cultures were embedded in by inverting Polybed 812-filled BEEM capsules on top of the cells. Blocks were cured overnight at 37°C, and then cured for two additional days at 65°C. Monolayers were pulled off the tissue culture plates. Ultrathin en face sections (60 nm) of the cells were obtained on a Riechart Ultracut E microtome, post-stained in 4% uranyl acetate for 10min and 1% lead citrate for 7 min. Sections were finally viewed on a JEOL JEM 1210 transmission electron microscope (JEOL, Peobody MA) at 80 KV.

Calcium chelation assays

The calcium chelation assay was essentially performed as described previously (Helwani et al., 2004; Rothen-Rutishauser et al., 2002). Briefly, MCF-7 cells were plated on fibronectin-coated coverslips, they were allowed to attach, and were then subject to serum starvation for 18 hours. The medium was then switched to DMEM supplemented with 4 mM EGTA and 1mM $MgCl_2$ and the cells were incubated at 37°C for 30 minutes. Cells were then washed twice with PBS and the medium was changed back to the regular calcium-containing culture medium. After incubation for periods of time as specified, cells were fixed and dually stained with mouse anti-migfilin antibody and rabbit anti-β-catenin antibody.

In some experiments, MCF7 mammary epithelial cells were transiently transfected with an expression vector encoding GFP-migfilin using LipofectaminePLUS. Twenty four hours following the transfection, cells were plated on fibronectin-coated coverslips and were then subject to serum starvation for 18 hours. The medium was then changed to DMEM supplemented with 4 mM EGTA, 1mM $MgCl_2$ and a function-blocking mouse monoclonal anti E-cadherin antibody (SHE78-7, 4 µg/ml) or an irrelevant mouse IgG (4 µg/ml) as a control. The cells were incubated at 37^oC for 1 hour and then washed twice with PBS and the medium was switched back to the normal culture medium, which again contained 4 µg/ml of either the function-blocking anti-E-cadherin antibody or the irrelevant control mouse IgG antibody. One hour following the switch to the normal calcium-containing medium, cells were fixed with 4% paraformaldehyde and stained with a rabbit polyclonal anti-β-catenin antibody and a Rhodamine Red^{TM}-conjugated anti-rabbit IgG antibody.

RNA interference

Human fibrosarcoma HT-1080 cells were transfected with a siRNA that specifically targets migfilin mRNA (sense sequence: 5'-AAAGGGGCAUCCACAGACAUC-3'), or a 21-nucleotide irrelevant RNA as a control, as previously described (Tu et al., 2003). The cells were analyzed by Western blotting and immunofluorescent staining two days after the siRNA transfection.

Cell dissociation assay

Cell dissociation assay was performed following a previously published method (Takeda et al., 1995). Briefly, the cells as specified in each experiment) were detached from culture plates with a rubber policeman and passed through glass Pasteur pipettes ten times. The cells were then fixed in 1% glutaraldehyde and pictures were taken under an Olympus IX70 inverted microscope equipped with a MagnaFireTM digital camera. The extent of cell dissociation was represented by the ratio of the number of particles (Np) over the number of cells (Nc) (Np/Nt). The values of Np/Nc were calculated by analyzing at least 500 cells from each sample.

2.3   RESULTS

Migfilin is a component of cell-cell junctions in epithelial and endothelial cells

Epithelial cells are attached not only to ECM but also to neighboring cells via highly specialized subcellular structures termed cell-cell junctions. To analyze the subcellular localization of migfilin in epithelial cells, we immunofluorescently stained human primary keratinocytes with a monoclonal antibody that specifically recognizes migfilin (Tu et al., 2003). Clusters of migfilin (Fig. 3A, arrows) were detected at cell-cell junctions where abundant β-catenin (Fig. 3B) and E-cadherin (not shown), which are welldescribed components of cell-cell junctions, were present. As expected, migfilin clusters were also detected at cell-ECM adhesions (Fig. 3A, arrowheads) lacking β-catenin (Fig. 3B) and E-cadherin (not shown). Colocalization of migfilin with β-catenin and E-cadherin at cell-cell adhesions was also observed in immortalized HaCat keratinocytes (not shown).
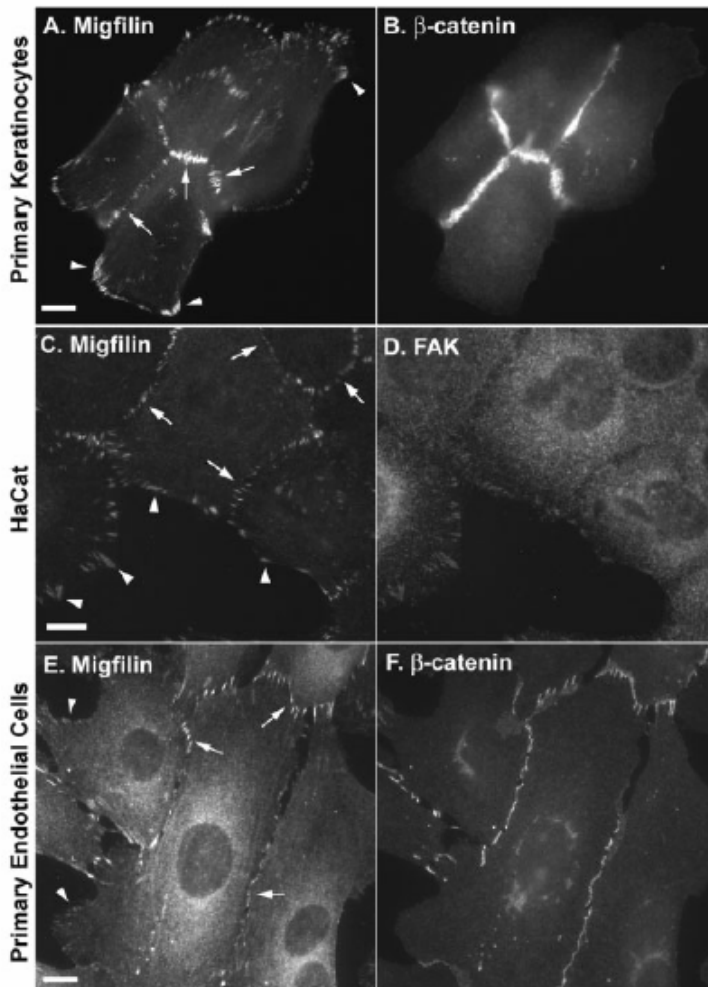
Figure 3. Migfilin localizes to cell-cell junctions in epithelial and endothelial cells. (A-D) Primary newborn human embryonic keratinocytes (A and B), immortalized human keratinocytes (HaCat) (C and D) and primary human microvascular endothelial cells (E and F) were double stained with a mouse monoclonal anti-migfilin antibody (clone 43) (A, C and E) and a rabbit polyclonal anti-β-catenin antibody (B and F) or anti-FAK antibody (D). The images were recorded using a Leica DM R fluorescence microscope equipped with a Hamamatsu ORCA-ER digital camera. The cell-cell and cell-ECM adhesions are indicated by arrows and arrowheads, respectively. Note that a fraction of migfilin was co-clustered with β-catenin at cell-cell junctions (arrows, C) that lack FAK (D). Migfilin was also detected at FAK-rich cell-ECM adhesions (arrowheads, C and D). Bars in A, C and E, 8 μm.

Double staining of the human keratinocytes with the mouse monoclonal anti-migfilin antibody and a rabbit polyclonal anti-FAK antibody confirmed that migfilin was clustered at both cell-ECM adhesions (Fig. 3C, arrowheads) where FAK was concentrated (Fig. 3D) and cell-cell adhesions (Fig. 3C, arrows) that lacked FAK (Fig. 3D). The localization of migfilin to both cell-cell and cell-ECM adhesions has also been observed in other epithelial cells that have been analyzed, including human mammary epithelial cells and Madin-Darby canine kidney epithelial cell (not shown). To test whether migfilin localizes to cell-cell junctions in endothelial cells, another major type of cells that assemble both cell-cell and cell-ECM junctions, we stained primary human microvascular endothelial cells with the monoclonal antimigfilin antibody. As in epithelial cells, migfilin was clustered at both cell-cell junctions (Fig. 3E, arrows), where abundant β-catenin was detected (Fig. 3F), and cell-ECM adhesions (Fig.3E, arrowheads) that lacked β-catenin (Fig. 3F).

A. Migfilin (lateral)   **B. β-catenin (lateral)**   **C. Merged (lateral)**

D. Migfilin (basal)   **E. β-catenin (basal)**   **F. Merged (basal)**

G. X-Z cross-section
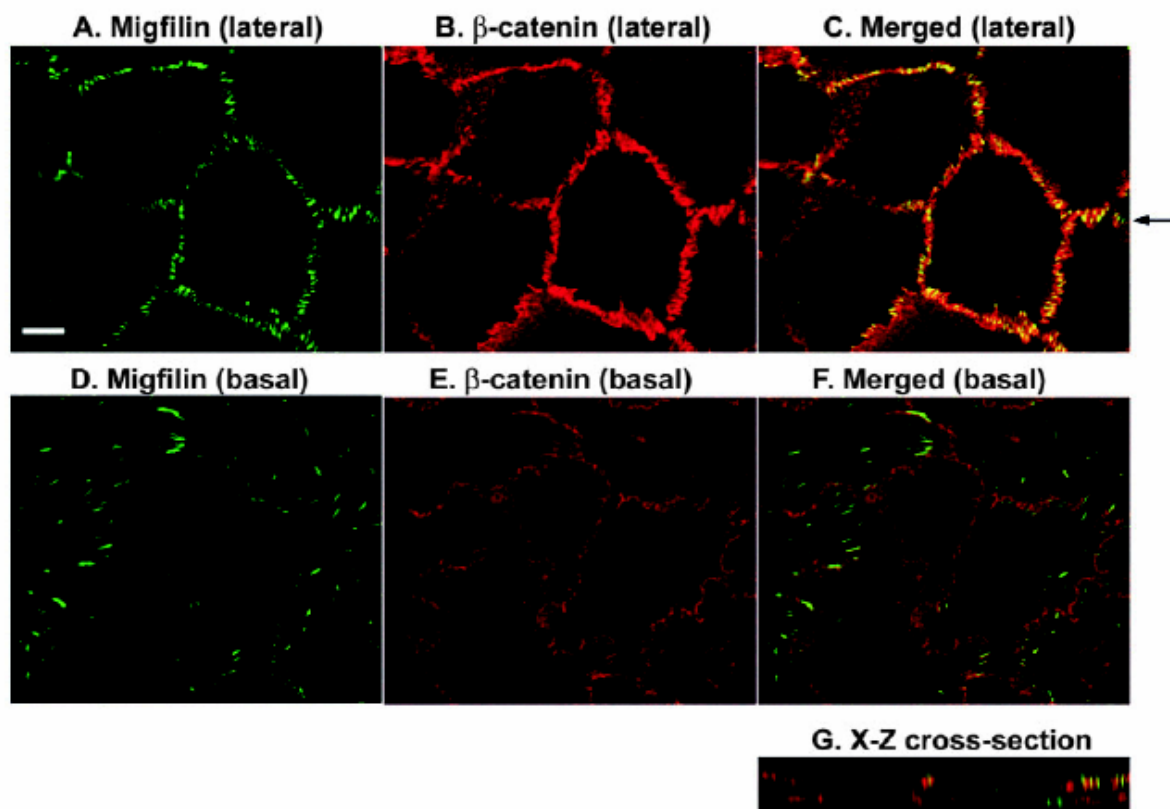
Figure 4. Immunofluorescent confocal microscopic analysis of cell-cell adhesion localization of migfilin. Human immortalized keratinocytes (HaCat cells) were double stained with monoclonal anti-migfilin antibody (clone 43) (A and D) and a rabbit polyclonal anti- β-catenin antibody (B and E) observed under an Olympus Fluoview BX61 confocal microscope. The *x-z* sections at the lateral (A and B) and basal (D and E) levels were shown. (C, F) Images merged from the migfilin (green) and β-catenin

(red) staining at the lateral and basal levels, respectively. The arrow in C indicates the position of the *xz* cross section (G). Bar, 8 μm.

To confirm that migfilin colocalizes with β-catenin at cell-cell adhesions, we analyzed human keratinocytes by confocal immunofluorescence microscopy. The results showed that migfilin was co-clustered with β-catenin at lateral cell-cell junctions (Fig. 4A-C,G). Clusters of migfilin were also detected at basal cell-ECM adhesions where β-catenin was not concentrated (Fig. 4D-G).

Migfilin forms detergent-resistant clusters that associate with actin bundles at cell-cell junctions

We next sought to characterize the association of migfilin with cell-cell junctions. We first tested whether migfilin could be removed from cell-cell junctions by extraction with nonionic detergents. To do this, we extracted HaCat cells with a Triton X-100-containing buffer. Analyses of the Triton X-100-extracted cells showed that migfilin remained to associate with β-catenin at cell-cell adhesions (Fig. 5A-C, arrowheads). Furthermore, double staining of the cells with anti-migfilin monoclonal antibody and phalloidin showed that migfilin was co-clustered with the anchoring sites of filamentous actin at cell-cell junctions, forming discrete structures that appeared to bridge neighboring cells (Fig. 5D).

It is well known that in epithelial cells, filamentous actin forms a network (Fig. 5G) linking the basal ECM adhesions with lateral cell-cell junctions, and the latter supports the connections between neighboring cells and the formation of epithelial sheets. To confirm that the migfilin clusters are physically associated with these two (basal cell-ECM adhesions and lateral cell-cell adhesions) adhesion structures, we physically separated cell-cell and cell-ECM adhesions using a cationic colloidal silica 'unroofing' protocol (Stolz and Jacobson, 1992). Staining of the 'unroofed' cells showed that migfilin clusters at cell-cell-junctions were removed with the apical and lateral plasma membrane and the actin bundles that were anchored, whereas migfilin clusters at the basal ECM adhesions (or 'cell footprints') and the associated filamentous actin remained (Fig. 5E,I). Additionally, the association of migfilin with the basal ECM adhesions, like that of migfilin with cell-cell junctions, resisted nonionic detergent extraction (Fig. 5F).
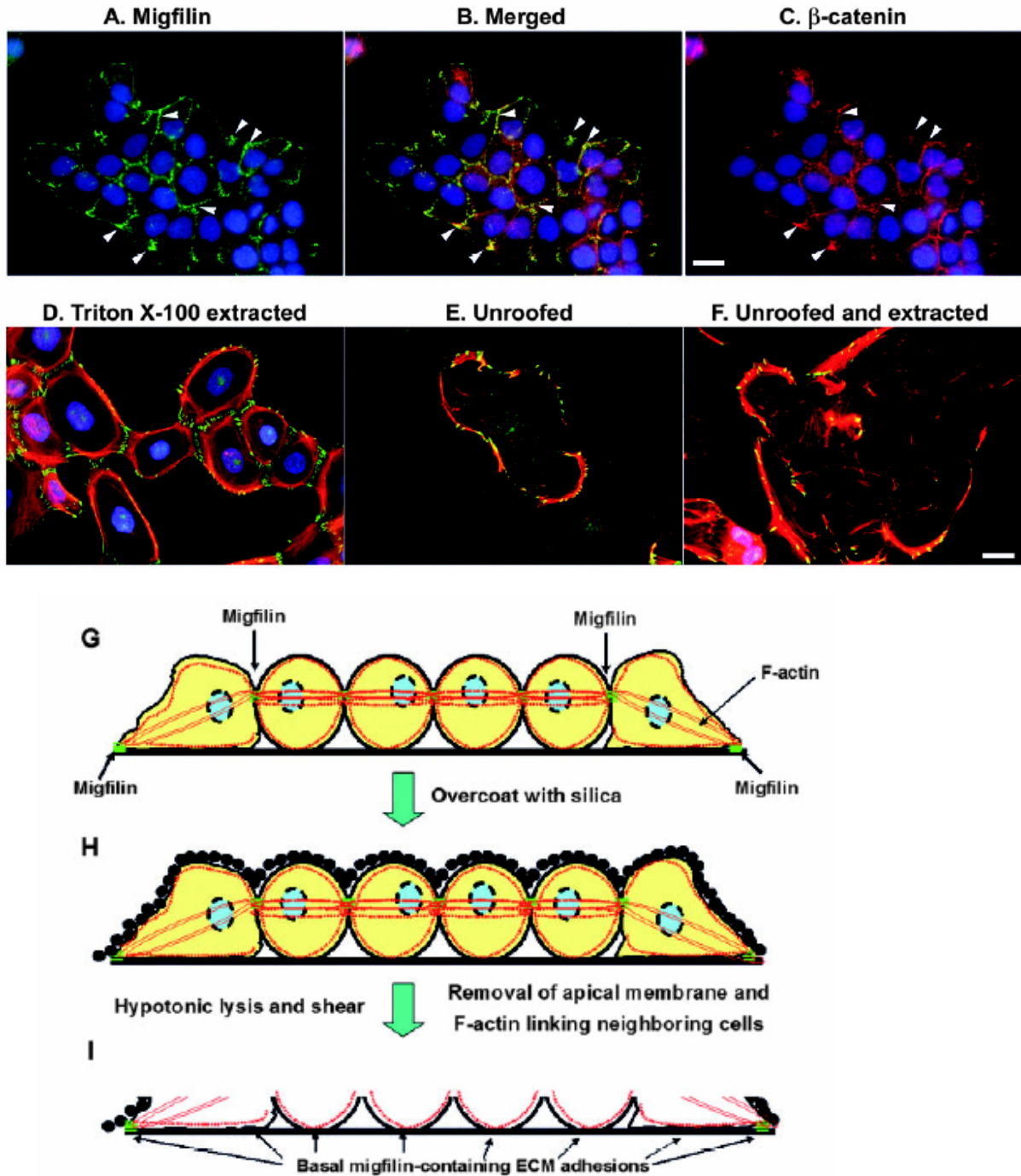
Figure 5.Detergent-resistant association of migfilin with filamentous actin at cell-cell junctions. (A-C) HaCat cells were subject to cytoskeletal extraction as described in Materials and Methods. The cells were then double stained with the mouse anti-migfilin (green, A) and rabbit anti-β-catenin (red, C) antibodies (arrowheads). The images were merged and are shown in B. (D-F) HaCat cells were Triton X-100-extracted (D), unroofed (E), or extracted and unroofed (F) as described in Materials and Methods. The cells were then costained with the monoclonal anti-migfilin antibody, which was detected with an Alexa 488-conjugated antimouse IgG antibody (green), Rhodamine-conjugated phalloidin (red) and Hoechst dye 33258 (blue). Bars, 25 μm. (G-I) Schematic representation of the Triton X-100-extracted and/or the cationic colloidal silica unroofed cells.

Immunoelectron microscopic analyses of migfilin clusters at cell-cell junctions

To define the localization and ultrastructure of migfilin at cell-cell junctions at higher magnification, we analyzed the cells by immunoelectron microscopy. Consistent with the immunofluorescent confocal microscopic results (Fig. 4), immunoelectron microscopic analysis of unextracted HaCat cells showed that migfilin is localized in the vicinity of β-catenin at cell-cell contacts (Fig. 6A).

To visualize filamentous actin and further test whether migfilin is closely associated with filamentous actin and β-catenin, we extracted the cells with a Triton X-100-containing buffer and analyzed them by pre-embedding immunotransmission microscopy as described in Materials and Methods.

The results showed that, consistent with the immunofluorescent microscopic analyses (Fig. 5), migfilin associated with actin bundles that linked neighboring cells (Fig. 6B, arrows). The migfilin clusters (Fig. 6C, arrowheads) were not associated with desmosomes (Fig. 6C, arrows).

Furthermore, double staining of cells with anti-migfilin and anti-β-catenin antibodies showed that migfilin was closely associated with β-catenin (often within 100 nm), and they formed electron dense, compact complexes that appeared to clamp actin bundles (Fig. 6D). These results suggest that migfilin forms a complex with both β-catenin and filamentous actin at adherens junctions.
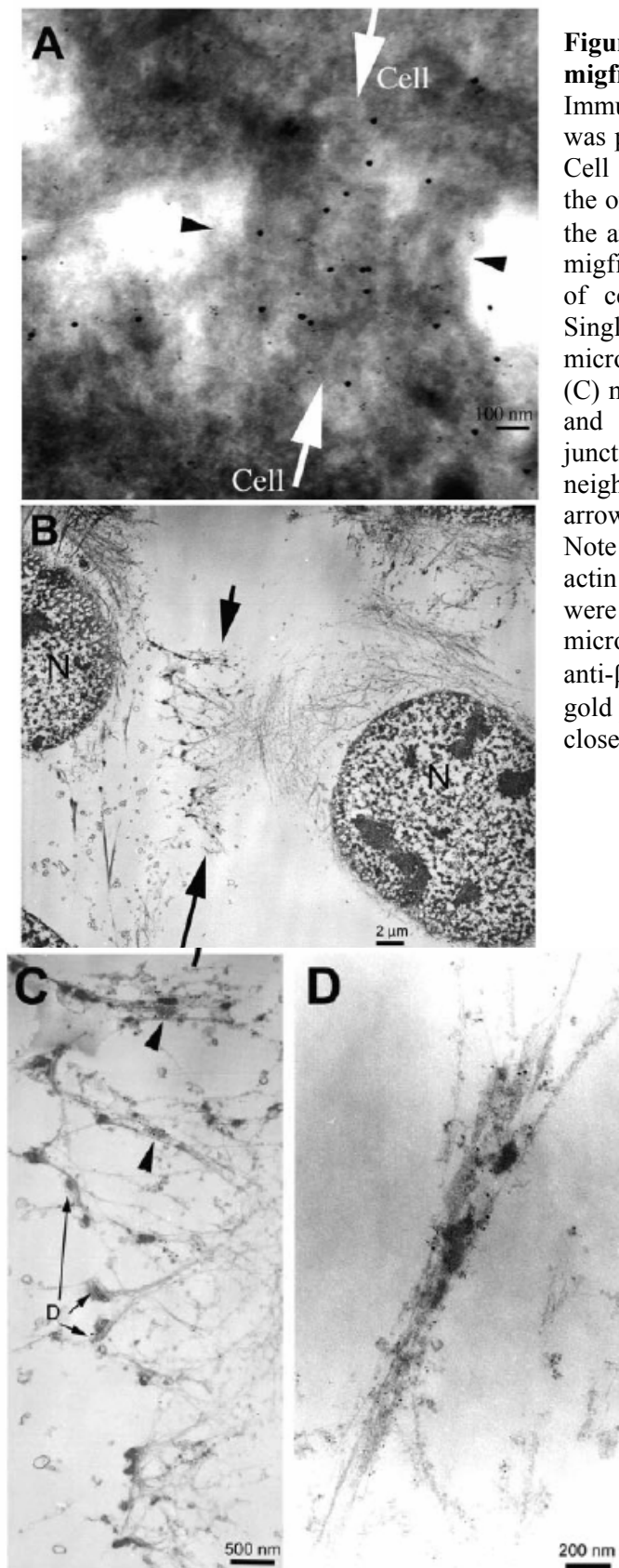
Figure 6. Immunoelectron microscopic analyses of migfilin clusters at cell-cell junctions. Immunoelectron microscopic analysis of HaCat cells was performed as described in Materials and Methods. Cell adhesions connecting the two cells are shown in the orientation between the two open arrows. Note that the anti-β-catenin antibody (10 nm gold) and the anti-migfilin antibody (5 nm gold) were colocalized at areas of cell-cell contacts (between arrowheads). (B, C) Single pre-embedding immunotransmission microscopic images of HaCat cells at low (B) and high (C) magnification. In B, migfilin (beads) was clustered and associated with the actin bundles at cell-cell junctions (arrows). N indicates the nuclei of two neighboring cells. In C, desmosomes are indicated by arrows, and migfilin clusters are shown by arrowheads. Note that migfilin clusters were associated with the actin bundles but not desmosomes. (D) HaCat cells were prepared for pre-embedding immunotransmission microscopy and double stained with anti-migfilin and anti-β-catenin antibodies. Note that migfilin (10 nm gold particles) and β-catenin (5 nm gold particles) were closely clustered with the actin bundles.

23

The recruitment of migfilin to cell-cell junctions is temporally separable from that of β-catenin

To analyze the temporal relation between migfilin and β-catenin recruitment to adherens junctions, we disassembled the adherens junctions by treating epithelial cells with a calcium-chelator (EGTA), and then added back medium that contains calcium, which is known to induce E-cadherinmediated adherens junction assembly (Nagafuchi et al., 1987). The epithelial cells were fixed at different time points after switching to calcium-containing medium.
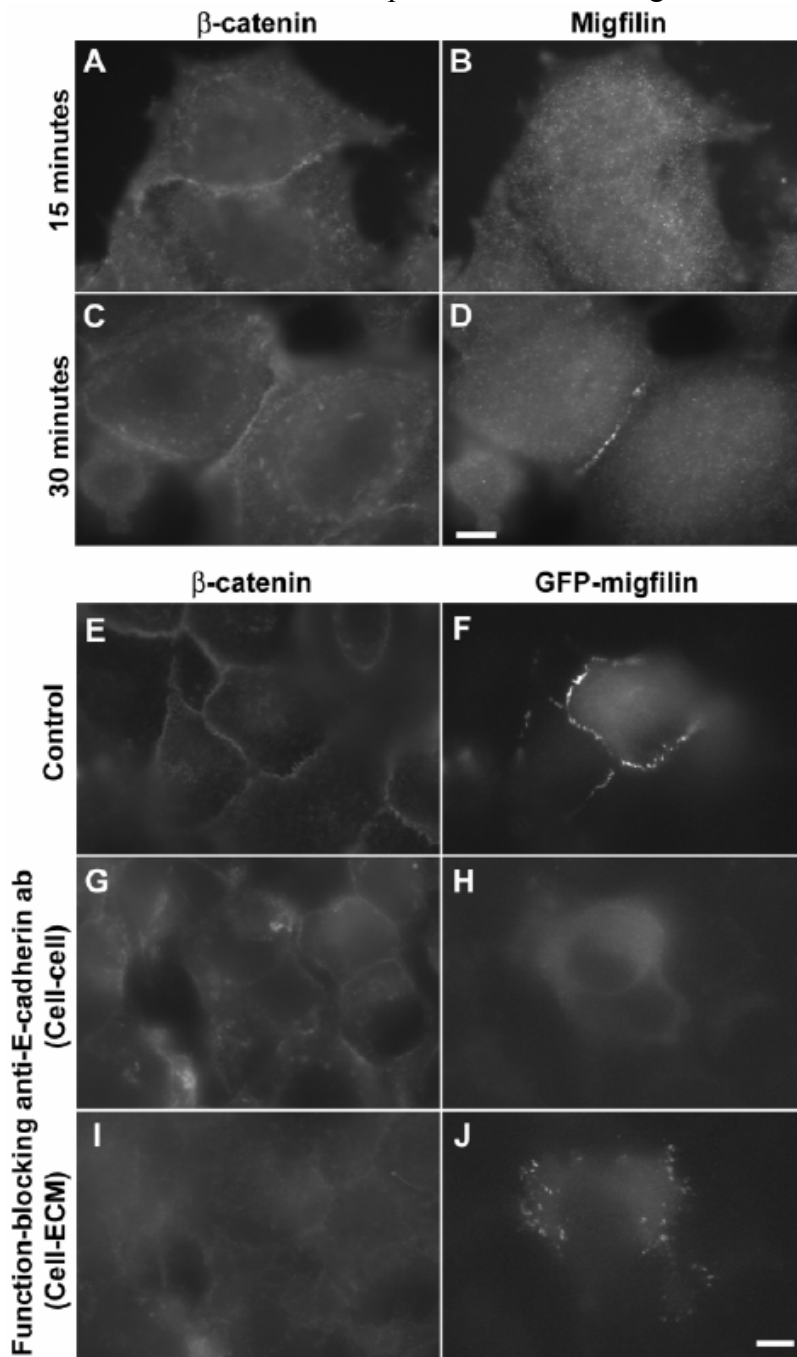
Figure 7. Calcium-induced migfilin localization to adherens junction. (A-D) MCF7 mammary epithelial cells were subject to calcium-chelation assay as described in Materials and Methods. The cells were fixed at 15 minutes (A and B) and 30 minutes (C and D) after switching to calcium-containing medium, and double stained with a rabbit anti-β-catenin antibody (A and C) and the mouse monoclonal anti-migfilin antibody (B and D). (E,F) MCF7 mammary epithelial cells were transiently transfected with an expression vector encoding GFP-migfilin. The cells were subject to calcium-chelation assay in the presence of a function-blocking mouse monoclonal anti-E-cadherin antibody (SHE78-7) (G-J) or a non-specific mouse IgG as a control (E and F) as described in Materials and Methods. The cells were fixed at 60 minutes after switching to calcium-containing medium, and stained with a rabbit anti-β-catenin antibody (E, G and I) and a Rhodamine RedTM-conjugated anti-rabbit IgG antibody. β-Catenin (E, G and I) and GFPmigfilin (F, H and J) at the cell-cell (E-H) or cell-ECM (I and J) adhesions were detected using a Leica DM R fluorescence microscope. Bars, 5 μm.

24

Immunofluorescence staining analysis with anti-migfilin and anti-β-catenin antibodies showed that β-catenin was clustered at adherens junctions within 15 minutes from the calcium switch (Fig. 7A), whereas at the same time point migfilin was not clustered at adherens junctions (Fig. 7B). Soon after the clustering of β-catenin (30 minutes from the calcium-switch), however, migfilin (Fig. 7D) was recruited to the adherens junctions where β-catenin (Fig. 7C) clusters were detected. Thus, the recruitment of migfilin to the adherens junctions appears to be temporally separable from that of β-catenin, which has been shown to be co-recruited with E-cadherin from ER to adherens junctions (Chen et al., 1999).

The recruitment of migfilin to cell-cell junctions depends on cadherin-mediated cell-cell adhesion

To test whether the localization of migfilin to cell-cell junctions depends on cadherin, we treated MCF-7 cells with a function-blocking mouse monoclonal anti-E-cadherin antibody (SHE78-7). Because the presence of the mouse monoclonal anti-E-cadherin antibody obscures the immunofluorescent detection of migfilin using the mouse anti-migfilin antibody, we transfected MCF-7 cells with an expression vector encoding GFP-migfilin and analyzed the effect of the function-blocking anti-E-cadherin antibody on the localization of GFP-migfilin.

Consistent with the results obtained with the monoclonal anti-migfilin antibody (Fig. 7C,D), GFP-migfilin was readily recruited to β-catenin-rich cell-cell adhesions in MCF-7 cells that were incubated with the control mouse IgG (Fig. 7E, F). By marked contrast, in MCF-7 cells that were incubated with the function-blocking anti-E-cadherin antibody, no GFP-migfilin clusters were detected at the cell-cell boundaries (Fig. 7G, H). The presence of the function-blocking anti-E-cadherin antibody, however, did not prevent the recruitment of GFP-migfilin to cell-ECM adhesions (Fig. 7I, J). Thus, the recruitment of migfilin to cell-cell junctions, but not that of migfilin to cell-ECM adhesions, depends on cadherin mediated cell-cell adhesion.
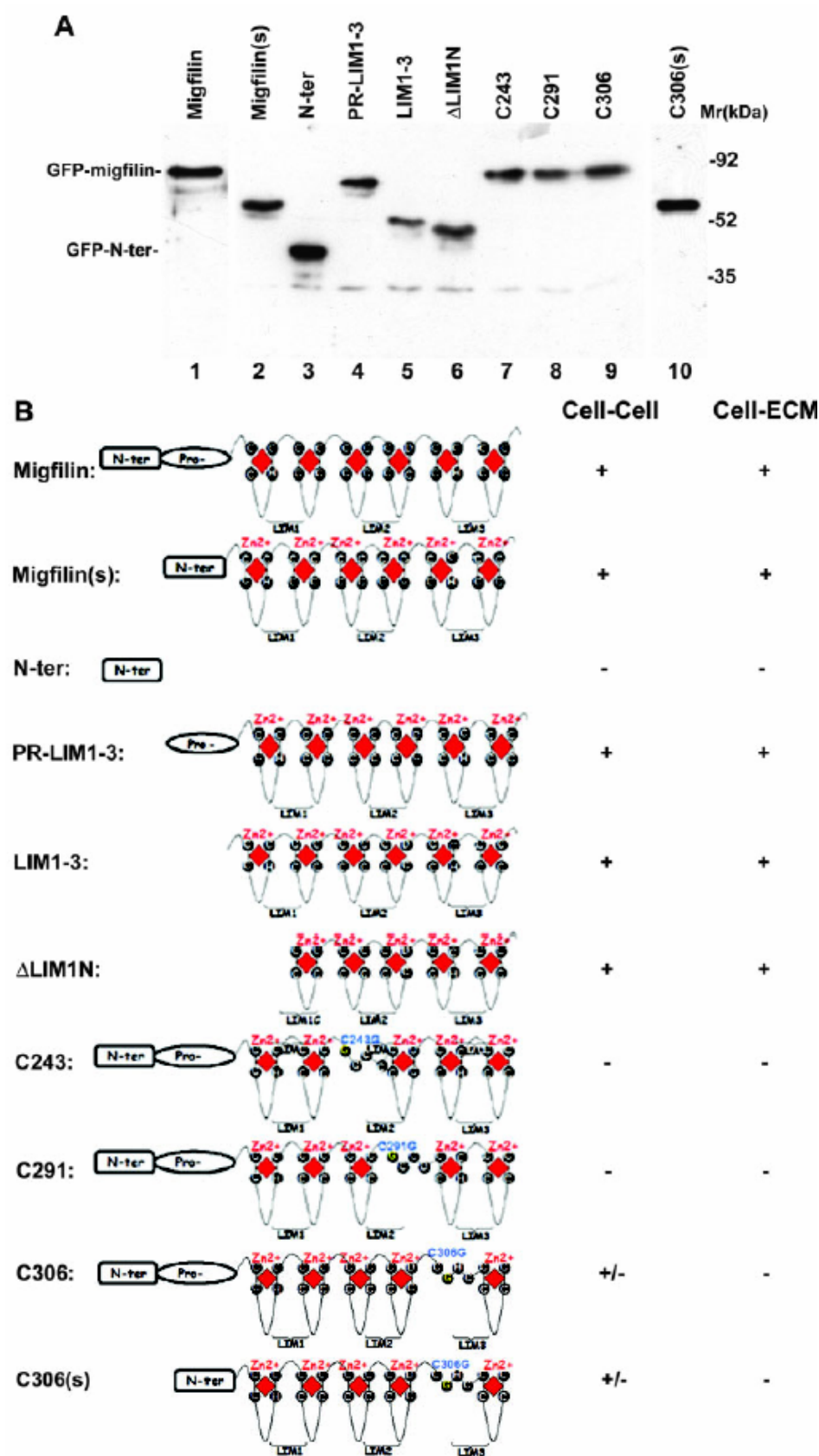
Figure 8. Expression and schematic representation of the wild-type and mutant forms of migfilin and their localization to cell-cell and cell-ECM adhesions. (A) Expression of GFP-tagged wildtype and mutant forms of migfilin. HaCat cells were transfected with expression vectors encoding the wild-type and mutant forms of migfilin as indicated in the figure. The cell lysates (15 µg/lane) were analyzed by western blotting with an anti- GFP antibody. N-ter, residues 1-85; PR-LIM1-3, residues 85-373; LIM1-3, residues 176-373; LIM1N, residues 205-373; C243, C291 and C306, migfilin bearing C243G, C291G or C306G point mutation. C306(s), migfilin(s) bearing the C306G point mutation. (B) Summary of the localization of the wild-type and mutant forms of migfilin to cell-cell and cell-ECM adhesions, based on the results presented in this paper.

26

The C-terminal LIM domains, but not the N-terminal filamin-binding domain, mediate migfilin localization to cell-cell junctions.

In addition to the central proline-rich domain, migfilin contains an N-terminal filamin-binding domain and a Mig-2-binding C-terminal region that consists of three LIM domains. To determine which of the migfilin regions mediates migfilin localization to adherens junctions, we generated expression vectors encoding GFP-tagged migfilin N-terminal domain (GFP-N-Ter), the proline-rich and the C-terminal LIM domains (GFP-PR-LIM1-3) and the C-terminal LIM domains (GFP-LIM1-3), respectively (Fig. 8B). HaCat cells were transfected with the GFP expression vectors encoding the different domains of migfilin. The expression of the GFP-tagged migfilin fragments in the corresponding transfectants was confirmed by Western blotting (Fig. 8A, lanes 3-5).
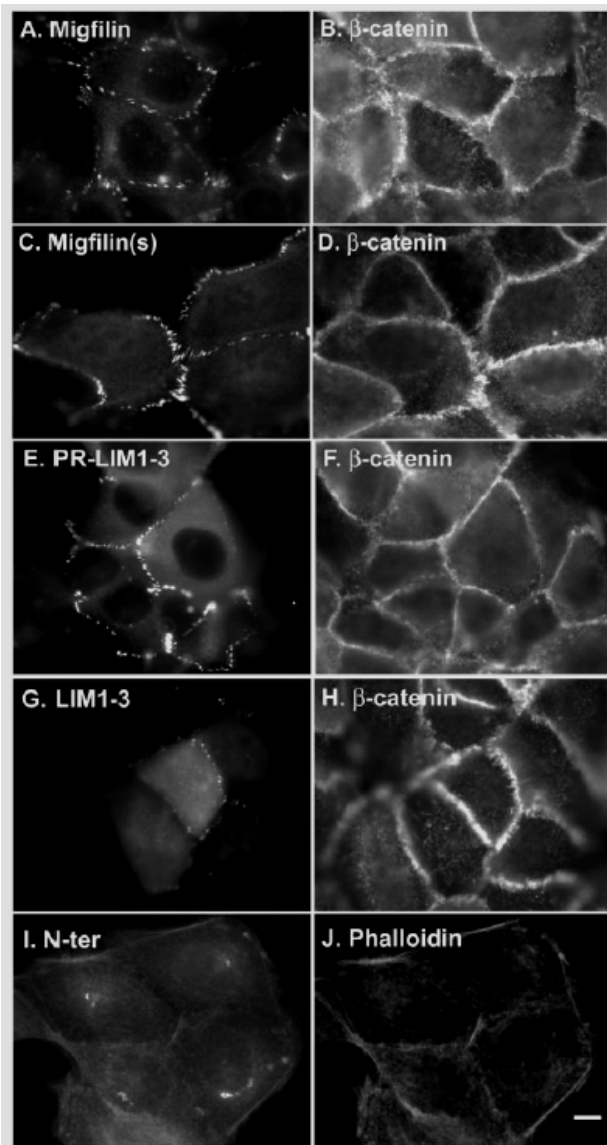
Figure 9. The C-terminal LIM domains, but not the N-terminal filamin-binding domain or the central proline-rich domain, mediate migfilin localization to adherens junctions. (A-D) The central proline-rich domain is not required for migfilin localization to cell-cell junctions. HaCat cells were transfected with expression vectors encoding GFPmigfilin (A and B) or GFP-migfilin(s) (C and D). The cells were stained with the rabbit anti-β-catenin primary antibody and Rhodamine RedTM-conjugated anti-rabbit IgG secondary antibody, and were observed under a Leica DM R fluorescence microscope equipped with GFP (A and C) or rhodamine (B and D) filters. (E-J) The C-terminal LIM domains, but not the N-terminal filamin-binding domain, are sufficient for mediating migfilin localization to adherens junctions. HaCat cells that were transiently transfected with expression vectors encoding GFP-PR-LIM1-3 (E and F), GFP-LIM1-3 (G and H) or GFP-N-ter (I and J) were stained with the anti-β-catenin antibody or phalloidin as indicated. Bar, 8 μm.

Analysis of the subcellular localization of the GFP-tagged migfilin mutants showed that GFP-PRLIM1-3 (Fig. 9E), like GFP-migfilin (Fig. 9A), was clustered at cell-cell junctions where abundant β-catenin was present (Fig. 9F), indicating that the N-terminal domain is not required for migfilin localization to cell-cell junctions. Clusters of GFP-LIM1-3 were also detected at β-catenin-rich adherens junctions (Fig. 9G, H), suggesting that the C-terminal LIM domains are sufficient for mediating migfilin localization to adherens junctions.

By contrast, the N-terminal fragment was not clustered at cell-cell junctions but instead it associated primarily with the actin ilaments (Fig. 9I, J). Taken together, these results suggest that the C-terminal LIM domains, but not the N-terminal domain, mediate migfilin localization to cell-cell junctions.

The LIM 2 domain is essential for migfilin clustering at cell-cell adhesions

To identify the LIM domain within the C-terminal region that is essential for mediating migfilin localization to cell-cell junctions, we introduced mutations into different migfilin LIM domains (Fig. 8B) and expressed the GFP-tagged migfilin mutants in HaCat cells (Fig. 8A, lanes 6-10). GFP-LIM1N, in which the first zinc finger in the LIM1 domain was deleted (Fig. 8B), was able to cluster at cell-cell junctions (Fig. 10A,B), suggesting that the first zinc finger of LIM1 domain is not absolutely required for migfilin clustering at these sites. Noticeably, GFP-LIM1N also accumulated in the nuclei (Fig. 10A).

However, substitution of C243 or C291 - which are crucial for the folding of the LIM2 domain (Fig. 8B) - with Gly eliminated the clustering of migfilin at cell-cell junctions, although they were still capable of associating with the actin filaments (Fig. 10C-F). Thus, the LIM2 domain is essential for migfilin clustering at cell-cell junctions.

We next analyzed the localization of migfilin or migfilin(s) mutants bearing a point mutation at C306, which is essential for the folding of the first zinc finger of LIM3 (Fig. 10B). The localization of migfilin(s) C306G point mutant (Fig. 8G, H, arrows) or that of migfilin C306G point mutant (not shown) to the β-catenin-containing cell-cell adhesions was compromised, suggesting that LIM3 also plays an important role in the recruitment of migfilin to

these sites. The C306G point mutants (Fig. 10G), like the C243G (Fig. 10C) and the C291G (Fig. 10E) mutants, efficiently associated with the actin filaments, which is reminiscent of that of migfilin N-terminal fragment (Fig. 9I). The migfilin(s) C306G point mutant (Fig. 10G), but not migfilin C306G point mutant that contains the proline-rich domain (Fig. 11K), was also detected in the nuclei.
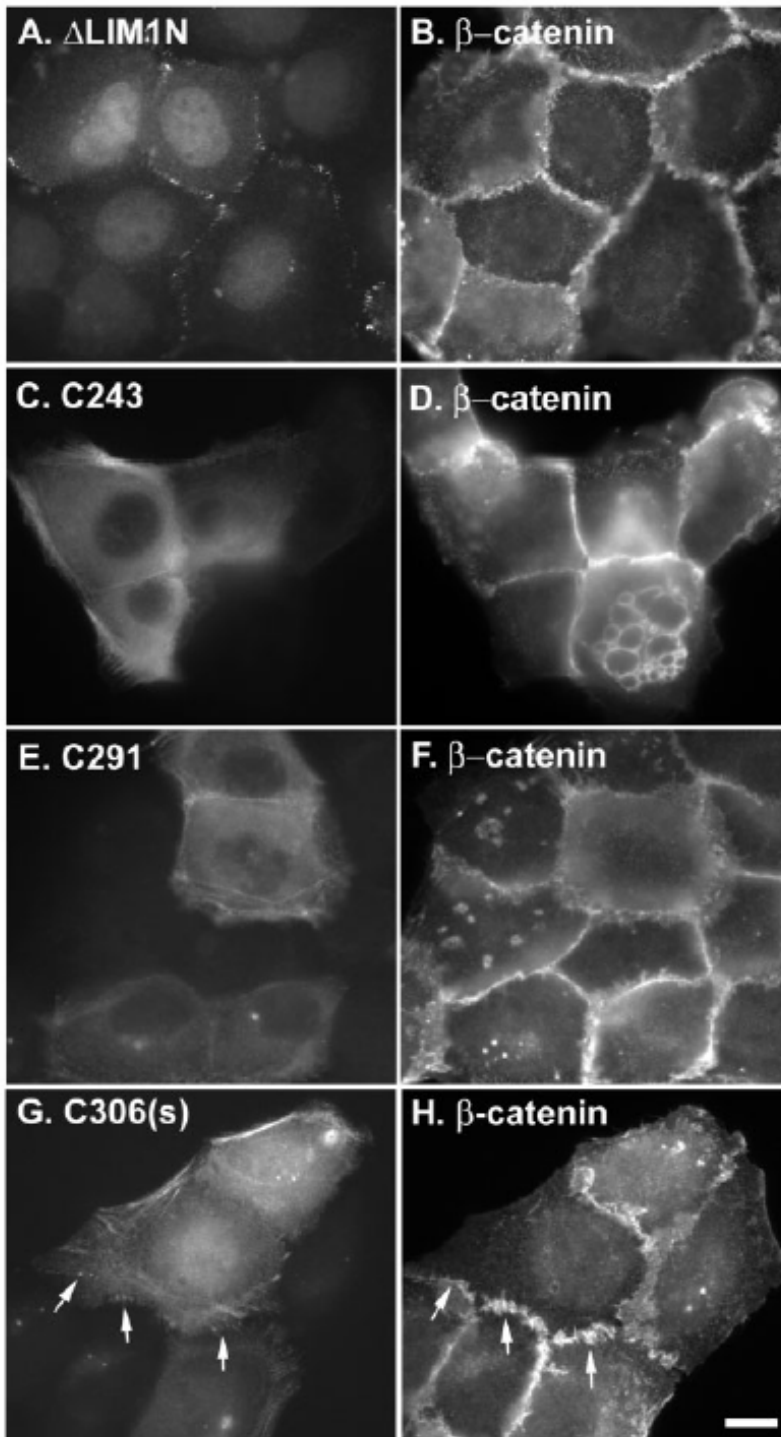
Figure 10. LIM2 is essential for migfilin localization to adherens junctions. HaCat cells were transfected with the expression vectors encoding GFP-LIM1N (A), GFP-C243 (C), GFP-C291 (E) and GFP-C306(s) (G). The cells were stained with the anti-β-catenin antibody as indicated (B, D, F and H). Notice that a small amount of GFP-tagged C306(s) mutant was detected in b-catenin-rich adherens junctions (G and H, arrows). Bar, 8 μm.

Mig-2 localizes to cell-ECM but not cell-cell adhesion

The finding that the C-terminal LIM domains, to which Mig-2 binds, mediate migfilin localization to cell-cell junctions prompted us to test whether Mig-2 also localizes to cell-cell junctions. To do this, we stained primary human keratinocytes with a monoclonal anti-Mig-2 antibody. The results showed that Mig-2 is clustered at cell-ECM adhesions (Fig. 11A, arrowheads) where actin filaments were anchored (Fig. 11B). Mig-2, however, was not clustered at junctions between the neighboring cells (Fig. 11A, arrow), suggesting that Mig-2 is not responsible for recruiting migfilin to cell-cell junctions.
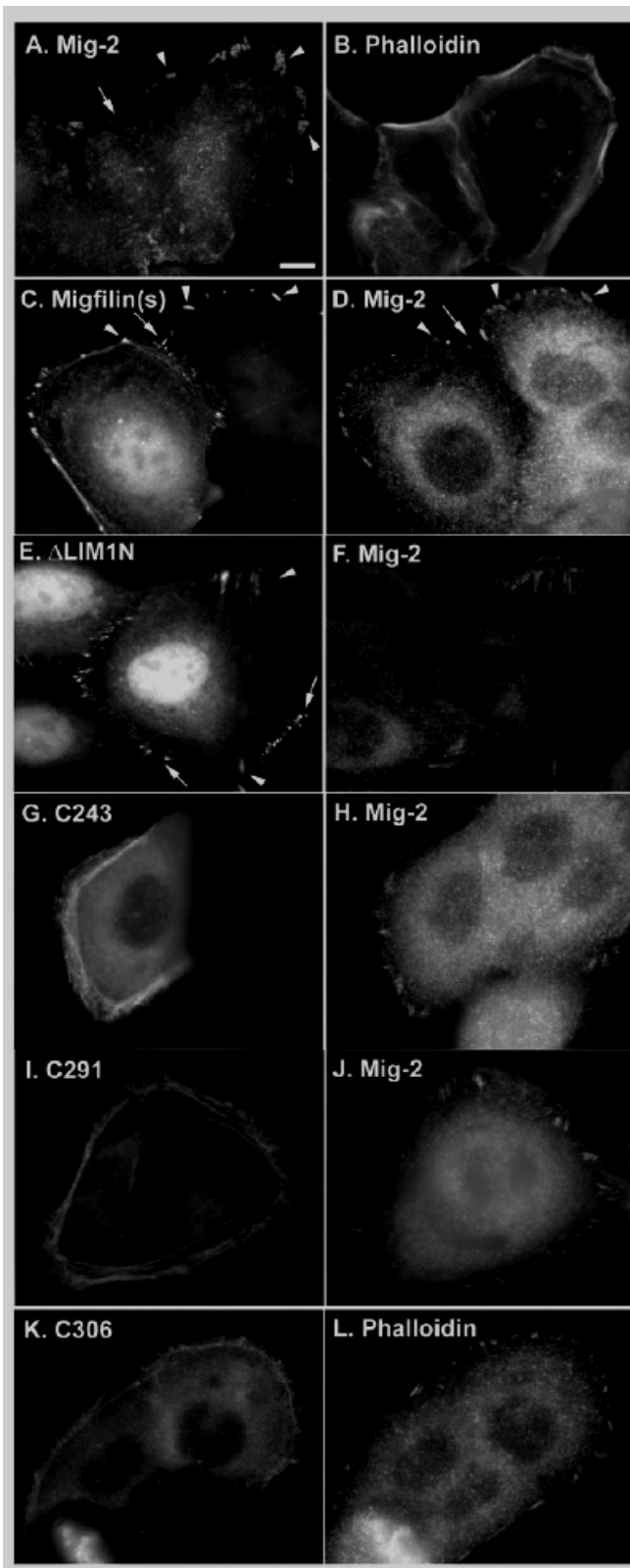
Figure 11. Effects of point mutations within the LIM domains on migfilin localization to cell-ECM adhesions. (A-D) Mig-2 localizes to cell-ECM but not cell-cell adhesions. Primary newborn human embryonic keratinocytes were double stained with mouse monoclonal anti-Mig-2 antibody 3A3 (A) and phalloidin (B). HaCat cells that were transiently transfected with the GFP-migfilin(s) vector (C) were stained with the mouse monoclonal anti-Mig-2 antibody (D). (E-L) HaCat cells that were transiently transfected with expression vectors encoding GFP-tagged migfilin mutants (as indicated) were stained with the mouse monoclonal anti-Mig-2 antibody (F, H, J and L). Bar, 8 μm.

30

Furthermore, these results suggest that the binding of Mig-2 to migfilin is insufficient for recruiting Mig-2 to cell-cell junctions. The LIM 2 and LIM3 domains, but not the LIM1 domain, are required for migfilin clustering at cell-ECM adhesions. We previously showed that the migfilin C-terminal region mediates its localization to cell-ECM adhesions (Tu et al., 2003). The specific LIM domains that are involved in the migfilin localization to cell-ECM adhesions, however, had not been determined.

To identify the site that mediates migfilin localization to cell-ECM adhesions, we transfected HaCat cells with expression vectors encoding the wild-type or mutant forms of migfilin (Fig. 8) and stained the transfectants with the monoclonal anti-Mig-2 antibody. The results showed that, as expected, GFP-migfilin(s) (Fig. 11C) and GFP-migfilin (not shown) localize to cell-cell adhesions as well as cell-ECM adhesions. In addition, abundant GFPmigfilin(s) was detected in the nuclei (Fig. 11C).

Consistent with the results obtained with primary keratinocytes (Fig. 11A), Mig-2 was co-clustered with migfilin in HaCat cells in cell-ECM adhesions but not cell-cell adhesions or the nuclei (Fig. 11D). GFP-LIM1N, which lacks the first zinc finger of the LIM1 domain, was clustered at cell-cell adhesions (Fig. 11E, arrows) as well as cell-ECM adhesions (Fig. 11E, arrowheads), where Mig-2 was detected (Fig. 11F), suggesting that the first zinc finger of migfilin LIM1 domain is not required for the cell-ECM adhesion localization. The C243 (Fig. 11G), C291 (Fig. 11I), C306 (Fig. 11K) or C306(s) (not shown) mutants, however, were not clustered at cell-ECM adhesions where abundant Mig-2 was detected, although they were associated with the actin filaments. Thus, LIM2 and LIM3, but not LIM1, are required for migfilin clustering at cell- ECM adhesions.

Depletion of migfilin compromises the organization of adherens junctions

We next tested whether migfilin is required for the proper organization of adherens junctions. Human HT-1080 fibrosarcoma cells were selected for these studies because (1) previous studies have shown that these cells form extensive β-catenin-containing adherens junctions (Chitaev and Troyanovsky, 1997; Sacco et al., 1995), (2) our preliminary studies have shown that migfilin is recruited to the β-catenin-containing adherens junctions in these cells (see

31

below) and (3) the level of migfilin in HT-1080 cells can be effectively reduced by RNA interference (see below).

To suppress the expression of migfilin, we transfected HT-1080 cells with an siRNA that specifically targets migfilin mRNA (Tu et al., 2003). Western blot analyses showed that the migfilin siRNA reduced the cellular level of migfilin by more than 50% (Fig. 12A, lanes 1 and 2). Equal loading was confirmed by probing the same samples with an anti-actin antibody (Fig. 12B, lanes 1 and 2).

Consistent with previous studies (Chitaev and Troyanovsky, 1997; Sacco et al., 1995), abundant β-catenin was detected in HT-1080 cells (Fig. 12C, lane 1). The level of β-catenin, unlike that of migfilin, was not reduced in the presence of the migfilin siRNA (Fig. 12C, lane 2), further confirming the equal loading and the specificity of the migfilin siRNA. Consistent with previous studies (Chitaev and Troyanovsky, 1997; Sacco et al., 1995), extensive β-catenin-containing adherens junctions were formed in HT-1080 cells that express a normal level of migfilin (Fig. 12D, F).

 Immunofluorescent staining of HT-1080 cells with a rabbit polyclonal anti- β-catenin antibody and a mouse monoclonal anti-migfilin antibody showed that, as expected, a substantial amount of migfilin was co-clustered with β-catenin at cell-cell junctions (Fig. 12, compare F and H). Noticeably, suppression of migfilin expression by RNA interference substantially impaired the organization of the β-catenin-containing adherens junctions (Fig. 12E, G, I), albeit the total cellular level of β–catenin was not reduced in these cells (Fig.12C).

Thus, migfilin is involved in the regulation of the organization of the β-catenin-containing adherens junctions but not the expression of β-catenin. Interestingly, migfilin-containing cell-ECM adhesions, unlike adherens junctions, were not eliminated in the migfilin siRNA transfectants under the experimental condition used, although they appeared somewhat smaller than those in the control cells (Fig. 12J, K).

A. Anti-migfilin **B. Anti-actin** **C. Anti-β-catenin**
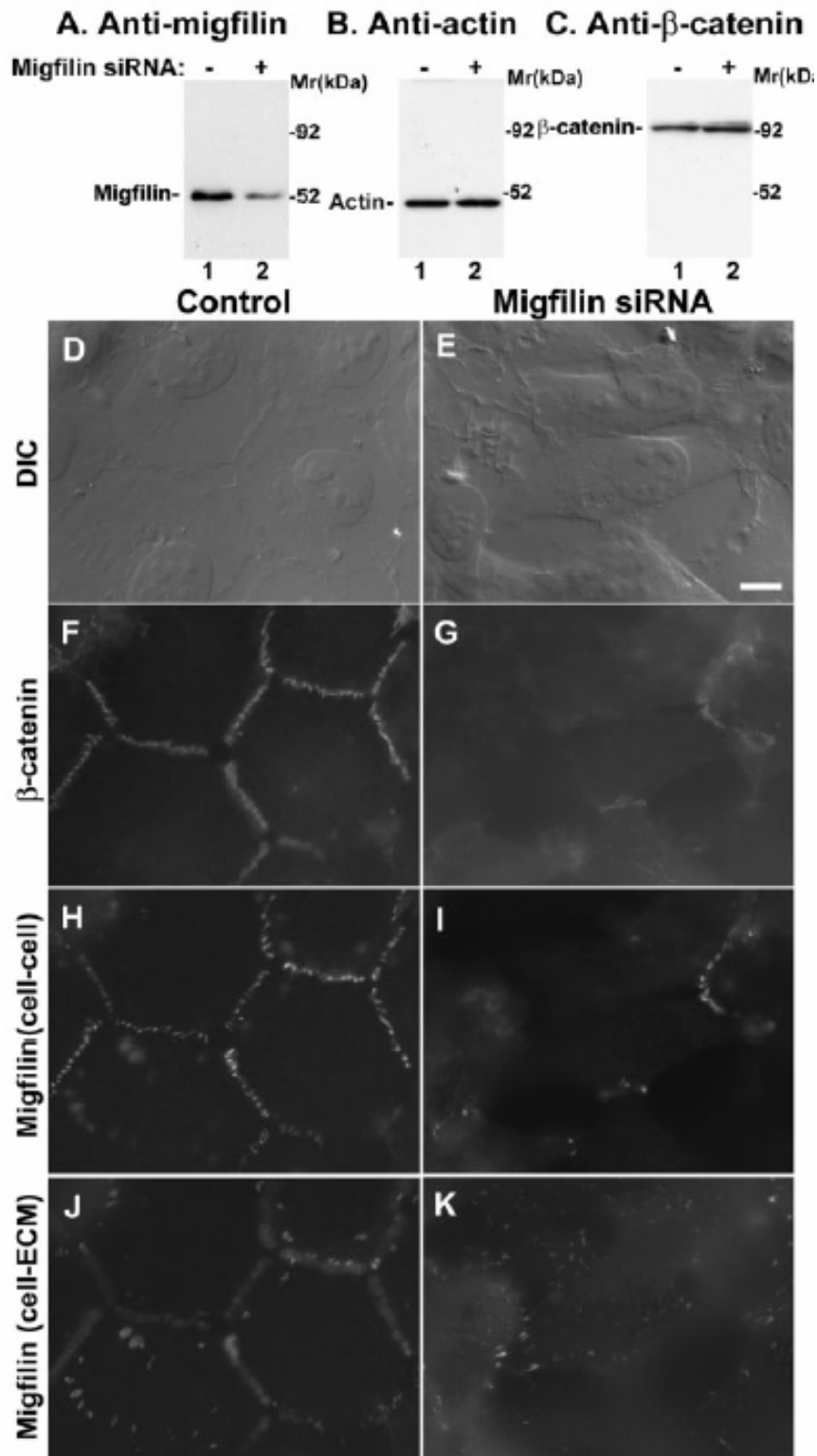
Figure 12. siRNA-mediated depletion of migfilin and its effect on β-catenin organization.

Human HT-1080 cells that were transfected with the migfilin siRNA (lane 2) or the control small RNA (lane 1) were analyzed by western blotting with monoclonal anti-migfilin antibody (clone 43) (A), monoclonal anti-actin antibody (B) or a polyclonal anti- β-catenin antibody (C). (D-K) HT-1080 cells transfected with the control RNA (D, F, H and J) or the migfilin siRNA (E, G, I and K) were double stained with mouse monoclonal anti-migfilin antibody (clone 43) (H-K) and rabbit-polyclonal anti- β- catenin antibody (F and G). The differential interference contrast (DIC) (D and E) and immunofluorescent (F-K) images were recorded using a Leica DM R fluorescence microscope equipped with a Hamamatsu ORCA-ER digital camera. Bar, 8 µm.

We next analyzed the effects of depletion of migfilin on F-actin and cadherin, another marker of cell-cell adhesions. To do this, we dually stained the cells with phalloidin and the monoclonal anti-migfilin antibody, or a rabbit polyclonal anti- β-catenin antibody and a mouse monoclonal anti-cadherin antibody. In control cells that express a normal level of migfilin, abundant F-actin was detected at cell-cell junctions where a substantial fraction was associated with clusters of migfilin (Fig. 13D, F, H).Furthermore, as expected, β-catenin and cadherin are co-clustered at cell-cell junctions(Fig. 13J, L, N).

By contrast, in migfilin siRNA transfectants that express a reduced level of migfilin, the actin cytoskeleton was disorganized (Fig. 13, compare H and I) and β-catenin and cadherin distributed rather diffusely in the cells (Fig. 13K, M, O). In parallel experiments, western blotting analyses showed that the cellular cadherin level (Fig. 13C, lanes 1 and 2), like that of β-catenin (Fig.12C, lanes 1 and 2), was not significantly reduced in migfilin siRNA transfectants in which the expression of migfilin was suppressed (Fig. 13A, lanes 1 and 2). Taken together, these results suggest that migfilin is crucially involved in the proper organization of adherens junctions.

To further assess the function of migfilin in cell-cell adhesion, we analyzed the parental HT-1080 cells, the control RNA transfectants and the migfilin siRNA transfectants using a cell dissociation assay. To do this, the cells were detached from culture plates with a rubber policeman and passed through Pasteur pipettes ten times. The majority of the migfilin siRNA transfectants, which expressed a reduced level of migfilin (Fig. 14A, lane 3), were dissociated from each other after pipetting (Fig. 14,C, F).

By contrast, under identical experimental conditions, significantly higher percentages of the control cells (i.e. the parental HT-1080 cells and the control RNA transfectants) that express a normal level of migfilin (Fig.14A, lanes 1 and 2) remained associated with each other (Fig.14D, E, F). Thus, consistent with the disorganization of β–catenin and cadherin (Fig. 13), depletion of migfilin weakened the cell-cell association.
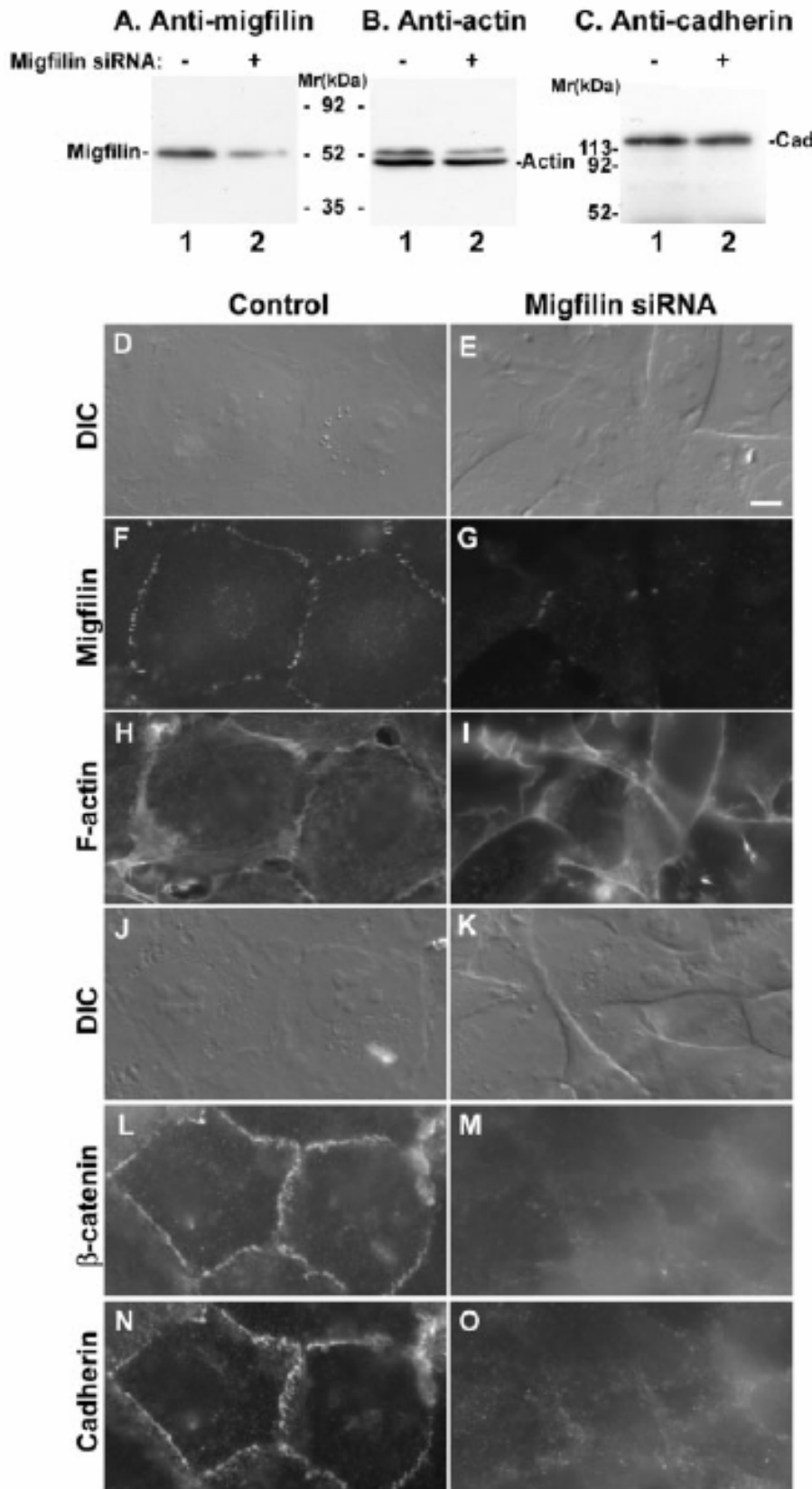
Figure 13. Depletion of migfilin compromises the organization of adherens junctions. Human HT-1080 cells that were transfected with the migfilin siRNA (lane 2) or the control small RNA (lane 1) were analyzed by western blotting with monoclonal anti-migfilin antibody (clone 43) (A) or an anti-cadherin antibody (C). Equal loading was confirmed by re-probing the migfilin membrane (A) with a monoclonal anti-actin antibody (B). (D-I) HT-1080 cells transfected with the control RNA (D, F and H) or the migfilin siRNA (E, G and I) were double stained with the mouse monoclonal anti-migfilin antibody (clone 43) (F and G) and Rhodamine-conjugated phalloidin (H and I). The mouse anti-migfilin primary antibody was detected with a FITC-conjugated anti-mouse IgG secondary antibody. (J-O) HT-1080 cells transfected with the control RNA (J, L and N) or the migfilin siRNA (K, M and O) were double stained with a rabbit polyclonal anti-β-catenin antibody (L and M) and a mouse monoclonal anti-cadherin antibody (clone CH-19) (N and O). The DIC (D, E, J and K) and immunofluorescent (F-I and L-O) images were recorded as described in Fig.10. Bar, 8 μm.
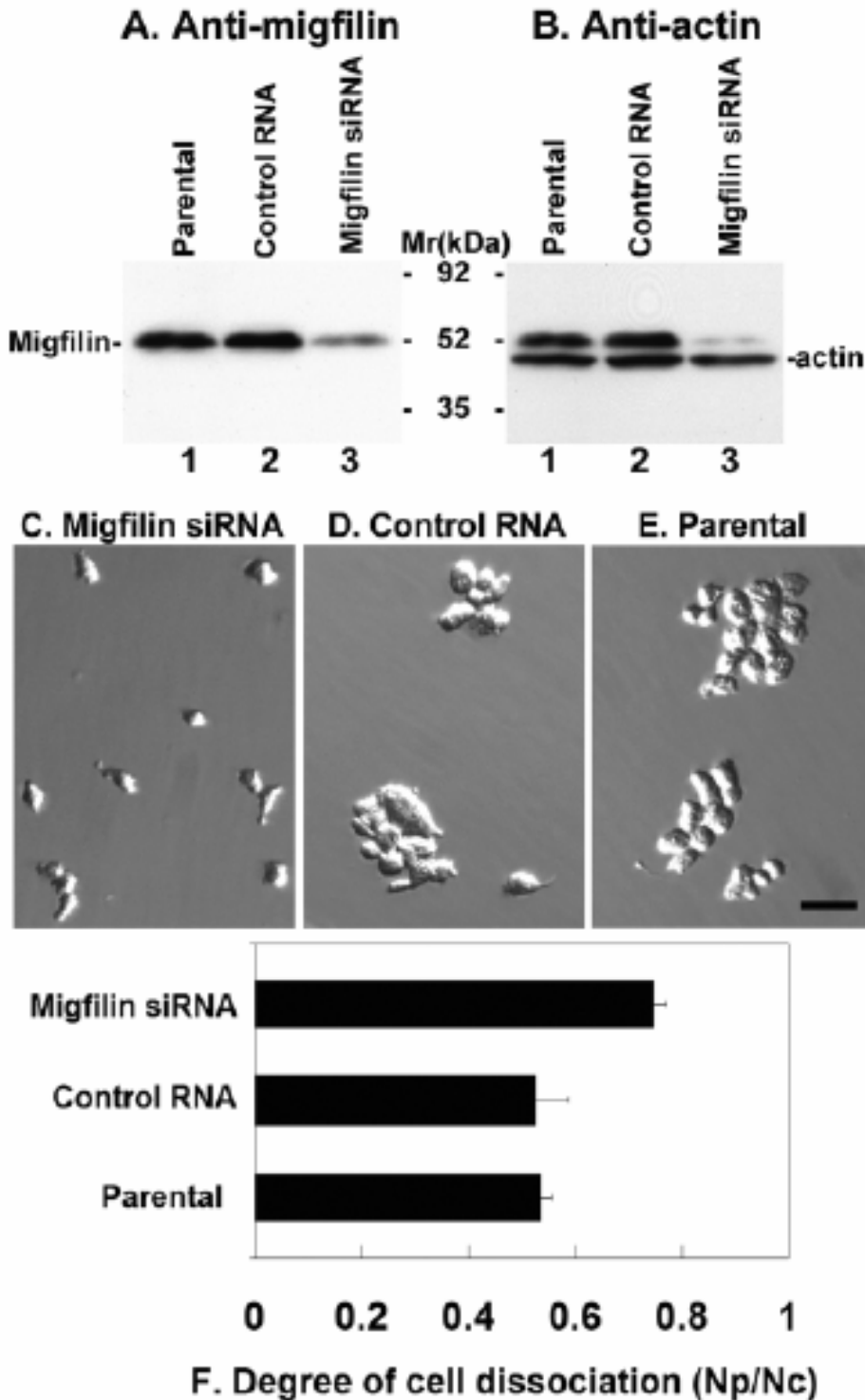
Figure 14. Depletion of migfilin weakens the cell-cell association. (A,B) The parental HT-1080 cells (lane 1) and HT1080 cells that were transfected with the control small RNA (lane 2) or the migfilin siRNA (lane 3) were analyzed by western blotting with the monoclonal anti-migfilin antibody (A). Equal loading was confirmed by re-probing the membrane with an anti-actin antibody (B). (C-F) Cell dissociation. The migfilin siRNA transfectants (C), control RNA transfectants (D) and the parental HT-1080 cells (E) were detached from culture plates, passed through Pasteur pipettes ten times and observed under an Olympus IX70 inverted microscope. Bar in E, 100 μm. The degree of cell dissociation (the number of particles (Np)/the number of total cells (Nc)) was calculated by analyzing at least 500 cells from each sample (F). Bars in F represent means + s.d. from two independent experiments.

2.4   DISCUSSION

Cell-cell junctions are highly specialized subcellular structures that are essential for epithelial and endothelial tissue formation and communication between neighboring cells. The studies presented in this paper have identified a new component of cell-cell junctions. Migfilin was identified and cloned based on its interaction with Mig-2, an important component of cell-ECM adhesions (Tu et al., 2003). In adherent cells lacking cell-cell junctions, migfilin is largely co-localized with Mig-2 at cell-ECM adhesions (Tu et al., 2003).

Using a combination of biochemical, cell biological, immunofluorescence and immunoelectron microscopic approaches, we have now shown that in epithelial as well as endothelial cells, migfilin localizes not only to cell-ECM adhesions but also to cell-cell junctions. In addition to showing that migfilin is a component of cell-cell junctions, we have characterized, both temporally and spatially, the localization of migfilin to cell-cell junctions. Migfilin localizes to cell-cell junctions soon after calciuminduced clustering of cadherin-â-catenin complex at these sites, suggesting that the localization of migfilin to cell-cell junctions is probably triggered by the presence of cadherin-β- catenin complex at these sites. Importantly, immunoelectron microscopic analyses have shown that migfilin is co-clustered with β-catenin at cell-cell junctions.

These findings raise an interesting possibility that migfilin binds to β-catenin or other components of the cadherin- β-catenin complex at adherens junctions, resulting in the formation of a supramolecular complex containing migfilin, β-catenin and other components of adherens junctions.

Using an siRNA-mediated knockdown approach, we have found that migfilin is functionally indispensable for proper organization of adherens junctions. It is worth noting that whereas the migfilin- and β-catenin-containing adherens junctions were largely eliminated in HT-1080 cells in which the expression of migfilin is suppressed, a substantial number of migfilin-containing cell-ECM adhesions were detected in the cells that lacked migfilin- and β-catenin-containing adherens junctions. These results suggest that the dynamics of these two

migfilin-containing adhesion structures (i.e. cell-cell and cell-ECM adhesions) are probably different. Migfilin in the cell-cell adhesions probably has a faster turnover rate than that in cell-ECM adhesions and therefore inhibition of migfilin synthesis by RNA interference resulted in a more dramatic down-regulation of migfilin at cell-cell adhesions and consequently the loss of adherens junctions. The loss of adherens junctions induced by the preferential elimination of migfilin at cell-cell adhesions in response to siRNA-mediated suppression of migfilin expression strongly suggests a direct role of migfilin in the organization or maintenance of the cell-cell adhesion structure. Consistent with this, siRNA-mediated depletion of migfilin significantly weakened the association of HT-1080 cells.

How does migfilin contribute to the organization or maintenance of adherens junctions? One characteristic of the migfilin-containing cell-cell adhesion structure is that it is highly resistant to detergent extraction, probably because of its cross-linking with filamentous actin at the adhesion sites (Fig. 5). Migfilin interacts with two important actin-binding proteins, VASP (Zhang et. al., 2006) and filamin (Tu et al., 2003; Takafuta et al., 2003). VASP, which binds to the central proline-rich domain of migfilin, is known to localize to adherens junctions (Grevengoed et al., 2002; Vasioukhin et al., 2000). However, VASP is unlikely to be responsible for recruiting migfilin to adherens junctions, as migfilin(s), which lacks the VASP-binding domain, also localizes to adherens junctions. Although VASP is unlikely to be functioning in mediating migfilin localization to adherens junction, it is possible that migfilin, through its interaction with VASP, functions in recruiting VASP to adherens junctions. Given the importance of VASP in the assembly and functions of epithelia (Comerford et al., 2002; Grevengoed et al., 2002; Lawrence et al., 2002; Vasioukhin et al., 2000), it will be interesting to test in future studies whether migfilin plays such a role.

Migfilin, through its N-terminal domain, binds to filamin (Tu et al., 2003; Takafuta et al., 2003). The interaction of migfilin with filamin is probably responsible for the tight association of migfilin with actin filaments, as a migfilin fragment containing the filamin-binding N-terminal domain but lacking the central proline-rich domain and the C-terminal LIM domains stably associates with actin filaments in cells (Fig.9I, J). Filamin cross-links actin filaments and is known to be crucial for the organization of the actin cytoskeleton (reviewed by Stossel et al.,

2001; van der Flier and Sonnenberg, 2001). Additionally, filamin binds to Cdc42, Rac, Rho and guanine nucleotide exchange factors that regulate the small GTPases (Bellanger et al., 2000; Ohta et al., 1999) and their effectors such as p21-activated kinase (PAK) (Vadlamudi et al., 2002) and Rho-kinase (ROCK) (Ueda et al., 2003). There is strong evidence now for a crucial role of actin polymerization and their regulators such as Cdc42 and Rac in the assembly as well as the signaling of cell-cell adhesions (reviewed by Adams and Nelson, 1998; Braga, 2002; Jamora and Fuchs, 2002; Perez-Moreno et al., 2003). It is likely that the interaction of migfilin with filamin contributes to the organization, maintenance or signaling of the intercellular adhesions.

Thus, the identification of migfilin as a functionally important component of adherens junctions and its characterization described in this paper shall facilitate future studies aimed at fully understanding the organization and signaling of this important adhesion structure.

In the present study, we have also identified the determinants that control migfilin localization to cell-cell and cell-ECM adhesions, two functionally coordinated but structurally distinct adhesion structures. Both LIM2 and LIM3 are crucially involved in the localization of migfilin to cell-cell and cell-ECM adhesions, whereas LIM1 (at least the first zinc finger of LIM1) is not required for migfilin localization to either adhesion site.

These results suggest that the sites that control the distribution of migfilin to cell-cell and cell-ECM adhesions are largely overlapping. Importantly, Mig-2, which recruits migfilin to cell-ECM adhesions, is present exclusively in cell-ECM adhesions (Fig. 11). Thus, it is attractive to propose a model in which Mig-2 competes with the components of adherens junction for interacting with migfilin. In cells with both cell-cell and cell-ECM adhesions, there exist at least two pools of migfilin. One pool of migfilin binds to Mig-2, which results in the recruitment of migfilin to cell-ECM adhesions, whereas the second pool of migfilin associates with components of adherens junction and therefore is recruited to cell-cell adhesions. Thus, an elevation of the Mig-2 level could translate into upregulation of migfilin localization to cell-ECM adhesions and concomitantly downregulation of migfilin localization to cell-cell junctions. The coupling or 'cross-talking' between cell-cell and cell- ECM adhesions is crucial for several biological and

39

pathological processes including epithelial-mesenchymal transition, wound healing, and carcinoma invasion. The 'competition' model of migfilin localization to cell-cell and cell-ECM adhesions could provide a potential mechanism by which cells coordinately regulate the assembly or signaling of cell-cell and cell-ECM adhesions.

3.0   THE ROLE OF RAS SUPPRESSOR-1 IN CELL SPREADING AND ADHESION

3.1   INTRODUCTION

Cell-ECM interactions are crucial for a number of essential cell functions.   Thus, a better understanding of the molecular mechanisms involved is essential.

Ras-suppressor-1 (RSU-1), a potent inhibitor of Ras-induced transformation(Masuelli and Cutler, 1996), has been recently shown to interact with PINCH at cell-ECM adhesion sites both in Drosophila (Kadrmas et al., 2004) and in mammalian cells(Dougherty et al., 2005).   In Drosophila, PINCH and RSU-1 together regulate the dorsal closure during Drosophila development(Kadrmas et al., 2004), while in mammalian cells RSU-1 binds to PINCH and regulates cell adhesion(Dougherty et al., 2005).

Intrigued by the fact that RSU-1 is strongly associated with PINCH, we wondered whether RSU-1 affects other PINCH-related functions as well.   Therefore, we employed two different approaches in order to shed more light upon the role of RSU-1 in adhesion-related cell functions;   first we knocked-down RSU-1 in HeLa cells and in parallel we used the overexpression approach.

Our results show that RSU-1 is involved in the regulation of cell spreading which is a function in which PINCH is also critically involved.   Interestingly however, RSU-1 does not affect cell survival as opposed to PINCH, depletion of which induces apoptosis(Fukuda et al., 2003a; Tu et al., 1999b; Wu, 1999).   Our results also demonstrate a connection of RSU-1 to the Rac activation but further studies are needed in order to further decipher the mechanism involved.

3.2   MATERIALS AND METHODS

Cell culture

HeLa cells were used for all the assays in the present study. Cells were cultured in DMEM medium (CellGro) supplemented with 10%FBS, 1%Glutamax and 1%Pennicilin/Strepromycin.

Cell spreading

Cell spreading was performed in HeLa cells plated on 30μg/ml collagen I, as described previously (Tu et al., 2003).

Caspase 3 activity assay

Apoptosis was assessed by caspase-3 activity measurement using the fluorogenic caspase-3 substrate VII (Ac-DEVD-aminofluoromethylcoumarin) from Calbiochem (San Diego, CA) following the company's protocol.

RNA interference

HeLa cells were transfected with two different siRNAs against RSU-1 using Lipofectamine 2000 from Invitrogen according to the company's guidelines. The sequence of the first siRNA against RSU-1 is as follows: UUA AAU CCA AGU UUC CUA GUU CUG G and CCA GAA CUA GGA AAC UUG GAU UUA A, while the sequence of the second siRNA is: AGA GGU AUU UGU AUG UCU CAG AAC G and CGU UCU GAG ACA UAC AAA UAC CUC U.

DNA transfections

All DNA transfections were performed using Lipofectamine 2000 from Invitrogen according to the protocol recommended by the company.

Immunoprecipitation and western blotting analysis

The immunoprecipitation and western blot analysis was performed as previously described(Tu, 2003).

Rac activation assay

HeLa cells were transfected with siRNA against RSU-1 or with Flag-tagged RSU-1 or Flag vector using Lipofectamine 2000 (Invitrogen), as indicated. Forty eight hours after transfection, cells were harvested and then plated in 60-mm dishes pre-coated with collagen I, and incubated at 37 °C for 10 min. Activated Rac was detected using a Rac activation assay kit (Cytoskeleton, Inc., Denver, CO) following the manufacturer's protocol, as described previously (Zhang et al, 2004).

3.3   RESULTS

RSU-1 binds to PINCH in HeLa cells

Ras suppressor-1 (RSU-1) has been recently shown to interact with PINCH both *in vivo* and *in vitro*, participating in several cell adhesion processes(Dougherty et al., 2005; Kadrmas et al., 2004). In order to confirm the binding between RSU-1 and PINCH in HeLa cells as well, we transfected the cells with Flag-RSU-1 and subsequently performed an immunoprecipitation with anti-Flag antibody. As shown in Figure 15 a strong binding is detected between RSU-1 and PINCH.
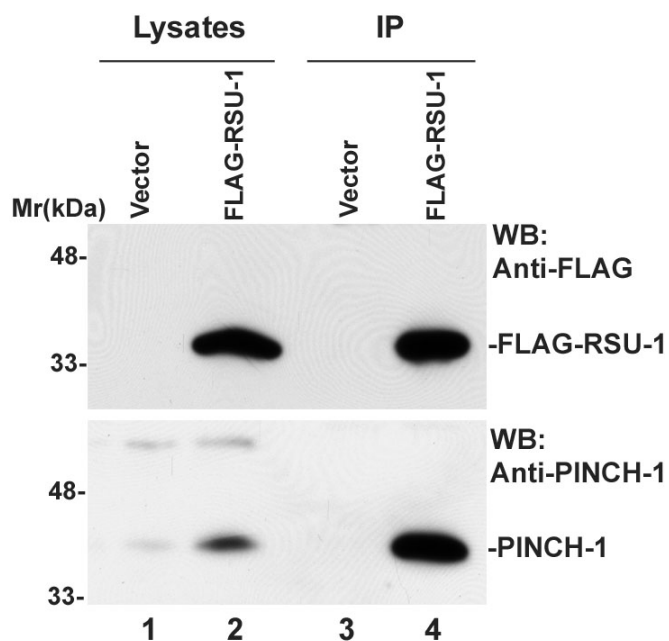
Figure 15. RSU-1 binds to PINCH in HeLa cells. HeLa cells were transfected with either a Flag vector or Flag-tagged RSU-1. Cells were then subject to immunoprecipitation and PINCH was detected in the immunoprecipitants.

Since PINCH is known to associate with ILK and parvin and form a well-characterized stable ternary complex at the cell-ECM adhesion sites(Zhang et al., 2002c), we wondered whether RSU-1 also associates with the whole PINCH-ILK-parvin complex at the cell-ECM adhesions. To test that, we performed an immunoprecipation in HeLa cells using an anti- α-parvin antibody. When α-parvin is precipitated, PINCH and ILK are found to be co-immunoprecipitated with α-parvin, as expected. Interestingly, RSU-1 is also immunoprecipitated with α-parvin, showing that RSU-1 is associated with the PINCH-ILK-parvin complex (Figure 16).
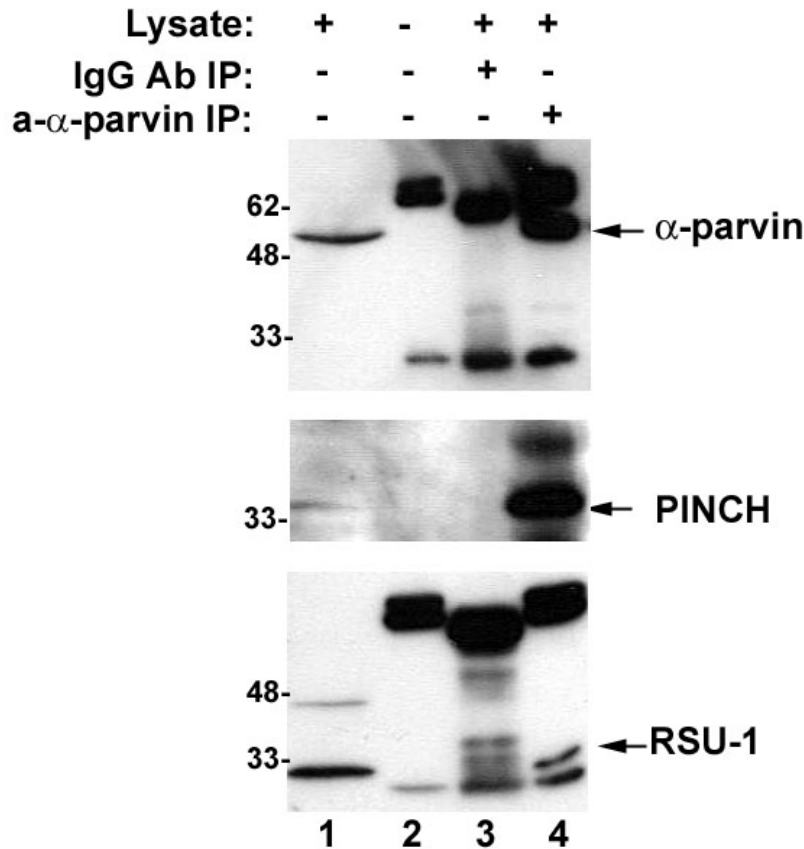
Figure 16. RSU-1 is immunoprecipitated with α-parvin in HeLa cells. HeLa cells were subject to immunoprecipitation with anti-α-parvin antibody and PINCH-1 and RSU-1 were detected by western blotting in the immunoprecipitated samples.

RSU-1 depletion from HeLa cells has no effect on cell survival but increases cell spreading and inhibits cell adhesion

In order to shed more light upon the role of RSU-1 in the cell, we used the RNA interference approach to deplete RSU-1 from HeLa cells. For that purpose two different siRNAs were used. As shown in Figure 17A, RSU-1 was efficiently inhibited. Inhibition of RSU-1 however, did not affect cell survival as shown by caspase 3 activity measurements (Figure 17B). Interestingly, however, RSU-1 inhibition led to an increase in cell spreading (Figure 17C) and a concurrent decrease in cell adhesion (Figure 17D).
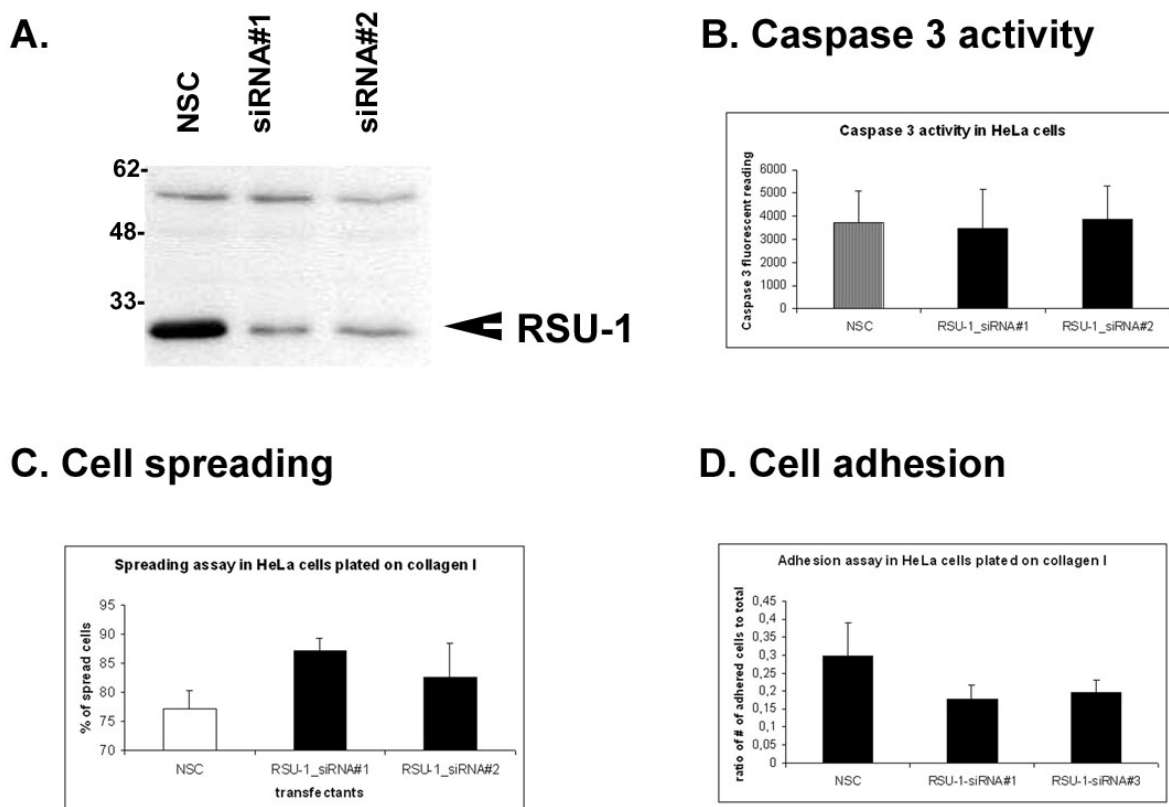
Figure 17. Effects of RSU-1 depletion in different cellular functions. A) Western blot showing that RSU-1 expression is dramatically inhibited by two different siRNA sequences. Note that the top non-specific band is equal in all lanes indicating equal loading. B) Caspase 3 activity in HeLa cells transfected with a non-specific control (NSC) siRNA or the two siRNA against RSU-1. C) Cell spreading in HeLa cells plated on 30µg/ml collagen I. D) Cell adhesion in HeLa cells also plated on 30µg/ml collagen I.

RSU-1 overexpression leads to decreased cell spreading and Rac activity

To further understand the role of RSU-1 in the cell, we employed the overexpression approach. Flag-tagged RSU-1 was efficiently overexpressed in HeLa cells (Figure 18A, bottom panel) and as with the knocking-down approach, cell survival was not affected by the Flag-RSU-1 overexpression (Figure 18C). Interestingly however, Flag-RSU-1 overexpression led to decreased cell spreading which is consistent with the increase in cell spreading induced by the depletion of RSU-1 (Figure 18B). To further test this effect on cell spreading, HeLa cells were tested for Rac activity which, as shown in Figure 18A, exhibited dramatic decrease in the cells that overexpressed Flag-RSU-1 as compared to the vector control (Figure 4A, compare Rac activity in the Rac pull down sample of the RSU-1 overexpressing cells to the control and in relation to the input in the lysate samples).
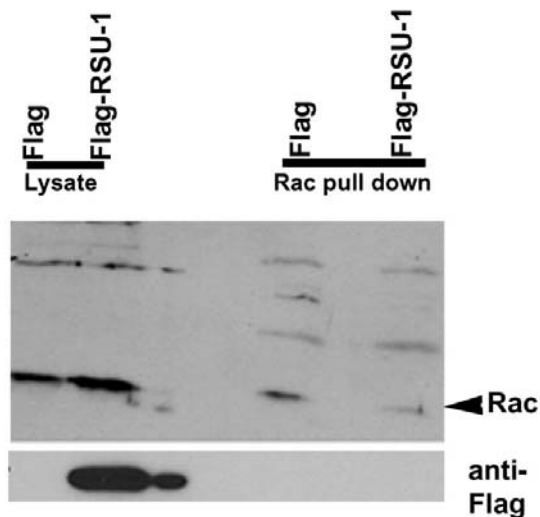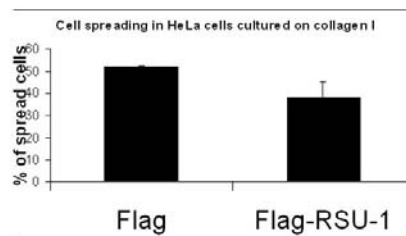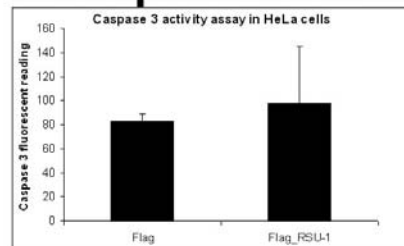
Figure 18. RSU-1 overexpression leads to decreased cell spreading and Rac activity and has no effect on apoptosis. A) Western blot of the Rac activation assay showing Rac decrease and the efficiency of RSU-1 overexpression. B) Cell spreading in HeLa cells plated on collagen I. C) Caspase 3 activity in HeLa cells overexpressing Flag, or Flag-RSU-1.

3.4   DISCUSSION

RSU-1 has been recently shown to bind to PINCH and function in regulating cell adhesion (Dougherty et al., 2005). Consistent with this finding, our study shows that inhibition of RSU-1 indeed leads to decreased cell adhesion. Interestingly, however, we also show that RSU-1 regulates cell spreading. More specifically, RSU-1 depletion induces an increase in cell spreading while RSU-1 overexression inhibits cell spreading. Furthermore, overexpression of RSU-1 inhibits Rac activation which may provide a mechanism to explain the decrease in cell spreading. Although there is an apparent connection between RSU-1, cell adhesion, and cell spreading, more research is required in order to decipher the exact mechanism by which RSU-1 regulates those processes and the extent in which PINCH is involved in this regulation.

Moreover, it is worth noting that although RSU-1 binds strongly to PINCH, which is essential for cell survival, RSU-1 itself does not seem to be directly involved in regulating this process since neither inhibition nor overexpression of RSU-1 induces cell death.

4.0 **PART II: INTRODUCTION TO LIVER BIOLOGY**

4.1 **LIVER ARCHITECTURE AND FUNCTION**

Liver is the second largest organ of the body after skin and it is considered as the "biochemical factory of the body" since most of the body's metabolic activities take place in the liver. Therefore, it is not surprising that the liver is one of the most complex organs of the body. To stress the importance of liver for the organism suffices to say that when more than 80% of liver function ceases, every other organ system of the body fails.

The liver parenchyma is organized in lobules which are hexagonal and consist of **portal triads** surrounding a central vein (Figure 19). Hepatocytes, the parechymal cells of the liver, are organized in plates around the portal triads. As shown in Figure 20, each portal triad consists of the following three vessels:

a) the **portal vein**, which brings to the liver blood enriched with nutrients from the intestines

b) the **hepatic artery**, which brings to the liver oxygenated blood from the lungs

c) the **bile duct**, which brings bile from the bile canaliculi of the liver to the main extrahepatic biliary duct.
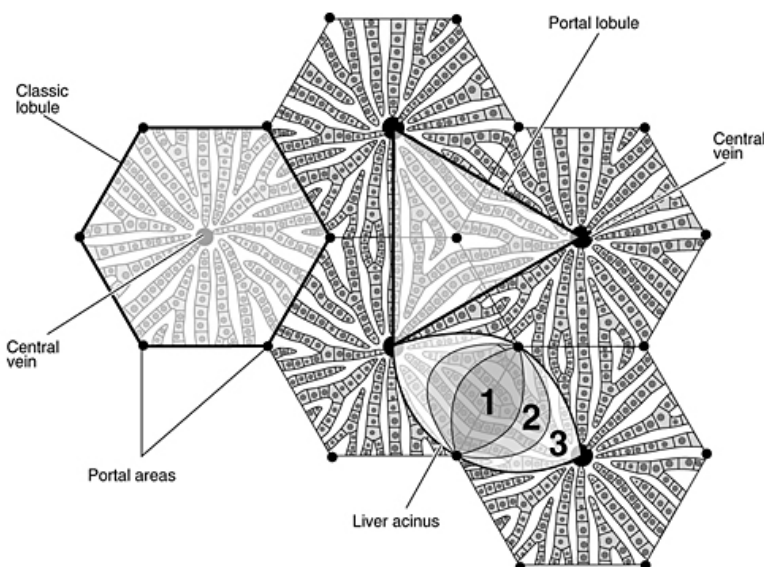
Figure 19. Lobular architecture of the liver. Schematic representation of portal triads surrounding a central vein in each lobule of the liver.

.

Figure 20. Liver architecture. Schematic representation of a portal triad around a central vein. The portal triad consists of a bile duct, a branch of the hepatic artery and a branch of the portal vein.
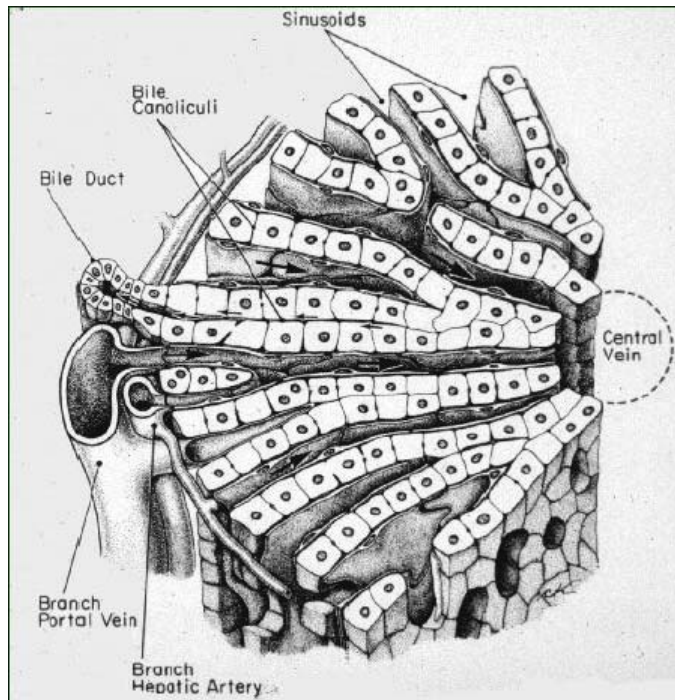
Thus, blood comes to the liver from two different sources; from the intestines through the portal vein, and from the lungs through the hepatic artery, while blood leaves the liver through the hepatic vein. In the meantime, blood from the portal vein and hepatic artery perfuses through the liver sinusoids between hepatocytes (see Figure 20), from the portal triads at the periphery to the central vein in the middle of the lobule (Figures 19 and 20).

The main synthetic functions that are performed by the liver are as follows:

❖ Production of albumin and coagulation proteins to facilitate the process of blood clotting.
❖ Production of bile. Bile produced by hepatocytes is secreted into the bile canaliculi which are connected to a network of intra-hepatic bile ducts, and through the bile canaliculi is transferred and stored in the gallbladder. From the gallbladder, bile is secreted to the intestines through the cystic and common bile ducts. The sectretion of bile facilitates the digestion of food by helping in the absorption of lipids and vitamins.

49

❖ Regulation of blood glucose by converting the excess glucose into glycogen for storage that can be again converted to glucose when needed. The liver also regulates lipids by producing cholesterol which in turn helps in carrying fats from the body.

❖ Storage of Vitamin A, D, B12 and iron.

❖ Detoxification of blood from toxins that originate from the food or drugs by filtering and breaking down the toxic substances in simpler compounds that can be used safely by the body.

4.2   LIVER CELL TYPES

Hepatocytes are the parenchymal cells of the liver that account for 80% of the cell population in the liver and carry out the major liver functions. They are large and exagonally-shaped and are arranged in plates with orientation from the portal triad to the central vein. The plates are separated by sinusoidal capillaries (see Figure 19 and 20) which are lined by endothelial cells.

Apart from the hepatocytes, liver also consists of non-parenchymal cells which include 4 different categories of cell types (Michalopoulos and DeFrances, 1997):

1. **stellate cells or Ito cells:** they store fat, and vitamin A and produce connective tissue as well as certain growth factors such as Hepatocyte Growth Factor (HGF), Transforming Growth Factor $\beta1$ (TGF$\beta1$).

2. **Kupffer cells:** the macrophages of the liver, which destroy microbes and foreign substances by phagocytosis.

3. **biliary epithelial cells or cholangiocytes:** they are the cells that line the bile ducts where bile is being transferred.

4. **sinusoidal endothelial cells:** they are the cells that line the blood vessels and have characteristic windows called fenestrae which allow maximal contact between hepatocytes and blood.

Since liver performs such important functions for the homeostasis of the whole body, it is essential to learn more about hepatocyte biology and the mechanisms governing fundamental processes such as hepatocyte differentiation and survival.

5.0 INTEGRIN-LINKED KINASE (ILK) IS INVOLVED IN MATRIX INDUCED HEPATOCYTE DIFFERENTIATION

5.1 INTRODUCTION

Hepatocytes, the parenchymal cells of the liver, have restricted proliferative capacity when maintained in culture and they de-differentiate over time losing both their hepatocyte-specific gene expression patterns and their characteristic cellular micro-architecture. Interestingly, addition of hydrated complex matrix preparations (Matrigel: a matrix extract from Engelbreth-Holm-Swarm (EHS) mouse sarcomas or Type I Collagen Gels)(Kleinman, 1986) over de-differentiated hepatocytes restores differentiation within three days(Block et al., 1996b; Kim et al., 1998). This highlights the importance of matrix for hepatocyte differentiation and normal function.

Signals from the extracellular matrix (ECM) are transmitted to the cells through integrins. Integrins in turn associate with a number of integrin-proximal proteins and, through those interactions, signals are transduced to actin cytoskeleton or the nucleus, thus enabling the cell to respond properly to environmental changes and signals(Hynes, 2002).

Integrin-Linked Kinase (ILK) is an important component of cell-matrix adhesions that has been shown to be critically involved in many fundamental cellular processes such as survival, and differentiation (Hannigan et al., 2005; Huang et al., 2000; Legate et al., 2006; Li et al., 2003; Terpstra et al., 2003; Wu, 2005). Furthermore, ILK overexpression has been associated with anchorage-independent growth, suppression of anoikis, and oncogenic transformation in general (Attwell et al., 2000a; Hannigan et al., 1996a; Persad and Dedhar, 2003; Radeva et al., 1997).

51

ILK can function as an adaptor protein in the cell and is capable of mediating several protein-protein interactions with other cell-ECM adhesion proteins. For instance, ILK interacts with the β1 and β3 subunits of integrin(Hannigan et al., 1996a), thus linking the ECM signaling to the intracellular compartment of the cell. Moreover, ILK has been shown to bind to PINCH and α-parvin, which are also focal adhesion proteins, forming a stable ternary complex at the cell-ECM adhesions sites(Sepulveda et al., 2005; Wu, 2004b). In fact, the PINCH-ILK-parvin complex is pre-formed and recruited to the cell-ECM adhesion sites as a complex(Zhang et al., 2002b), and it has been implicated in several crucial cellular processes. Furthermore, each one of the components of the complex has been shown to be crucial for cell survival(Fukuda et al., 2003a; Fukuda et al., 2003b), and cell spreading. Interestingly, α-parvin is directly connected to actin thus linking the whole PINCH-ILK-parvin complex with the cytoskeleton(Wu and Dedhar, 2001b). ILK is also capable of binding to another focal adhesion protein termed Mitogen-inducible gene 2 (Mig-2) (Mackinnon et al., 2002a), which is important for the regulation of cell shape and spreading (Tu et al., 2003b).

Finally, it is worth noting that ILK, as well as PINCH, α-parvin and Mig-2 are all widely expressed in the human tissues and well-conserved among different species(Clark et al., 2003; Mackinnon et al., 2002a; Wu, 2004b), suggesting an essential role in many different organisms and processes.

In the present study, we investigated the role of ILK as well as its binding partners PINCH, α-parvin and Mig-2 in hepatocyte differentiation induced by matrix. Primary hepatocytes were isolated from the rat liver by collagenase perfusion and cultured for eight days in collagen-coated plates. As shown previously(Block et al., 1996b), hepatocytes de-differentiated over time in culture and addition of Matrigel restored differentiation within three days. This model culture system for studying hepatocyte differentiation was previously used to determine the expression and distribution of focal adhesion (integrins, Focal Adhesion Kinase, paxillin) and cell adhesion molecules (E-cadherin)(Kim et al., 1998), as well as the regulation of the β-catenin pathway (Monga, 2006).

In this study, we show that ILK is present in the rat liver and localizes at the cell-ECM adhesion sites of primary rat hepatocytes in culture. Interestingly, the expression level of ILK in whole cell lysates of re-differentiated hepatocytes following Matrigel overlay is reduced, and this reduction is even more striking when we examine the Triton-X-100-soluble cellular fraction during re-differentiation, suggesting that ILK is involved in cellular control of hepatocyte differentiation induced by matrix. Furthermore, we show that PINCH and α-parvin, the other two members of the PINCH-ILK-parvin complex at focal adhesions, follow the same changes in solubility and expression level as ILK, while Mig-2, another binding partner of ILK, total expression level remains unchanged while the level of Mig-2 in the Triton-X-100-insoluble fraction increases and the level of Mig-2 in the Triton-X-100-soluble fraction decreases. Our results suggest that ILK, PINCH, and α-parvin play an important role in the process of matrix-induced hepatocyte differentiation, as their expression is dramatically changing during this process, while Mig-2, which also associates with ILK, seems to be unaffected.

5.2   MATERIALS AND METHODS

Antibodies and reagents

Matrigel was purchased from BD bioscience (BD Bioscience, Bedford, MA). Plates were coated with 10% vitrogen (Cohesion, Palo Alto, CA), and were air-dried under a hood and ultraviolet light overnight.

The following primary antibodies were used in this study: mouse monoclonal (mAb) anti-ILK antibody (clone 69), rabbit polyclonal anti-PINCH, mAb anti-α-parvin (clone3B5), mAb anti-Mig-2 antibody as described previously(Fukuda et al., 2003a; Fukuda et al., 2003b; Tu et al., 2003b), sheep anti-rat albumin (Immunology Consultants Laboratory, Newberg, OR), and anti-β-actin mAb (Chemicon, Temecula, CA). All secondary Abs were from Jackson ImmunoResearch Laboratories (West Grove, PA).

Hepatocyte isolation from rat liver and Matrigel overlay

Primary rat hepatocytes were isolated from male Fischer 344 rat livers by a calcium two step collagenase perfusion technique, as described previously(Block et al., 1996b). Freshly isolated hepatocytes were plated at a density of 400,000 cells per ml, on collagen-coated 6-well plates, in MEM medium (Sigma, St. Louis, MO) supplemented with 500 ng/ml insulin and 50 mg/ml gentamycin. Three to four hours after plating, the medium was replaced with Hepatocyte Growth Medium (HGM) containing 40 ng/ml Epidermal Growth Factor (EGF) and 20 ng/ml Hepatocyte Growth Factor (HGF) as described previously(Block et al., 1996b). The rat hepatocytes were kept in culture for a total of 15 days and the HGM medium was changed every two days.

Rat hepatocytes in half of the plates were overlaid with diluted Matrigel on the eighth day following the liver perfusion (Day 0 corresponds to the day of the perfusion), and cultured for one week, while the rest of the hepatocytes were maintained in normal culture conditions without Matrigel treatment. Matrigel was diluted 1:3 with HGM, and the medium was changed in all cultures every two days.

Immunofluorescent staining

Immunofluorescent staining was performed as described previously. Briefly, cells were plated on collagen-coated coverslips, fixed with 4% paraformaldehyde and stained with the anti-ILK mouse monoclonal antibody (clone 69) or anti-Mig-2 mouse monoclonal antibody. A rhodamine-red conjugated goat anti-mouse antibody was used as a secondary antibody (Jackson ImmunoResearch Laboratories (West Grove, PA).

Immunohistochemistry

Immunohistochemical staining for ILK and Mig-2 was performed on formalin-fixed paraffin embedded livers, as described previously (Kim et al., 2000).

Protein isolation and immunoblotting analysis

Total cell lysates were isolated from Matrigel-treated primary rat hepatocytes at different time points following the overlay of Matrigel (Days 10 and 15) and at the same time points lysates were isolated from untreated cultures. Whole cell lysates were generated using 1% sodium

dodecyl sulfate (SDS) in RIPA buffer (20 mM Tris/Cl pH 7.5, 150 mM NaCl, 0.5% NP-40, 1% TX-100, 0.25% Sodium Deoxycholated (DOC), 0.6-2 µg/ml aprotinin, 10µM Leupeptin, 1µM Pepstatin). The Triton-X-100-soluble fractions were isolated by lysing the cells for 30min on ice in RIPA buffer without SDS, followed by centrifugation at 14,000rpm for 15 min, and collection of the supernatant. The pellet from that centrifugation was then dissolved in RIPA buffer supplemented with 1% SDS, and it constituted the Triton X-100-insoluble fraction.

Protein concentrations of all lysates were determined using the bicinchoninic acid protein assay reagents (BCA method) (Pierce Chemical Co., Rockford, IL). Lysates were run on 10% reducing SDS-polyacrylamide gels. Actin was used as a loading control.

5.3   RESULTS AND DISCUSSION

ILK and Mig-2 are both present in the liver and they localize at the cell-ECM adhesions of primary rat hepatocytes in culture

In order to determine the expression and localization of ILK, PINCH, α-parvin and Mig-2 in the liver, we performed immunohistochemical staining on formalin-fixed paraffin-embedded liver sections. Only the anti-ILK and anti-Mig-2 antibodies worked for that purpose. As shown in Figure 21, both ILK and Mig-2 are present in the liver (Fig.21A-C). In fact, Mig-2 appears to be more concentrated in the periportal and centri-lobular regions (Fig.21C).
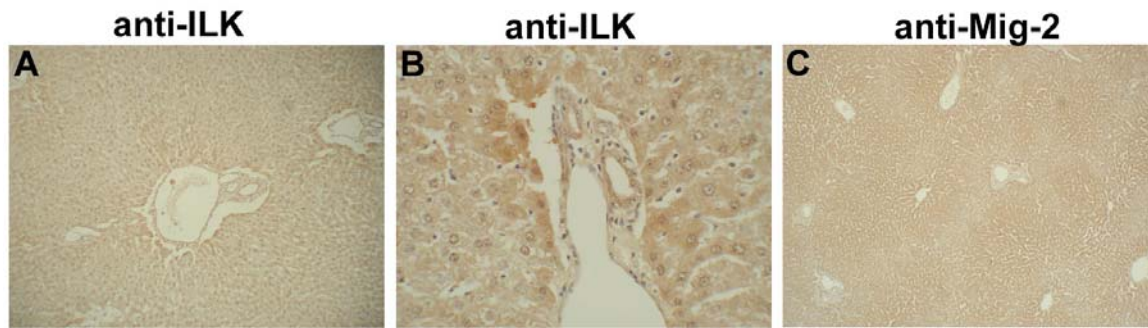
Figure 21: Immunohistochemical localization of ILK and Mig-2 in the liver. A) Formalin-fixed-paraffin embedded liver sections from normal rat liver were stained with anti-ILK antibody (20X magnification), B) Formalin-fixed-paraffin embedded liver sections from normal rat liver were stained with anti-ILK antibody (40X magnification), C) Formalin-fixed-paraffin embedded liver sections from normal liver were stained with anti-Mig-2 antibody (10X magnification).

Both ILK and Mig-2 have been shown to be present in the cell-ECM adhesions sites of multiple cell types (Li et al., 1999b; Tu et al., 2003b). To test whether the localization is the same in hepatocytes, we performed cell immunostaining of primary rat hepatocytes cultured on collagen. Indeed, both ILK (Fig.22B) and Mig-2 (Fig.22C) are abundant in primary cultured rat hepatocytes, forming nice and strong focal adhesions. A picture of the cells stained with just the secondary antibody (Fig.22A) serves as negative control for the cell immunostaining.
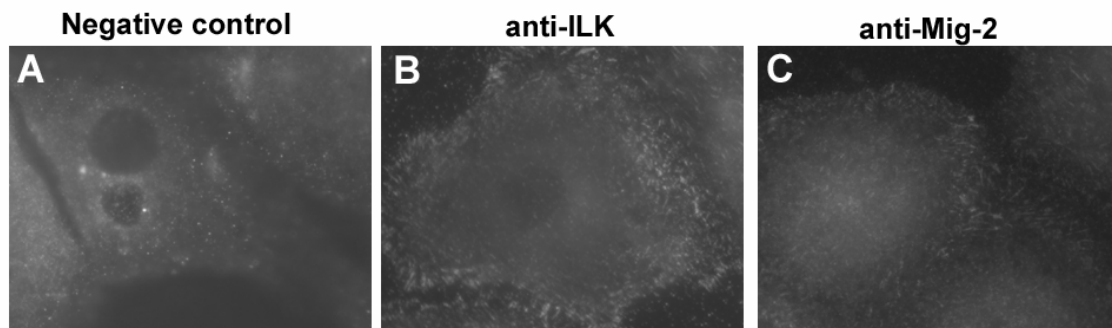
Figure 22: Localization of ILK and Mig-2 at the cell-ECM adhesions of primary rat hepatocytes. Primary rat hepatocytes stained with A) the secondary antibody only (as a negative control), B) the anti-ILK antibody, C) the anti-Mig-2 antibody.

Differentiation of hepatocytes is restored following addition of Matrigel

Intrigued by the finding that ILK is abundant at the cell-ECM adhesion sites of primary hepatocytes in culture, we sought to find whether its total expression level changes during hepatocyte differentiation induced by matrix. For that purpose, primary rat hepatocytes were cultured for eight days in collagen-coated plates using the chemically defined hepatocyte growth medium (HGM), which allows serum-free clonal expansion of primary hepatocytes in the presence of hepatocyte growth factor (HGF) and epidermal growth factor (EGF)(Block et al., 1996b). During that time primary hepatocytes lost albumin gene expression (Fig.23, compare albumin in lane 1 with lanes 2 and 3) as described previously(Block et al., 1996b). On the eighth day, Matrigel was added on half of the plates with the de-differentiated hepatocytes and re-differentiation occurred as shown by the increased albumin expression (Fig.23, compare lane 2 and 3 to lane 4) as well as the characteristic hepatocyte morphology (data not shown). Albumin was used as a hepatocyte-specific differentiation marker and the results were consistent with previous studies done in the same model system of matrix-induced hepatocyte differentiation(Block et al., 1996b; Kim et al., 1998), demonstrating that Matrigel overlay indeed restores hepatocyte differentiation.
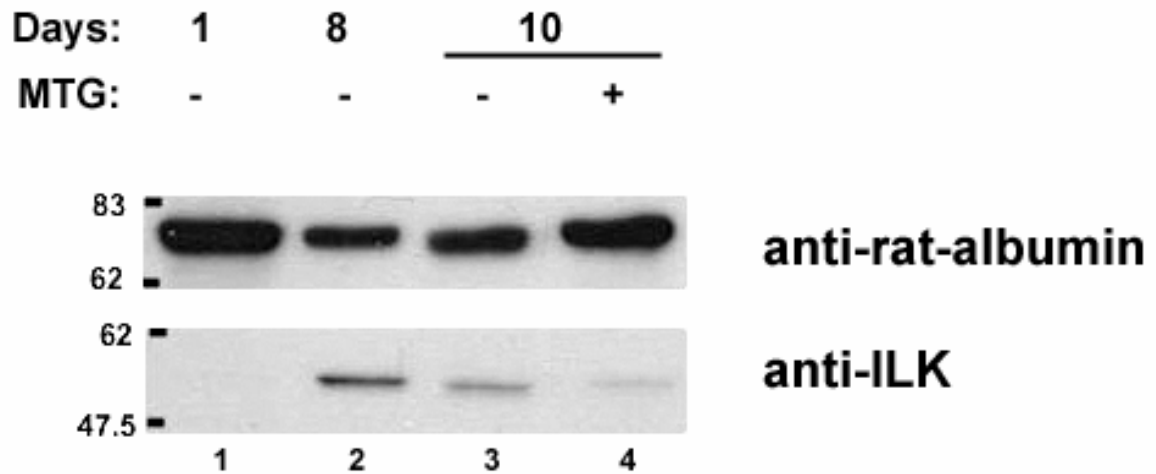
Figure 23: Hepatocytes re-differentiate in culture following addition of Matrigel, and ILK total expression level is reduced. Western blot of total cell lysates from hepatocytes harvested on Days 1, 8 and 10 following isolation from the liver. Matrigel was added on Day 8. Western blot using an anti-rat-albumin antibody (upper panel) or the anti-ILK antibody (bottom panel). Note that the same membrane was first probed with ILK and then reprobed without stripping with the anti-rat albumin antibody.

57

In order to investigate the role of ILK in this process, we analyzed the total protein level of ILK in de-differentiated and re-differentiated hepatocytes. As shown in Figure 23, ILK total level was significantly reduced following Matrigel overlay in primary cultured hepatocytes (Fig.23, compare lanes 3 and 4), while albumin level has been restored to the initial levels. This result suggests that ILK is involved in the cellular control of hepatocyte differentiation induced by matrix, and that a relatively low level of ILK is characteristic of differentiated hepatocytes.

The total protein expression of ILK, PINCH, and α-parvin is reduced during the matrix-induced hepatocyte differentiation, while the level of Mig-2 is not affected

To gain further knowledge on the role of ILK in the matrix-induced hepatocyte differentiation, we analyzed the total expression level of the ILK-binding proteins, PINCH, α-parvin and Mig-2. As shown in Figure 4, the total levels of all three components of the PINCH-ILK-parvin complex were reduced following addition of Matrigel over de-differentiated hepatocytes (Fig.24, compare lanes 2 and 3, for ILK, PINCH, and α-parvin). Interestingly, however, the total expression level of Mig-2, another ILK-binding protein, was not affected (Fig.24, compare lanes 2 and 3 for Mig-2).
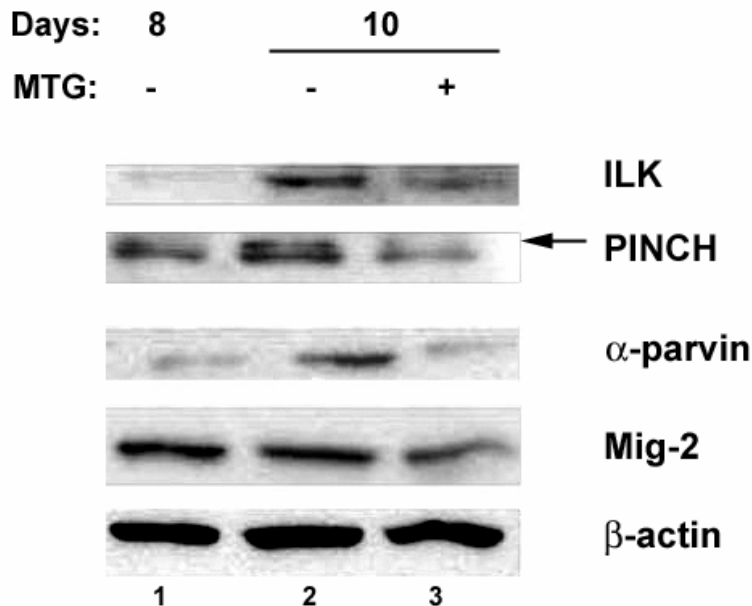
Figure 24: Total expression level of PINCH, ILK, α-parvin and Mig-2 during the matrix-induced hepatocyte differentiation. Western blot analyses of whole cell lysates from primary rat hepatocytes treated with matrigel on Day 8 post isolation, using antibodies against ILK, PINCH, α-parvin, and Mig-2. β-actin serves as a loading control.

In a study by Kim et al. (Kim et al., 1998) using the same model system, it was shown that the expression level of paxillin and Focal Adhesion Kinase (FAK), two other focal adhesion proteins, is increased in the Matrigel-treated hepatocytes. Thus, the data of the present study and

the study by Kim et al., suggest that during the matrix-induced hepatocyte differentiation, there is an interesting re-distribution of the different focal adhesion molecules, and some are increased while others are decreased as a response to Matrigel overlay and matrix in general. Therefore, understanding the regulation or the mechanism behind it would provide new insights into hepatocyte biology and thus facilitate hepatocyte-oriented therapeutic approaches.

The expression levels of ILK, PINCH and α-parvin are dramatically reduced in the Triton-X-100-soluble cellular fraction during hepatocyte differentiation

To shed more light upon the mechanism regulating this complex process of matrix-induced hepatocyte differentiation, we examined the intracellular distribution of ILK, PINCH, and α-parvin during the re-differentiation process. Triton-X-100-soluble cellular fractions, which contain the cytosol, were isolated from dedifferentiated or re-differentiated primary rat hepatocytes (at least 3 days following the addition of Matrigel). As shown in Figure 25, ILK and PINCH levels were dramatically reduced in the re-differentiated hepatocytes following Matrigel overlay (Fig.25, A, and B), and α-parvin follows the same pattern. However, the anti-α-parvin antibody is far stronger than the anti-ILK or anti-PINCH and thus the change seems less dramatic (Fig.25C). Examination of the actin loading though shows clearly that α-parvin level is also reduced in the Triton-X-100-soluble cellular fraction. These findings show that all members of the PINCH-ILK-parvin complex are dramatically downregulated from the cytosol during the matrix-induced hepatocyte differentiation, suggesting a biological relevant role of the PINCH-ILK-parvin complex in hepatocyte biology and the process of differentiation.

A.

no MTG   no MTG   +MTG   +MTG

50.7- .... **ILK**

50.7- .... β-actin

B.

no MTG   no MTG   +MTG   +MTG

35.5- .... **PINCH**

50.7- .... β-actin

C.

no MTG   no MTG   +MTG   +MTG

50.7- .... α-parvin

50.7- .... β-actin
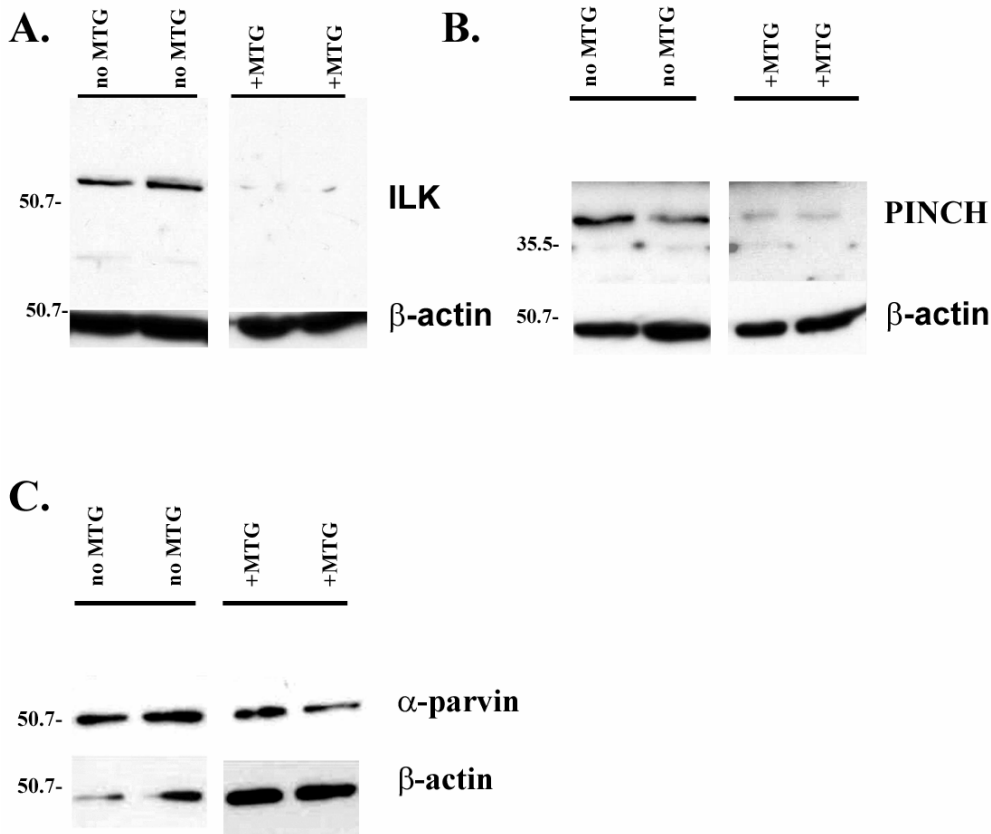
Figure 25: Expression level of ILK, PINCH, and α-parvin in the Triton-X-100-soluble cellular fraction during the matrix-induced hepatocyte differentiation. Triton-X-100-soluble fractions from dedifferentiated and re-differentiated hepatocytes 10 and 15 days after the addition of Matrigel (MTG) were subject to western blot analysis for A) ILK, B) PINCH, C) α-parvin. β-actin is used as a loading control.

Consistent with the above, a similar reduction in ILK in the Triton-X-100 soluble cellular fraction was also observed during the myogenic differentiation(Huang et al., 2000), indicating that ILK plays an important role in differentiated cells and corroborating the finding of the present study.

Intracellular redistribution of Mig-2 during matrix-induced hepatocyte differentiation

Finally, we sought to determine the cellular distribution of Mig-2, whose total expression level was not affected by the Matrigel overlay (Fig.24). Thus, Mig-2 expression level was examined both in the Triton-X-100-soluble fractions, and Triton-X-100-insoluble fractions. As shown in Figure 26, Mig-2 was significantly reduced in the Triton-X-100-soluble or cytosolic fraction (Fig.26A), while it was increased in the Triton-X-100-insoluble fraction (Fig.26B),

which explains why there was no significant change in the total expression level of Mig-2 (Fig.24).

A. Mig-2 in TX-100-soluble fraction
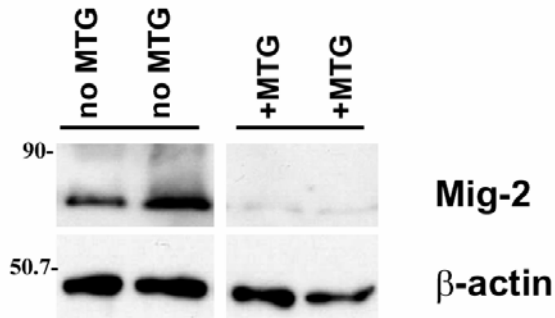
B. Mig-2 in TX-100-insoluble fraction
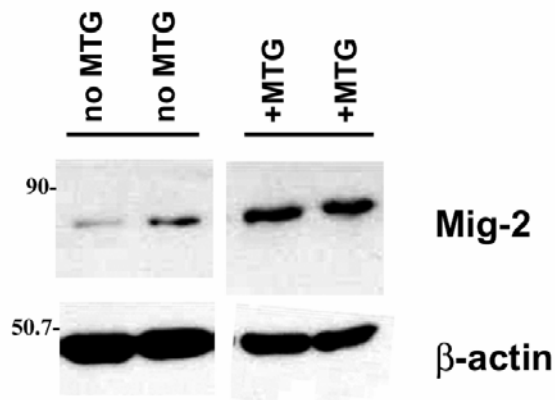
Figure 26: Mig-2 cellular re-distribution following the matrix-induced hepatocyte differentiation. Triton-X-100-soluble (A) and insoluble fractions (B) from dedifferentiated and re-differentiated hepatocytes after the addition of Matrigel (MTG) were subject to western blot analysis for Mig-2. β-actin is used as loading control.

In conclusion, it is worth noting that all proteins examined in this study, namely ILK, PINCH, α-parvin and Mig-2 have reduced expression levels in the Triton-X-100-soluble cellular fractions which correspond to the cytosol. In contrast, other focal adhesion proteins such as FAK, and paxillin (Kim et al., 1998), are elevated in those fractions, indicating the complexity of the mechanism regulating the matrix-induced hepatocyte differentiation. Furthermore, Mig-2 is increased in the Triton-X-100-insoluble fraction that is associated with the cytoskeleton suggesting that during the matrix-induced hepatocyte differentiation, different focal adhesion proteins are differently distributed within the cell, highlighting the complexity of the mechanism and the importance of cell-ECM adhesion proteins in this process.

In the present study, we have shown that the redistribution of components of the cell-ECM adhesion molecules is an important element of restoring differentiation in Matrigel-treated hepatocyte cultures. Although the molecular mechanisms governing the hepatocyte differentiation process are far from being deciphered, the present work provides new insight that could enhance our understanding of the whole process, and ultimately enable us to apply this information in the field of cell transplantation of hepatocytes in critically ill liver patients or other hepatocyte-based therapies.

6.0   LOSS OF INTEGRIN-LINKED KINASE FROM MOUSE HEPATOCYTES IN VITRO AND IN VIVO RESULTS IN APOPTOSIS AND HEPATITIS

6.1   INTRODUCTION

Extracellular matrix (ECM) is of great importance for the survival, differentiation, and normal function of the cells within a tissue. This is particularly true for hepatocytes, the parenchymal cells of the liver (Block et al., 1996b; Kumaran et al., 2005; Otsu et al., 2001; Pinkse et al., 2004). In fact, hepatocytes in culture maintained in the absence of matrix rapidly lose patterns of hepatocyte-specific gene expression and characteristic cellular micro-architecture. Interestingly, however, when hydrated complex matrix preparations (Matrigel: a matrix extract from Engelbreth-Holm-Swarm (EHS) mouse sarcomas or Type I Collagen Gels)(Kleinman, 1986) are added over de-differentiated hepatocytes, differentiation is restored within three days (Block et al., 1996b; Kim et al., 1998).

Moreover, ECM remodeling is an essential part of liver regeneration after partial hepatectomy (Kim et al., 1997; Michalopoulos and DeFrances, 1997; Mohammed, 2005), again highlighting the importance of ECM for the normal function of hepatocytes in liver.

Signals from the ECM are transmitted to the interior of the cell via integrins. Integrins not only interact with components of the ECM and physically link them to the cytoskeleton, but they also associate with multiple receptor-proximal proteins, which in turn serve as scaffolds for the attachment of enzymes that modify and regulate these complex interactions (Hynes, 2002).

Integrin-Linked Kinase (ILK) is a Ser/Thr kinase that is emerging as a key regulator of cell-ECM adhesions. Activation of ILK, either by integrin clustering or by growth factors,

affects multiple cell signaling pathways that regulate different processes such as survival, differentiation, proliferation, migration, and angiogenesis (Friedrich et al., 2004a; Huang et al., 2000; Tan et al., 2004a; Terpstra et al., 2003). Additionally, there is evidence that ILK also plays a role in oncogenic transformation (Hannigan et al., 1996a; Radeva et al., 1997; Yoganathan et al., 2002a).

From the signaling perspective, ILK activation results in the phosphorylation and subsequent activation of protein kinase B (PKB/Akt) (Persad et al., 2000a; Troussard et al., 2003b; Wu and Dedhar, 2001b) and Mitogen Activated Protein Kinase (Wu and Dedhar, 2001b), as well as inhibition of Glycogen Synthase Kinase 3-beta (Delcommenne et al., 1998b; Tan et al., 2001a). Through these pathways, ILK regulates survival, differentiation, cell cycle progression and many other crucial processes.

As an adaptor protein, ILK mediates multiple protein-protein interactions (Wu, 2001a; Wu, 2004b). Apart from interaction with the β1-and β3-subunits of integrin (Hannigan et al., 1996a), ILK also binds to PINCH (Li et al., 1999b; Tu et al., 1999a) and α-parvin, member of the CH-ILKBP/α-parvin/actopaxin/affixin protein family (Fukuda et al., 2003a; Tu et al., 2001b; Zhang et al., 2002b; Zhang et al., 2002), resulting in the formation of a ternary complex within cells. This stable ternary complex of PINCH-ILK-parvin at the cell-ECM adhesion sites, has been shown to be crucial for cell survival (Fukuda et al., 2003a; Fukuda et al., 2003b; Tu et al., 2001b; Tu et al., 1999a).

Although, extensive research has been done on ILK signaling and functions in the cell, little is known about the function of ILK in hepatocytes. There is, however, evidence suggesting that integrin signaling is important for hepatocyte survival (Pinkse et al., 2005; Pinkse et al., 2004; Su, 2005).

Our aim in the present study was to elucidate the role of ILK in mouse hepatocytes both *in vitro* and *in vivo*. In order to pursue this, we utilized the loxP-Cre system to directly eliminate ILK from primary mouse hepatocytes in culture or from the whole animal.

6.2   MATERIALS AND METHODS

Antibodies

The following primary antibodies were used in this study: mouse monoclonal (mAb) anti-ILK antibody (clone 69) (Santa Cruz biotechnology, Santa Cruz, CA), rabbit polyclonal anti-PINCH1, mAb anti-α-parvin (clone3B5), mAb anti-Mig-2 antibody as described previously(Tu et al., 2001b; Tu et al., 2003b), rabbit polyclonal anti-phospho-Akt (Ser 473) (Cell Signaling Technology, Danvers, MA), and anti-β-actin mAb (Chemicon, Temecula, CA). All secondary Abs were from Jackson ImmunoResearch Laboratories (West Grove, PA).

Animals

The ILK-floxed animals that were used in the present study were generated as described previously(Terpstra et al., 2003). All animals were housed in the animal facility of the University of Pittsburgh and they were treated in a humane manner according to the criteria outlined in the "Guide for the Care and Use of Laboratory Animals" prepared by the National Academy of Sciences and published by the National Institutes of Health. All experiments were performed under protocols approved by the Institutional Animal Care and Use Committee (IACUC) of the University of Pittsburgh.

Eight wild type animals, purchased from the Jackson Laboratory (Bar Harbor, Maine), were used to investigate the inherent toxicity of the injected Cre-expressing adenovirus. As the ILK-floxed animals were on a mixed genetic background, four of the controls were of the 129X1/SvJ strain and the remaining four were of the C57BL/6J strain.

Isolation of hepatocytes from the mouse liver

Mouse hepatocytes from the ILK-floxed animals were isolated by an adaptation of the calcium two step collagenase perfusion technique, as described previously(Block et al., 1996b). Hepatocytes were plated at a density of 300,000 cells per ml, in 6-well (35mm) plates, and the medium was renewed 3-4h after plating. The medium used was MEM (Sigma, St. Louis, MO) supplemented with 10% fetal bovine serum (FBS), 1% glutamine, and 1% penicillin and streptomycin.

Adenoviral vectors

The recombinant adenoviruses used in this study were either control adenoviral expression vector encoding β-galactosidase (β-gal), Cre-recombinase-expressing adenovirus (Cre), or adenoviral expressing vector encoding a FLAG-tagged full length mouse ILK. The control β-gal adenovirus was kindly provided by Drs. Tong-Chuan He and Bert Vogelstein (Howard Hughes Medical Institute, The Johns Hopkins Oncology Center, Baltimore, MD). The Cre expressing adenovirus was kindly provided by Dr. Jorge Sepulveda (Department of Pathology, University of Pittsburgh School of Medicine).

The FLAG-tagged full length mouse ILK expressing adenovirus was generated by cloning the cDNA encoding the FLAG-tagged full length mouse ILK into the *Sal*I/*Xba*I sites of the pAdTrack-CMV shuttle vector and mixed with supercoiled pADEsay-1, as previously described (29).

The amplified adenoviruses were subsequently purified by cesium chloride (CsCl) density gradient ultracentrifugation, dialyzed in sterile virus storage buffer, aliquoted, and stored at −80°C until use (Graham, 1991; Kolls, 1994). Viral titers were initially calculated by measuring the optical density of the viral DNA at 260 nm (OD_{260}). Titer was considered equal to the optical density at 260nm divided by 9.09×10^{-13} particles/ml.

However, before using the adenovirus in our cultured cells, we also measured the viral titer by plaque formation assay (pfu/ml) performed according to the protocol provided by BD biosciences.

Adenoviral infections of ILK-floxed mouse hepatocytes in culture

Twenty four hours after liver perfusion (Day 1), the cultured ILK-floxed mouse hepatocytes were infected with 10^7pfu/well of either control β-gal or Cre adenovirus. The medium was changed the following day and cells were kept in culture for a total of seven days.

For the rescue experiments, hepatocytes were co-infected with either β-gal adenovirus and ILK-adenovirus, or Cre adenovirus and ILK adenovirus, one day after isolation from the

mouse liver. The viral titer used for these experiments was 10^7 pfu/well for the β-gal and Cre adenoviruses, and 8×10^6 pfu/well for the ILK adenovirus.

Tail vein injections of adenoviral expressing vectors in ILK-floxed animals

PBS, 10^{10} particles/mouse (10^9 pfu/mouse) of control β-gal adenovirus, Cre-expressing adenovirus, or vehicle only (phosphate buffered saline) as an additional control, were administered into 78 ILK-floxed mice via tail vein injection. The same number of viral particles of Cre adenovirus was also injected via tail vein in eight wild type animals to test for the inherent toxicity of the Cre-recombinase.

Immunofluorescent staining

Immunofluorescent staining was performed as described previously (Li et al., 1999b; Tu et al., 2003b). Briefly, cells were plated on collagen-coated coverslips, fixed with 4% paraformaldehyde and stained with the anti-ILK mouse monoclonal antibody (clone 69). A rhodamine-red conjugated goat anti-mouse antibody was used as a secondary antibody.

Histology scoring

Hematoxylin-and-eosin (H&E) staining was performed both on formalin-fixed-paraffin-embedded sections, and paraformaldehyde-fixed frozen sections of the livers from ILK-floxed mice injected with β-gal or Cre-adenovirus. The histology was evaluated in a blind fashion by the pathologist (G.K.M.) and scored according to the following characteristics: Score 0; normal liver, Score 1; inflammation and/or fatty change, Score 2; inflammation and/or fatty change, with very few apoptotic cells, Score 3; inflammation and/or fatty change, with apoptosis, Score 4; inflammation, and/or fatty change, apoptosis, ballooning degeneration, and abnormal mitoses, Score 5; inflammation, and/or fatty change, apoptosis, ballooning degeneration, abnormal mitoses, hydropic degeneration, and necrosis.

Polymerase Chain Reaction (PCR)

DNA was isolated from the ILK-floxed mouse hepatocytes using the Trizol reagent from Invitrogen (Carlsbad, CA). Subsequently, the DNA was tested by PCR using a set of primers designed to detect the deleted ILK gene; forward: 5'-CCA GGT GGC AGA GGT AAG TA-3',

reverse: 5'-CAA GGA ATA AGG TGA GCT TCA GAA-3'. The conditions of the PCR reaction were as follows: 94°C for 5min, 94 ^{o}C for 1min, 55 ^{o}C for 1min, 72 ^{o}C for 3 min, (40 cycles for the last three steps), 72 ^{o}C for 10min, 55 ^{o}C for 5min and hold at 4 ^{o}C. The PCR products were separated through a 1% agarose gel at 80V for 4h and visualized with eithidium bromide staining.

DNA was also isolated from livers of ILK-floxed mice injected with either PBS, β-gal-adenovirus, or Cre-expressing adenovirus using again the Trizol reagent. Subsequently, the DNA was subject to PCR using the following primers for the amplification of the Cre gene; forward: 5'- GCG GTC TGG CAG TAA AAA CTA TC-3', reverse: 5'- GTG AAA CAG CAT TGC TGT CAC TT -3'. The conditions of the PCR reaction were as follows: 94°C for 3min, 94 ^{o}C for 30sec, 68 ^{o}C for 1min, 72 ^{o}C for 1min, (35 cycles for the last three steps), 72 ^{o}C for 2min, and hold at 10 ^{o}C. The PCR products were separated using a 2% agarose gel at 80V for 2h and visualized with ethidium bromide staining.

Protein isolation for immunoblotting

Total protein was isolated from the ILK floxed mouse hepatocytes or livers of the ILK-floxed mice injected with PBS, β-gal or Cre-expressing adenovirus using 1% sodium dodecyl sulfate (SDS) in RIPA buffer (20 mM Tris/Cl pH 7.5, 150 mM NaCl, 0.5% NP-40, 1% TX-100, 0.25% Sodium Deoxycholated (DOC), 0.6-2 μg/ml aprotinin, 10μM Leupeptin, 1μM Pepstatin).

Caspase-3 activity measurement

Apoptosis was assessed by caspase-3 activity measurement as described in the materials and methods section in Chapter 3.

TUNEL assay

Apoptosis in livers from adenovirus-injected animals was assessed by terminal deoxynucleotidyltransferase-mediated dUTP-biotin nick end-labeling (TUNEL) assay using the ApopTag In Situ Apoptosis Detection Kit from Chemicon (Temecula, CA).

6.3   RESULTS

ILK is localized to the cell-ECM adhesions of primary mouse hepatocytes in culture

ILK has been shown to localize to the cell-ECM adhesions in a number of different cell types (Li et al., 1999b). In order to test whether the localization of ILK is the same in hepatocytes, we stained primary mouse hepatocytes with anti-ILK monoclonal antibody. ILK is indeed abundant at the cell-ECM adhesion sites in primary mouse hepatocytes (Fig.27A), and it also appears to be present in the canaliculi formed between hepatocytes in culture (Fig.27B).
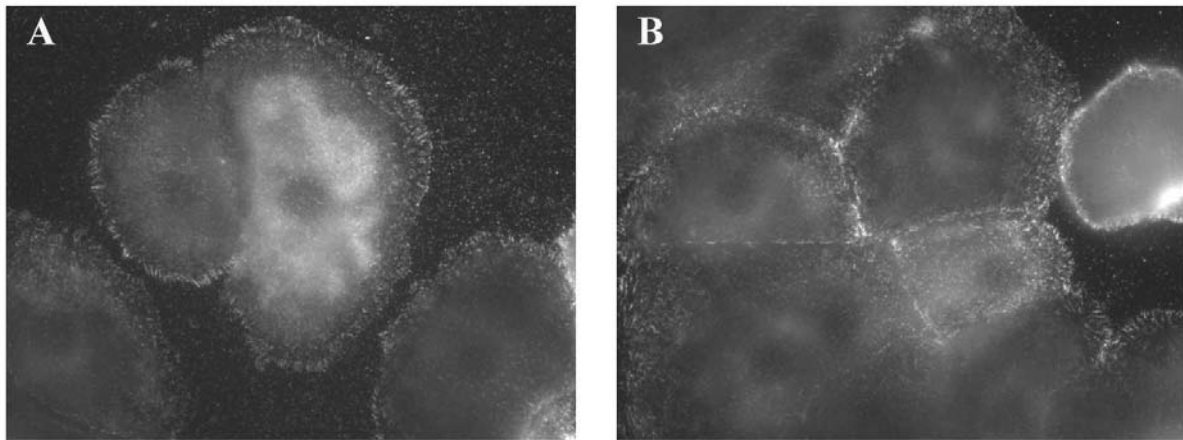
Figure 27: Localization of ILK to the cell-ECM adhesions of primary hepatocytes. A, and B) Primary hepatocytes stained with anti-ILK antibody.

ILK gene and protein are removed by infection of the ILK-floxed mouse hepatocytes with Cre adenovirus

To test the significance of ILK in hepatocytes, we employed the loxP-Cre system approach. Specifically, primary mouse hepatocytes were isolated from ILK-floxed mice by liver perfusion (Day 0) and twenty four hours after plating (Day 1), cells were subject to adenovirus infections to introduce either Cre-recombinase (Cre-adenovirus) or β-galactosidase (β-gal adnovirus) as a control. DNA was isolated from the adenovirus-infected cells and subsequently tested by PCR using a set of primers designed to detect the excised ILK gene.
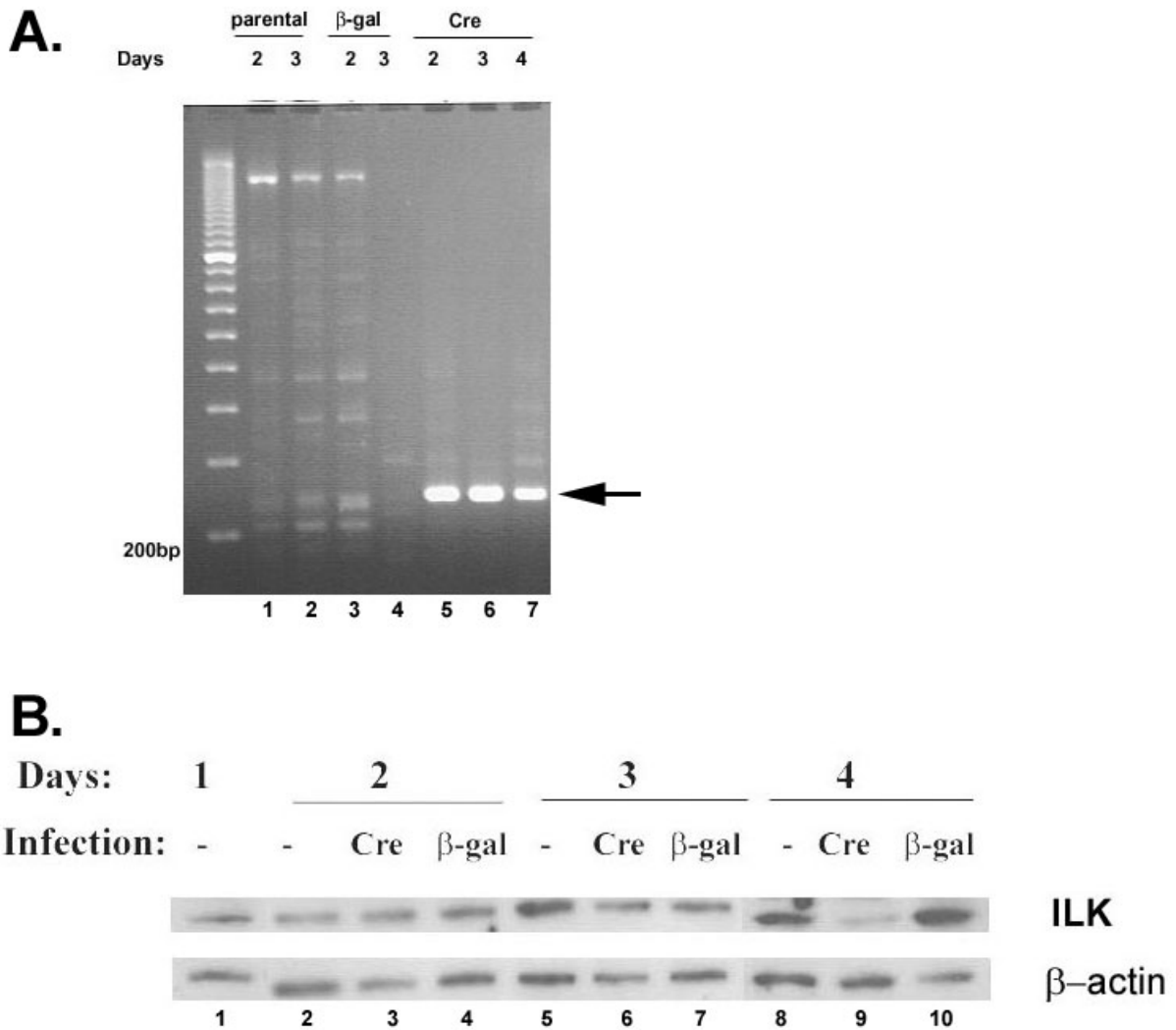
Figure 28: Excision of the ILK gene and removal of the ILK protein from primary ILK-floxed mouse hepatocytes. A) PCR products showing the excised ILK gene (arrow) in the cells-infected with Cre-adenovirus 2, 3, and 4 days post-infection (lanes 5-7). Note that the uninfected cells (lanes 1 and 2), and the β-gal-infected cells (lanes 3 and 4) do not have the excised ILK band, B) Western blot showing that ILK protein is not removed from the uninfected cells (lanes 1, 2, 5 and 8), nor the β-gal-infected cells (lanes 4, 7 and 10), but it is removed from the Cre-infected cells 4 days post-infection with Cre adenovirus (compare lane 9 to lanes 3 and 6). Actin is used as loading control.

As shown in Figure 28A, the ILK gene was excised by the Cre-recombinase as early as one day after infection of the cells with Cre-adenovirus (Day 2). The ILK protein however, was not completely depleted until day 4, as shown in Figure 28B.

Depletion of ILK from ILK-floxed mouse hepatocytes leads to massive apoptosis

The ILK-floxed mouse hepatocytes that were infected with control β-gal adenovirus exhibited normal hepatocyte morphology for at least five days in culture. On the other hand, the ILK-floxed hepatocytes that were infected with an equal number of plaque forming units (pfu/ml) of the Cre-adenovirus showed abnormal morphology, and increasing numbers of dead cells were observed over time. The accumulation of dead cells in the Cre-infected-ILK-floxed hepatocytes started on day 3 (two days following infection with Cre-adenovirus), as shown in Figure 36A.

In order to determine whether the cells were dying as a result of apoptosis, caspase 3 activity was measured at different time points after infection. Starting on day 3 following adenoviral infections, caspase 3 activity was 4-9 fold increased in the Cre-infected cells compared to the uninfected cells or the cells infected with the control β-gal adenovirus (Fig.29B, compare the solid black bars with the solid white or striped bars).

These results suggest that ILK is crucial for hepatocyte survival since depletion of the protein from primary cultured hepatocytes leads to massive apoptosis.

A **ILK-floxed mouse hepatocytes**

	Parental	β-gal	Cre	

Day 2

Day3

Day4

Day5

B

Caspase 3 activity in ILK floxed mouse hepatocytes
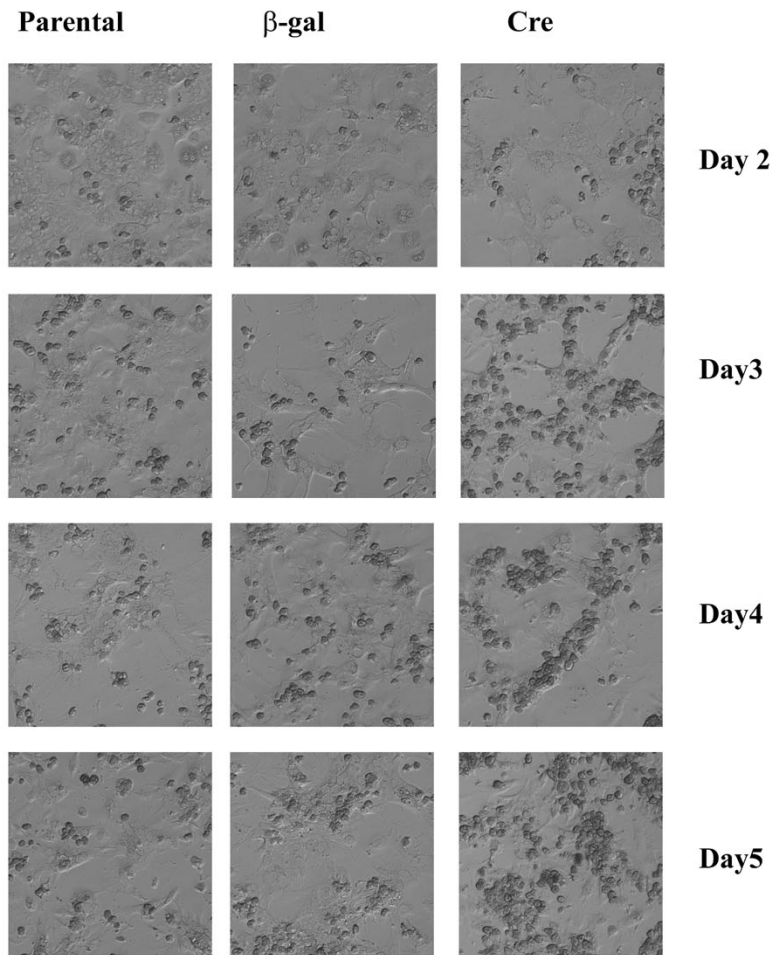
Figure 29: Cell morphology and caspase 3 activity in mouse hepatocytes following ILK knock-down. A) Cell morphology of uninfected (parental), control-adenovirus (β-gal)-infected, or Cre-infected hepatocytes, 2, 3, 4 and 5 days post-infection. Cells were observed under an Olympus IX70 fluorescence microscope and images were captured with a digital camera. Note that the parental or β-gal-infected hepatocytes have normal morphology during days 2-5, while the Cre-infected hepatocytes show increasing numbers of dead cells over time, B) Caspase 3 activity 2, 3, 4, and 5 days post-infection. Cre-infected hepatocytes have significantly elevated caspase 3 activity compared to the parental and control infected cells. Compare the solid black bars with the solid white or striped bars.
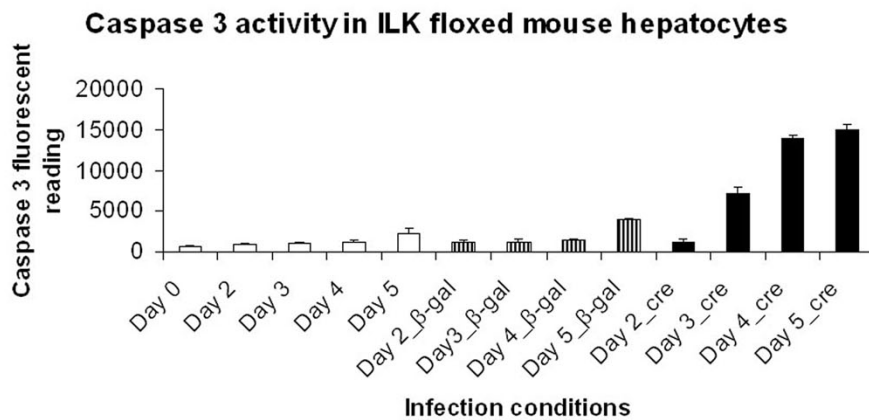
ILK overexpression substantially rescues apoptosis induced by the removal of ILK

We next sought to find whether the effect of ILK depletion on apoptosis could be rescued via re-introduction of the protein. Cells were co-infected with either β-gal adenovirus and an adenovirus expressing ILK (ILK-adenovirus), or Cre-adenovirus and ILK-adenovirus, and harvested four days after infection for western blot analysis. As shown in Figure 4A, ILK was effectively removed by the Cre-recombinase (Fig.30A, lanes 3 and 5) and it was efficiently overexpressed in the cells that were co-infected with ILK-adenovirus (Fig.30A, lanes 4 and 5).

Interestingly, parallel caspase 3 activity measurement experiments for the same sets of cells revealed a reduction of approximately 36% in the caspase 3 activity in the cells that were co-infected with Cre and also overexpressed ILK, compared to the ones that were solely infected with the Cre adenovirus. This indicates that the dramatic apoptotic effect in the Cre-infected-ILK-floxed hepatocytes results from the loss of ILK.
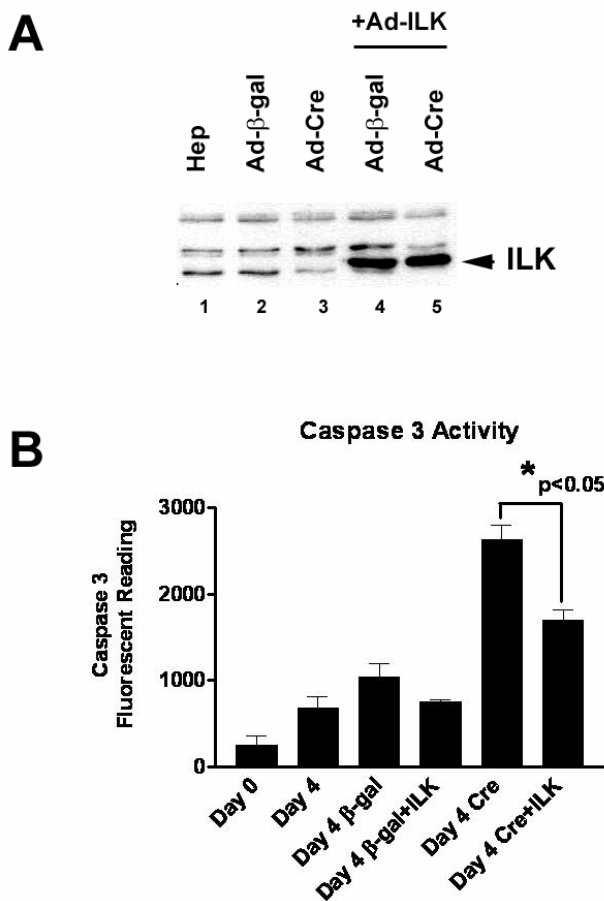
Figure 30: ILK overexpression substantially rescues the effect on apoptosis induced by the loss of ILK. A) Western blot showing ILK knock-down (lanes 3 and 5), and overexpression (lanes 4 and 5), four days post-infection. B) Caspase 3 activity four days post infections. The same sets of cells were used for A and B.

PINCH-1 and a-parvin expression levels are reduced in the ILK-depleted hepatocytes

To further investigate the mechanism by which ILK removal induces apoptosis in hepatocytes, we first sought to determine whether ILK-associated proteins are affected. To do so, we tested the levels of PINCH and α-parvin which, together with ILK, form a stable ternary complex at the cell-ECM adhesion sites (Tu et al., 2001b; Tu et al., 1999a; Wu, 2004b; Zhang et al., 2002b; Zhang, 2002).

ILK-floxed hepatocytes that were infected with Cre-adenovirus and had reduced levels of ILK (Fig.31A), also showed a dramatic reduction in both PINCH (Fig.31B) and α-parvin protein expression levels (Fig.31C). Interestingly, the level of Mitogen-inducible gene-2 (Mig-2), another cell-matrix adhesion protein closely associated with ILK (Mackinnon et al., 2002a; Tu et al., 2003b), was not altered after the removal of ILK from hepatocytes (Fig. 31D).
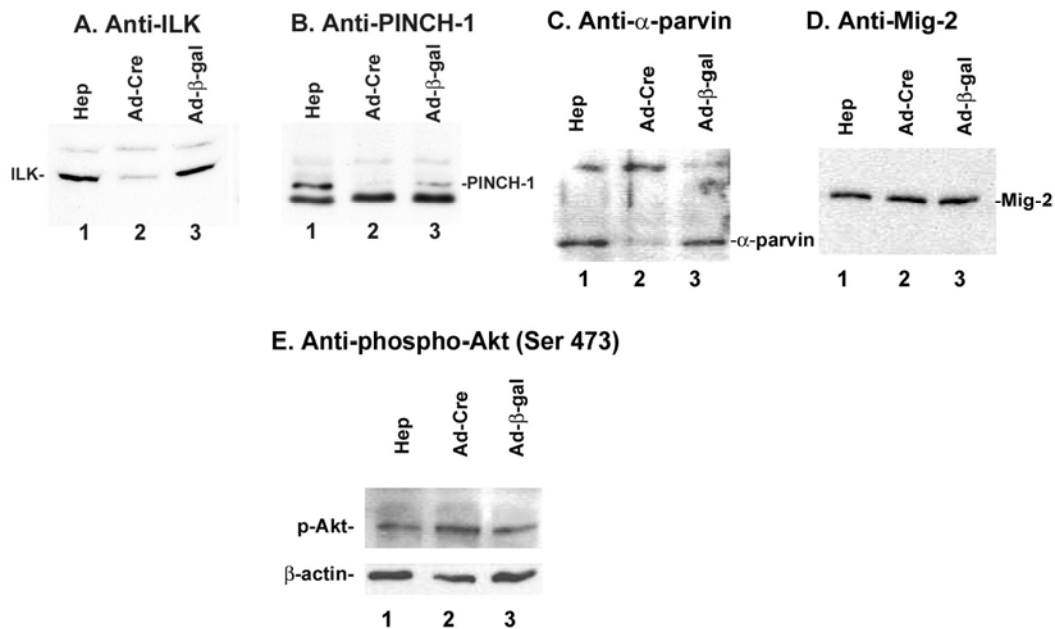
Figure 31: Changes in the expression level of other proteins as a result of removal of ILK from ILK-floxed mouse hepatocytes. Western blot analysis for A)ILK, B)PINCH, C) α-parvin, D)Mig-2, E)phosphor-Akt (Ser473), 5 days post infection with either β-gal or Cre-adenovirus.

The phosphorylation of PKB/Akt is not affected by the loss of ILK from hepatocytes

Previous studies have shown that inhibition of either ILK, PINCH, or α-parvin induces extensive apoptosis in HeLa cells, and that the activation of PKB/Akt, a key regulator of cell survival, is also impaired (Fukuda et al., 2003a; Fukuda et al., 2003b). In order to test whether depletion of ILK from primary hepatocytes leads to apoptosis through the PKB/Akt pathway, we examined the expression level of phosphorylated-Akt at Ser473, the phosphorylation site that activates Akt (Fukuda et al., 2003a; Fukuda et al., 2003b; Troussard et al., 2003b). As shown in Fig.31E, the level of phosphorylated Akt at Ser473 does not change after removal of ILK.

ILK protein is significantly reduced in animals injected with Cre-adenovirus, in vivo

To gain further knowledge on the significance of ILK for hepatocytes, we employed an *in vivo* approach. PBS, β-gal or Cre-adenovirus were delivered into ILK-floxed animals via the tail vein, which has been shown to be an effective way of administrating adenovirus in the liver in a homogeneous fashion with high reproducibility of expression (Herrmann, 2004). Injections were performed in 78 ILK-floxed mice (19-31 weeks old), and mice were sacrificed two, four, five, seven, eight or ten days later.
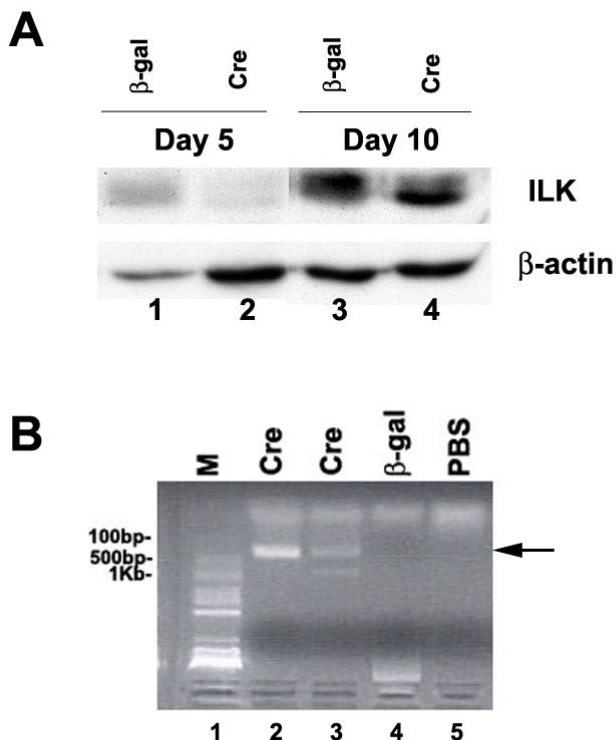
Figure 32: Elimination of ILK from the mouse liver by administration of Cre-recombinase expressing adenovirus via tail vein. A) Western blot showing the expression level of ILK in samples from ILK-floxed mouse livers injected with either β-gal or Cre adenovirus (Day 5 and 10 post-injection) using anti-ILK antibody. Equal loading was confirmed by actin reprobing of the same membrane. B) PCR using primers that detect the presence of Cre gene (arrow). Note that only the Cre-injected animals have the Cre gene (compare lanes 2 and 3 to 4 and 5).

As shown in Fig.32A the ILK protein level was reduced in the Cre-adenovirus-injected animals compared to the β-gal adenovirus injected animals in all animals injected with Cre-adenovirus at all the time points tested. This corresponds with specific expression of Cre recombinase in the Cre adenovirus injected mice (Fig.32B, compare lanes 2 and 3 to lanes 4 and 5. The band that corresponds to the Cre gene is shown with an arrow).
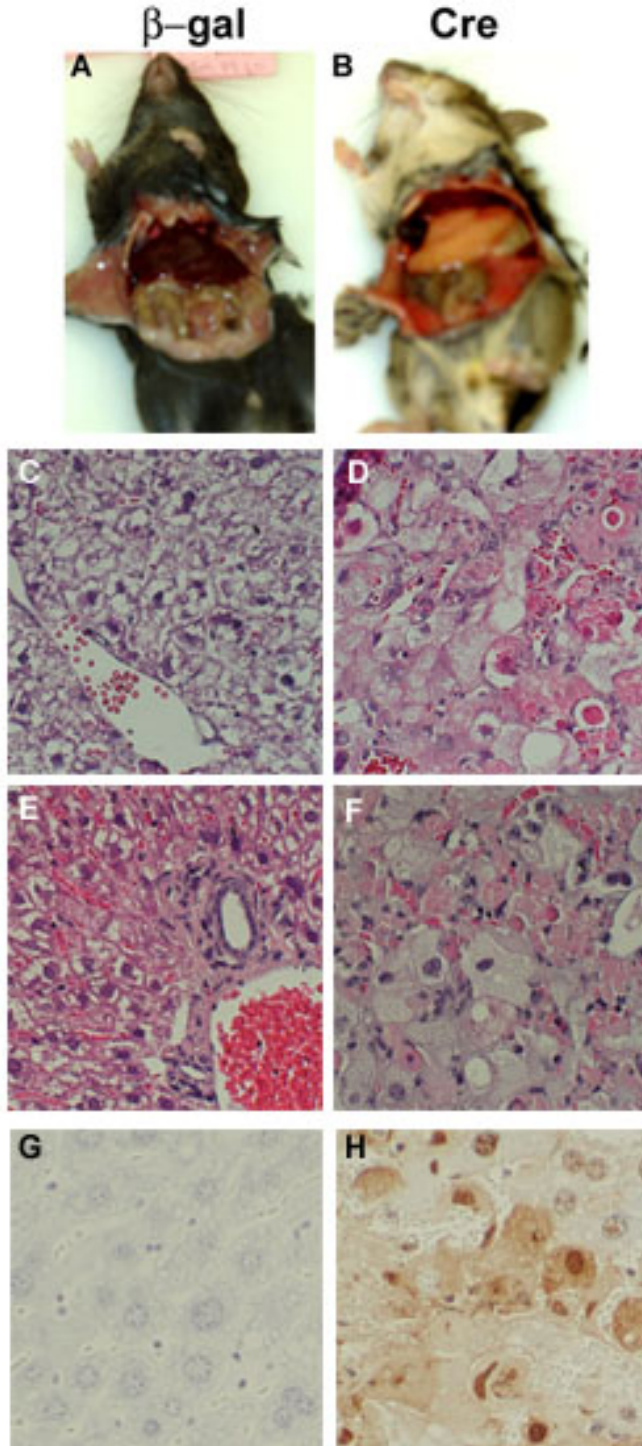
Figure 33: Gross appearance and H&E staining of the livers from β-gal or Cre-injected animals
A) Gross appearance of the liver of a control β-gal-adenovirus-injected mouse, B) Gross appearance of the liver of a mouse injected with Cre-recombinase expressing adenovirus, C) H&E staining on frozen liver sections taken from a β-gal-adenovirus-injected mouse, D) H&E staining on frozen liver sections taken from a Cre-adenovirus-injected mouse. Arrows point to apoptotic cells, E) H&E staining on formalin-fixed, paraffin embedded sections from a β-gal-adenovirus-injected mouse liver, F) H&E staining on formalin-fixed, paraffin embedded sections from a Cre-adenovirus-injected mouse liver. Arrows point to apoptotic cells, while arrowheads show necrotic cells with ballooning degeneration. G) TUNEL staining on formalin-fixed, paraffin embedded sections from a β-gal-adenovirus-injected mouse liver, H) TUNEL staining on formalin-fixed, paraffin embedded sections from a Cre-adenovirus-injected mouse liver

Livers from the animals injected with Cre adenovirus are significantly impaired and show signs of hepatitis

  ILK floxed mice were sacrificed at two, four, five, seven, eight, or ten days after injection with either β-gal or Cre-adenovirus, and liver histology was examined. Livers were further analyzed by PCR and immunoblotting. The gross appearance of the livers from most of the Cre-adenovirus injected animals (35 out of 45) was greatly altered. Livers were larger, with a coarse granular surface and very pale, compared with control livers from β-gal adenovirus injected mice (Fig.33, compare A and B).
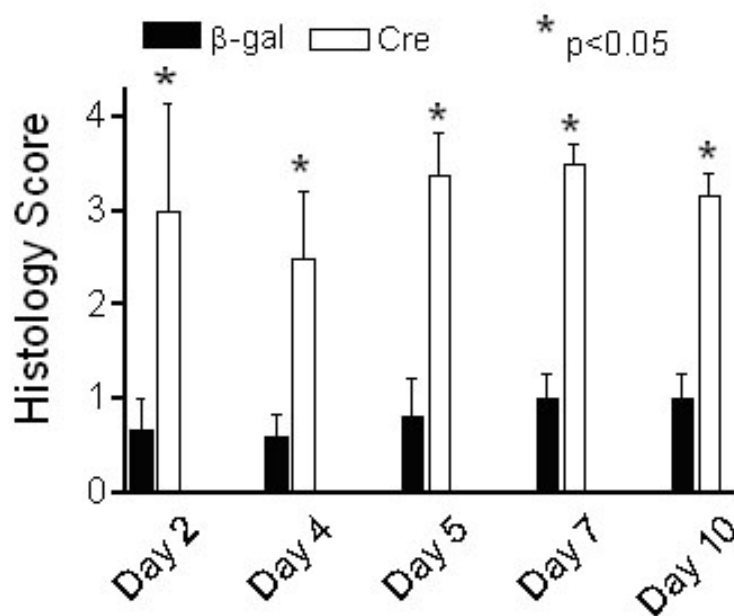
Figure 34: Statistical analysis of the differences in the histology between β-gal and Cre-adenovirus-injected ILK-floxed mouse livers. The bar graph shows the differences in the liver histology scores between β-gal control and Cre-adenovirus-injected ILK-floxed animals, at different time points after injection. The day of injections is considered as day 0. The statistical analysis was conducted using the Mann-Whitney test and the Statgraphics Plus statistics software. A p value of less that 0.05 was considered as statistical significant.

At the microscopic level, the liver histology exhibited a variety of abnormal characteristics and it was blindly scored on a scale of 0 to 5 (experimental procedures section). The highest score (five) was attributed to livers with the worst histology, exhibiting inflammation, and/or fatty change, apoptosis, ballooning degeneration, abnormal mitoses, hydropic degeneration, and necrosis. Collectively, 85% (23 out of 27) of the β-gal-adenovirus injected animals had normal livers (score 0-1) whereas the remaining 15% exhibited signs of mild inflammation and had a few apoptotic cells (score 2). In the Cre adenovirus-injected animals, 78% (35 out of 45) had abnormal liver histology (score 3-5), while 22% appeared to have relatively normal histology (score 1-2). That can be attributed to problems with the tail vein administration of the virus which resulted in the actual delivery of only a portion of the intended amount of virus in some of the animals. The Cre-adenovirus-injected animals, at each one of the time points tested, had more severe pathology and thus higher scores than the control β-gal-injected ones and the difference was statistically significant as shown by Mann-Whitney test ($p < 0.05$) (Fig.34).

Interestingly, three animals from the Cre-injected group died 2, 4 and 5 days after being injected and their livers showed the most severe pathology. Representative images of the histology of the control and Cre-adenovirus-injected animals are shown in Fig.33 (compare C and E to D and F). Finally, confirming the apoptosis observed from the H&E staining, the livers of the Cre-adenovirus-injected animals exhibited dramatically increased TUNEL staining (Fig.33, compare G and H).

Lastly, to determine whether genetic susceptibility to Cre recombinase toxicity played a role in the results that we obtained, eight wild type mice of the strains 129X1/SvJ and C57BL/6J (the background of the ILK-floxed mice) were injected with Cre adenovirus using the same exact titer as the one utilized in the ILK-floxed animals. Wild type livers were normal, both macroscopically and microscopically. This indicates that the severe phenotype observed in the Cre-injected animals was a response to loss of ILK and not a side effect of the Cre-adenovirus.

6.4   DISCUSSION

Hepatocytes are the parenchymal cells of the liver and thus, they perform a number of complicated functions to maintain homeostasis. Of particular importance for normal hepatocyte function, both *in vivo* and *in vitro,* is the surrounding matrix (Block et al., 1996b; Kumaran et al., 2005; Michalopoulos et al., 1999; Ohashi and Kay, 2004).

ILK is a cell-ECM adhesion protein that mediates signal transduction between integrins, ECM, and the interior of cells. It directly interacts with PINCH and α-parvin and, together they form a stable ternary complex at the cell-ECM adhesion sites. In fact these proteins are pre-assembled in a ternary complex and the entire complex is then localized to the cell-ECM sites (Zhang et al., 2002b). ILK, as well as PINCH and α-parvin are widely expressed in the human tissues and well-conserved among different species (Clark et al., 2003; Mackinnon et al., 2002a; Wu and Dedhar, 2001b). As such, it is not surprising that ILK is critically involved in many fundamental cellular processes (Hannigan et al., 2005; Legate et al., 2006; Wu, 2005).

In the present study, we investigated the role of ILK in mouse hepatocytes by specifically eliminating it *in vitro* from primary hepatocytes in culture and *in vivo* from the whole liver. *In vitro,* the ILK-depleted cells underwent dramatic apoptosis, as assessed by morphological changes and caspase 3 activity measurements. Interestingly, re-introduction of ILK substantially reversed the effect on apoptosis suggesting that apoptosis is indeed due to the removal of the ILK and that the protein itself helps prevent cell death.

Cells lacking ILK also display reduced levels of PINCH and α-parvin, while Mig-2, another ILK-binding protein, is not affected. The reduction in the level of PINCH, and α-parvin following ILK-depletion has been shown previously in other cell types (Fukuda et al., 2003a; Fukuda et al., 2003b), while both PINCH and α-parvin have been implicated in cell survival (Fukuda et al., 2003a; Fukuda et al., 2003b). Therefore reduction of their level could contribute to or enhance the apoptosis induced by the decreased level of ILK. Hence, in cultured primary hepatocytes, the components of the PINCH-ILK-parvin complex appear to function in concert to mediate cellular signaling for survival.

Mig-2 is a cell-ECM adhesion protein closely associated with the PINCH-ILK-parvin complex and integrin signaling and has been shown to regulate cell shape and spreading (Legate et al., 2006; Tu et al., 2003b; Wu, 2005). Mig-2 level does not change following ILK removal from hepatocytes, which indicates that not all the cell-matrix adhesion proteins are affected by the depletion of ILK, but rather the two proteins that form the ternary complex with ILK are the ones that are most dramatically affected.

Several studies in cancer cell lines or immortalized cells, have shown that ILK regulates survival through the PKB/Akt pathway (Delcommenne et al., 1998b; Fukuda et al., 2003a; Persad et al., 2000a; Persad et al., 2001; Troussard et al., 2003b). In this study, we tested the expression level of active-phosphorylated-Akt (Ser473) following depletion of ILK from primary hepatocytes and found that it was not affected (Fig.5B), indicating that ILK regulates primary hepatocyte survival through a pathway other than the PKB/Akt. Our finding is in accordance with other studies using ILK deficient fibroblasts (Legate et al., 2006; Sakai et al., 2003) that also showed no alterations in the phosphorylation status of Akt. The reason for the discrepancy is unclear but may be attributed to either cell-type specific differences or possibly differences in the mechanisms that are activated in primary cells versus immortalized and/or cancerous cell lines.

Consistent with our *in vitro* data, *in vivo* elimination of ILK from ILK-floxed mice, resulted in severe liver abnormalities ranging from inflammation, apoptosis, and fatty change to acute, full-scale hepatitis. The finding that the liver was the most obviously affected organ by the ILK elimination is explained by the fact that administration of Cre-adenovirus through the tail vein leads to higher infectivity of the adenovirus with higher recombination levels in the liver and spleen, as opposed to other organs (Wang, 1996).

Furthermore, it is worth noting that the adenoviral injection itself caused some inflammation as shown by the results of the β-gal-injected animals, 15% of which show signs of inflammation and small scale apoptosis. This is consistent with previous studies demonstrating toxicity effects of adenovirus vectors in hepatocytes(Shayakhmetov, 2004).

Altogether, our results clearly show that elimination of integrin signaling by removal of ILK is detrimental to primary hepatocyte survival in culture, as well as to the function of the whole liver. Thus, ILK is of great importance for the liver in general, consistent with recent work by Shafiei *et al*. highlighting the importance of ILK in liver wound healing (Shafiei, 2006). Nevertheless, more research is needed in order to decipher the exact mechanisms involved. Understanding the mechanisms that regulate survival in hepatocytes *in vitro* and *in vivo* is of utmost importance since the balance between cell survival and death is delicate and can be easily disrupted in cases of liver injury.

7.0 TARGETED GENETIC ELIMINATION OF ILK IN THE LIVER LEADS TO ABNORMAL LIVER ARCHITECTURE AND BILIARY MALFORMATIONS

7.1 INTRODUCTION

The liver is the biochemical factory of the body performing numerous functions at the same time and it is thus essential for the normal function of the whole body. It consists of hepatocytes, the parenchymal cells of the liver, as well as the non-parenchymal cells which include the endothelial cells, the stellate cells, the Kupffer cells and the biliar cells(Michalopoulos and DeFrances, 2005). In order for all those cells to function properly, the interaction with the extracellular matrix (ECM) is of utmost importance.

In fact, how essential ECM is for normal liver function is shown by the fact that the liver is undergoing matrix breakdown and remodeling at the earliest stages of regeneration after partial hepatectomy (Kim et al., 2000; Kim et al., 1997; Michalopoulos and DeFrances, 2005; Michalopoulos and DeFrances, 1997). Moreover, hepatocytes are greatly depended on the ECM for their differentiation. Hepatocytes in culture rapidly lose expression of their differentiation markers when maintained in the absence of matrix but differentiation and normal hepatocyte architecture is quickly restored upon addition of complex matrix environments (e.g. Matrigel, or collagen gels)(Block et al., 1996b; Bucher, 1990; Kim et al., 1998). Finally, the importance of ECM for liver is again demonstrated in cases such as cirrhosis, where alterations of liver matrix affect hepatocyte growth and differentiation.

The communication between cells and the ECM is achieved through integrins and the associated integrin-proximal adhesion molecules(Hynes, 2002). Through multiple protein-

protein interactions and signaling events, these molecules transmit signals from the ECM to the inside of the cell and regulate many fundamental cellular processes.

Integrin-Linked Kinase (ILK) is a β1- and β3-integrin-interacting cell matrix adhesion protein that has been proven to be crucial for a number of cellular processes such as survival, differentiation, proliferation, migration, and angiogenesis(Huang et al., 2000; Legate et al., 2006; Li et al., 2003; Wu, 2001a; Wu, 2004b), while there is strong evidence that overexpression of ILK leads to oncogenic transformation with all the accompanied attributes (Persad and Dedhar, 2003; Radeva et al., 1997; Troussard et al., 2000).

Despite massive evidence that ECM signaling affects hepatocyte structure and function, the impact of this at the level of the whole organ has not been assessed at a genetic level and the role of ILK in the liver has not been investigated either.

In the present work, in order to study the contribution of ILK in the biology and function of the liver, we used the genetic mouse model of targeted elimination of a gene in a specific organ by the LoxP-Cre system and we eliminated ILK from the mouse liver.

To do that we crossbred ILK-floxed animals (Terpstra et al., 2003) with three strains of transgenic animals that express Cre-recombinase under the control of promoters related to hepatocyte-associated transcription factors and genes; the albumin promoter, Alpha Fetoprotein (AFP) enhancer-albumin promoter, and Foxa3-promoter. The albumin promoter and AFP-enhancer-albumin-promoter are turned on after liver specification. Albumin expression, even though present during liver embryonic development, becomes stronger after birth whereas AFP expression is stronger during embryonic life and declines after birth. Previous studies have shown that although albumin is expressed early in development, the Cre-recombinase under an albumin promoter can completely ablate a floxed gene from the liver at about 6 weeks of age, while the recombination is not complete at earlier stages after birth(Postic and Magnuson, 2000).

Thus, in the present work, most of our studies were done in 8 week old mice. Regarding the Cre-recombinase expressed under the control of an AFP-enhancer-albumin-promoter, it is known that it allows position-independent expression of Cre-recombinase in mice at the same

time at which the endogenous albumin gene gets activated during embryoegesis(Kellendonk, 2000; Tronche, 1999). Finally, the Cre-recombinase expressed under the Foxa3 promoter, also known as HNF3 gamma, is expressed in the ventral endoderm just prior to hepatic specification(Lee, 2005).

Cre-recombinase expression under the three different promoters allows assessment of ILK ablation at different stages (from the very earliest stages in liver development to a few weeks after birth), and thus provides us with a more complete picture of the role of ILK in the liver.

7.2   MATERIALS AND METHODS

Antibodies

The following primary antibodies were used in this study: mouse monoclonal (mAb) anti-ILK antibody (clone 69) (Santa Cruz biotechnology, Santa Cruz, CA), PCNA, Ki67, and anti-β-actin mAb (Chemicon, Temecula, CA). Goat-anti-mouse secondary Abs was purchased from Jackson ImmunoResearch Laboratories (West Grove, PA).

Animals

The ILK-floxed animals that were used in the present study were generated as described previously(Troussard et al., 2003c). The ILK-floxed mice were crossbred with three strains of mice expressing Cre-recombinase under the control of promoters related to hepatocyte-associated transcription factors and genes; the albumin promoter, AFP-enhancer-albumin promoter, and Foxa3-promoter. The AFP-enhancer-albumin promoter and the Foxa3-promoter Cre expressing mouse strains were kindly provided by Dr. Klaus Kaestner (University of Pennsylvania), while the albumin-promoter Cre-expressing mice were purchased from Jackson's laboratories. All animals were housed in the animal facility of the University of Pittsburgh and all experiments were performed under protocols approved by the Institutional Animal Care and Use Committee (IACUC) of the University of Pittsburgh. Animals were treated humanely according to the criteria outlined in the "Guide for the Care and Use of Laboratory Animals"

prepared by the National Academy of Sciences and published by the National Institutes of Health.

Liver-specific inactivation of the ILK gene

The ILK-floxed mice were mated with mice from three strains of mice expressing Cre-recombinase under the control of hepatocyte-specific promoters; the albumin promoter, Alpha Fetoprotein (AFP) enhancer-albumin promoter, and Foxa3-promoter. Genotyping was performed by PCR from DNA isolated from the mice tails using previously published primer sequences(Troussard et al., 2003c).

Liver perfusion with collagenase and separation of hepatocytes from non-parenchymal cells of the liver

Mouse hepatocytes from the AFP-albumin-ILK-knock-out animals, albumin-ILK-knock-out animals or Foxa3-ILK-knock-out animals, as well as their respective controls, were isolated by an adaptation of the calcium two step collagenase perfusion technique, as described previously(Block et al., 1996a). Following the liver perfusion, hepatocytes were separated from the non-parenchymal cells of the liver by several centrifugation steps.

Briefly, the cell pellet obtained from the liver perfusion was centrifuged at 500 rpm for 5min and the supernatant was saved. The pellet was subsequently washed with Hanks HBSS buffer and centrifuged at 500rpm for 5min, and the supernatant was again saved for later use while the pellet was kept as the fraction that corresponds to hepatocytes. The supernatants from the last two centrifugations were combined and centrifuged at 600 rpm for 5min. The resulting supernatants were then centrifuged at 1,500 rpm for 5min and the pellet was saved and washed once again with HBSS buffer. This pellet contained all the non-parenchymal cells of the liver (stellate cells, endothelial cells, Kupffer cells, biliar cells).

Immunohistochemistry

Immunohistochemical staining of formalin-fixed, paraffin-embedded liver sections was performed as described previously.

Protein isolation for immunoblotting

Total protein was isolated from the mouse hepatocytes, non-parenchymal cells of the liver or whole livers from the AFP-albumin-ILK-knock-out, albumin-ILK-knock-out or Foxa3-ILK-knock-out animals using 1% sodium dodecyl sulfate (SDS) in RIPA buffer (20 mM Tris/Cl pH 7.5, 150 mM NaCl, 0.5% NP-40, 1% TX-100, 0.25% Sodium Deoxycholated (DOC), 0.6-2 µg/ml aprotinin, 10µM Leupeptin, 1µM Pepstatin).

Light and Transmission Electron Microscopy

Mouse livers were perfusion-fixed through the heart with 2.5% glutaraldehyde in PBS. Liver was removed and immersed in the same fixative for 2 additional days at 4°C. Several 1mm^3 cubes were removed from the liver, were washed 3 times in PBS and were then post-fixed in aqueous 1% OsO_4, 1% $K_3Fe(CN)_6$ for 1 hour. Following 3 PBS washes, the pellet was dehydrated through a graded series of 30-100% ethanol, 100% propylene oxide then infiltrated in 1:1 mixture of propylene oxide: Polybed 812 epoxy resin (Polysciences, Warrington, PA) for 1 hr. After several changes of 100% resin over 24 hrs, the pellet was embedded in molds, cured at 37°C overnight, followed by additional hardening at 65°C for two more days. Ultra thin (60 nm) sections were collected on copper grids, stained with 2% uranyl acetate in 50% methanol for 10 minutes, followed by 1% lead citrate for 7 min. Sections were on a JEOL JEM 1210 transmission electron microscope (Peabody, MA) at 80 kV using am AMT 2K digital camera (Advanced Microscopy Technologies, Danvers MA).

TUNEL assay

Apoptosis in livers from the AFP-albumin-ILK-knock-out, albumin-ILK-knock-out or Foxa3-ILK-knock-out animals was assessed by terminal deoxynucleotidyltransferase-mediated dUTP-biotin nick end-labeling (TUNEL) assay using the ApopTag In Situ Apoptosis Detection Kit from Chemicon (Temecula, CA).

Microarray analysis

cRNA preparation: Total RNA was extracted and purified with Qiagen RNeasy kit (Qiagen, San Diego, CA) from whole livers harvested from 8-week-old AFP-albumin-ILK-knock-out, albumin-ILK-knock-out or Foxa3-ILK-knock-out animals and their respective controls. Five

micrograms of total RNA were used in the first strand cDNA synthesis with T7-d(T)$_{24}$ primer (GGC CAG TGA ATT GTA ATA CGA CTC ACT ATA GGG AGG CGG-(dT)$_{24}$) by Superscript^{TM} II (GIBCO-BRL, Rockville, MD). The second strand cDNA synthesis was carried out at 16°C by adding E. coli DNA ligase, E. coli DNA polymerase I and RnaseH in the reaction. This was followed by the addition of T4 DNA polymerase to blunt the ends of newly synthesized cDNA. The cDNA was purified through phenol/chloroform and ethanol precipitation. The purified cDNA were then incubated at 37°C for 4 hours in an *in vitro* transcription reaction to produce cRNA labeled with biotin using MEGAscript^{TM} system (Ambion, Inc, Austin, TX).

Affymetrix chip hybridization: Fifteen to 20 μg of cRNA were fragmented by incubation in a buffer containing 200 mM Tris-acetate, pH 8.1, 500 mM KOAc, 150 mM MgOAc at 95°C for 35 minutes. The fragmented cRNA were then hybridized with a pre-equilibrated Affymetrix chip (R430 2.0) at 45°C for 14-16 hours. After the hybridization cocktails were removed, the chips were then washed in a fluidic station with low-stringency buffer (6x SSPE, 0.01% Tween 20, 0.005% antifoam) for 10 cycles (2 mixes/cycle) and stringent buffer (100 mM MES, 0.1 M NaCl and 0.01% Tween 20) for 4 cycles (15 mixes/cycle), and stained with SAPE (Strepto-avidin Phycoerythrin). This was followed by incubation with biotinylated mouse anti-avidin antibody, and restained with SAPE.

The chips were scanned in a HP ChipScanner (Affymetrix Inc, Santa Clara, CA) to detect hybridization signals. For quality assurance, all samples were run on Affymetrix test-3 chips to evaluate the integrity of RNA. Samples with RNA 3'/5' ratios less than 2.5 were accepted for further analysis.

7.3   RESULTS

ILK elimination during embryonic development does not affect hepatic embryonic growth
To study the effects of ablation of ILK *in vivo*, we mated the ILK floxed animals with mice expressing Cre-recombinase under three promoters related to hepatocyte-associated transcription factors and genes; AFP-enhancer albumin promoter, albumin promoter or Foxa3 promoter.

DNA from mouse tails from the resulting offspring was used for genotyping the mice. The mice that had a copy of the Cre gene and were homozygous for the floxed-ILK gene were considered to be conditional knock-out animals.

Mice were sacrificed at different time points after birth and their livers were harvested. More specifically, livers were collected starting as early as 1 day after birth, at 14 days, 5 weeks, 8-10 weeks, and 30-39 weeks of age.

Although the complete ILK knock-out is embryonic lethal at the pre-implantation stage, suggesting that ILK is indispensable for normal development, all three types of the ILK conditional knock-out mice in the liver are born normal with normal liver histology, which at birth is indistinguishable between the knock-out and the control WT mice.

This suggests that ILK is most likely not essential for the liver development. Soon after birth, though, the growth of the Foxa3-Cre ILK knock-out mice becomes stunted and the mice at 2 weeks of age are about have the size of their normal litter-mates. This phenomenon however is not true for the albumin-ILK-knock-outs or the AFP-albumin-ILK knock-outs, which appear normal in size.
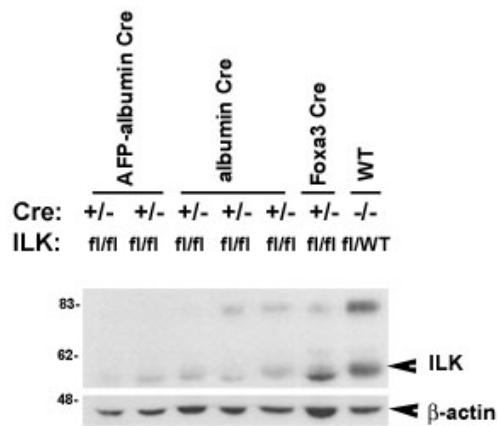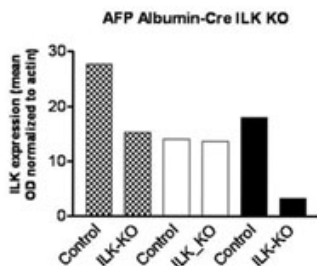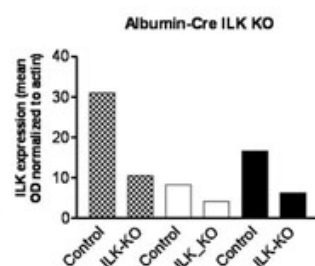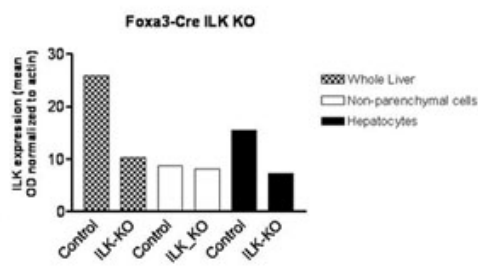
Figure 35: ILK expression level is dramatically reduced in the liver of the conditional knock-out animals and the reduction is due to elimination of the ILK from the hepatocytes A) Western blotting analysis with an anti-ILK monoclonal antibody performed on total cell lysates extracted from whole livers from the AFP-albumin-Cre, albumin-Cre and Foxa3-Cre conditional knock-out animals. β-actin is used as loading control. The last lane corresponds to a wild type animal (WT). B) Bar graph showing the ILK expression level in whole liver, isolated non-parenchymal cells (solid white bars) and isolated hepatocytes (solid black bars) from the control and AFP-albumin-Cre-ILK-knock-out animals. C) Bar graph showing the ILK expression level in whole liver, isolated non-parenchymal cells (solid white bars) and isolated hepatocytes (solid black bars) from the control and albumin-Cre-ILK-knock-out animals. D) Bar graph showing the ILK expression level in whole liver, isolated non-parenchymal cells (solid white bars) and isolated hepatocytes (solid black bars) from the control and Foxa3-Cre-ILK-knock-out animals.

ILK is removed from the liver of the conditional knock out animals

In order to find out whether ILK was indeed removed from those animals, we performed western blot analysis with anti-ILK antibody in whole cell lysates isolated from whole liver. As shown in Figure 35A, ILK was efficiently knocked down in AFP-albumin-ILK-knock-out,

albumin-ILK-knock-out and Foxa3-ILK-knock-out animals. However, there was still a certain amount of ILK remaining in the knock-out animals (see Fig.35A).

ILK is removed from the hepatocytes and not the non-parenchymal cells of the liver

Thus, we next sought to find which population of liver cells the ILK was removed from. To do that we performed a liver perfusion and subsequently we separated the hepatocytes from the non-parenchymal cells. As shown in Fig.35B-D, ILK expression level is almost the same between the control and the conditional knock-outs in the non-parenchymal cells of the AFP-albumin and Foxa3 ILK conditional knock-outs, while it is dramatically reduced in the hepatocyte fraction of the same mice (compare the 2 white bars with the 2 black bars in Fig.35B-D).

This suggests that ILK is indeed removed from the hepatocytes but not the non-parenchymal cells of the liver (endothelial cells, Kupffer cells, stellate cells and biliar cells), explaining why a significant amount of ILK is still present in whole cell lysates from the liver tissue of the conditional knock-out animals (Fig.35A, and Fig. 35B-D, stripped bars).

The ILK conditional knock-out animals exhibit abnormal liver architecture, apoptosis, and biliar malformations

As mentioned above, the liver phenotype of the 1-day old ILK-conditional knock-outs in the liver was normal (data not shown) but as the mice progressed in age their livers exhibited severe abnormalities as compared to the control animals. Macroscopically, while the rest of the organs appeared normal the livers from the ILK conditional knock-outs were paler and their texture was extremely hard.

The abnormalities were confirmed in the microscopic level as well. At the stage of 4 weeks, hepatocytes in all three categories of knock-out mice are not organized in standard (one cell thick) hepatic plates, but they remain in disorganized clumps (Fig.36, compare B to A, D to C, and F and G to E).
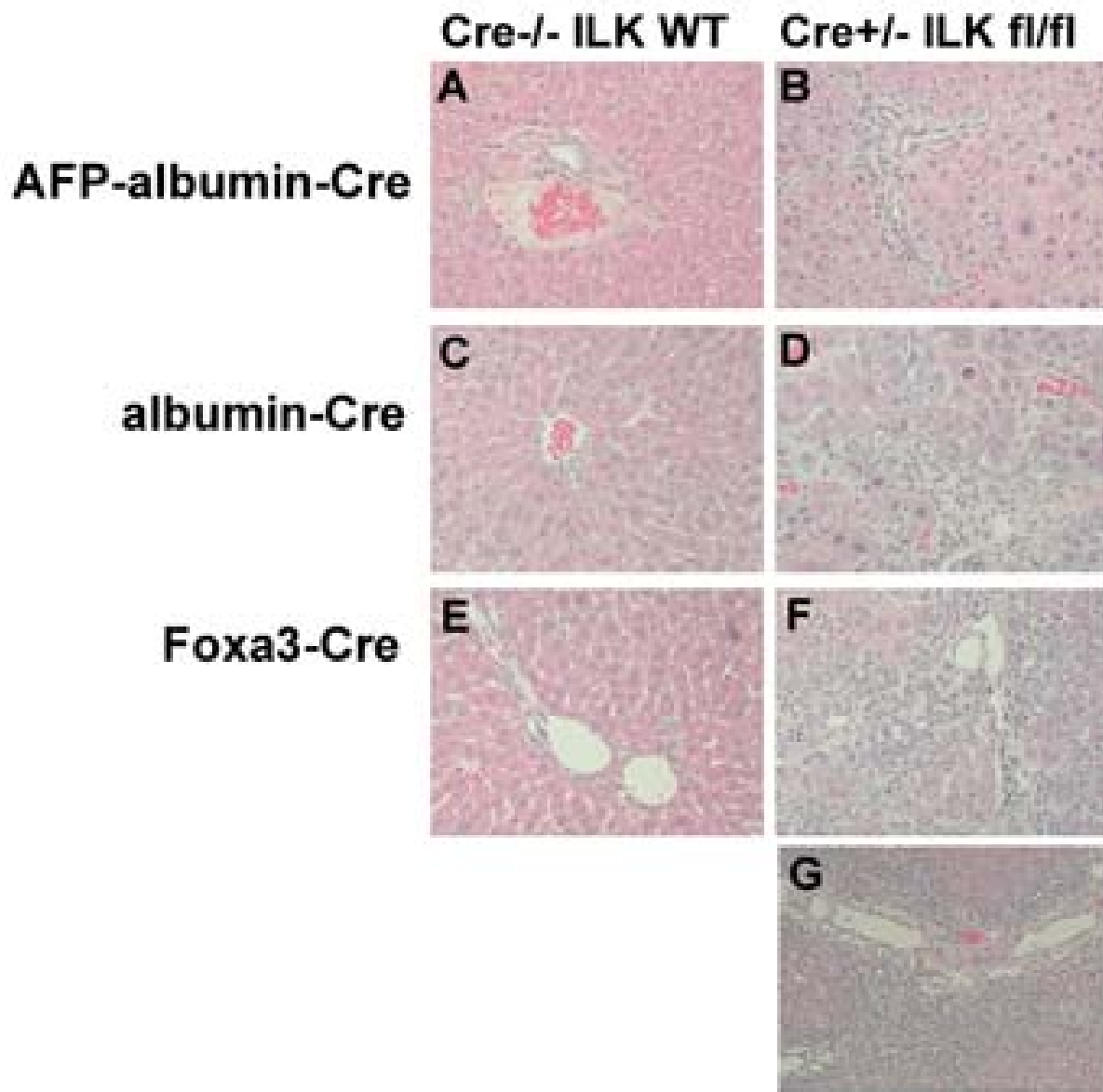
Figure 36: H&E staining from the ILK-conditional knock-out animals in the liver shows dramatic abnormalities H&E staining in the liver of: A, C and E) control WT animals, B) AFP-albumin-ILK knock-out animals, D) albumin-ILK knock-out animals, F and G) Foxa3-ILK knock-out animals.

More importantly, there is diffuse hepatocyte apoptosis, associated with compensatory proliferation and apparent infiltration by inflammatory cells. Finally, livers develop fibrosis akin to cirrhosis.

Interestingly, Foxa3 mice had the most severe phenotype and were completely lacking bile ducts in their portal triads (Fig. 36, compare F and G to E), whereas the other two categories had bile ducts in about 1/3 of the portal triads.

Thus, ablation of ILK from hepatocytes *in vivo* caused severe defects in hepatic tissue architecture, suggesting that ILK is essential for normal liver organization and the formation of the biliar tree.

There is no dosage effect in heterozygous Cre+/- ILK fl/WT animals and there is no toxicity in the Cre+/- ILK WT/WT animals

In order to test whether there was any toxicity effect associated with the observed apoptosis and inflammation in the conditional knock-out animals that could be attributed to the expression of one copy of the Cre-recombinase gene in these mice, we examined the liver histology of Cre positive mice that expressed non-floxed Wild Type (WT) ILK. As shown in Fig.37 A, C, and E, the livers from those animals were completely normal, excluding the possibility of Cre-induced toxicity.
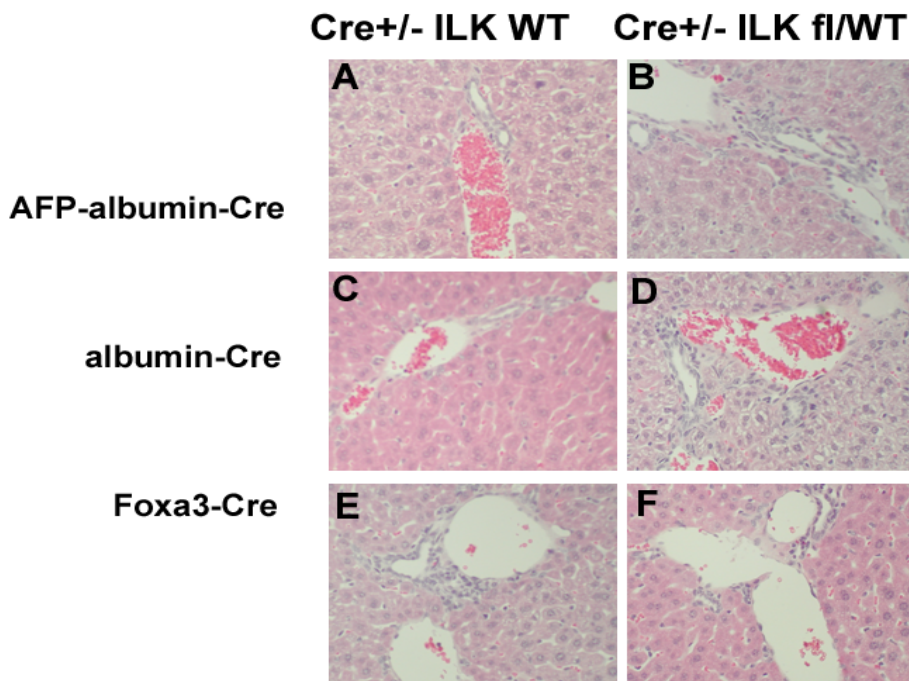
Figure 37: H&E staining of liver sections from mice that are Cre+ and have WT ILK or Cre+ with one copy of the floxed ILK gene A, C, and E) H&E from the Cre+ ILKWT mice livers, B, D and F) H&E from the Cre+ ILK Fl/WT livers.

We next examined whether there was an abnormal phenotype in Cre-positive mice that only had one copy of the floxed ILK gene and one of the WT (ILKfl/WT). No abnormalities were observed in the liver of these ILK heterozygous Cre-positive animals (Fig.37, B, D and F), suggesting that expression of only one allele of the ILK gene is enough for the livers to be normal, and thus there is no dosage effect.

Abnormal ultra-structure of the cell-cell junctions in the conditional knock out animals

In order to better characterize the phenotype observed in the ILK-conditional knock-out animals in the liver, we performed a light and transmission electron microscopy (TEM) study on perfusion-fixed 8-week-old male mice. Interestingly, TEM images show presence of blunted microvilli or complete absence of microvilli from the bile canaliculi (Fig. 38), while the junctional complexes are also compromised. It seems that only tight junctions are present along the canaliculi and not gap junctions or desmosomes (Fig.38). Moreover, all the livers from the conditional knock-out mice have excessive collagen deposition (Fig.38), which explains the hard texture of those livers.
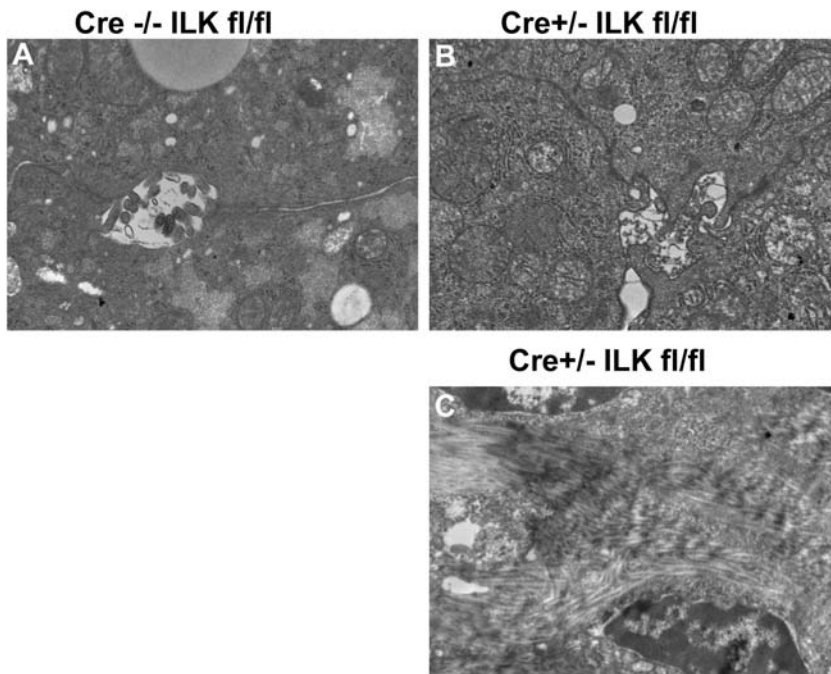
Figure 38: Transmission Electron Microscopic (TEM) analysis of livers from the ILK-conditional knock-out animals. A) TEM image from the liver of a control animal where the microvilli of the canaliculus are visible, B) TEM image from an ILK knock-out animal where there is absence of microvilli, C) TEM image from an ILK knock-out animal where there is evident excessive collagen deposition.

Increased apoptosis in all the ILK- conditional knock-out animals in the liver

Since ILK is known to be involved in regulating cell survival(Attwell et al., 2000a; Persad et al., 2000a), it would be anticipated that elimination of the protein would likely result in cell death. To test whether this is true *in* vivo as well following genetic removal of ILK from the liver, we performed TUNEL staining in formalin-fixed paraffin-embedded liver sections from 8 week-old female mice. Consistent with the apoptotic cells observed by H&E staining, the control livers were negative for TUNEL staining, but the livers from the ILK-conditional knock-out mice had many TUNEL-positive hepatocytes (Fig.39), indicating that there is an ongoing apoptosis in these animals.
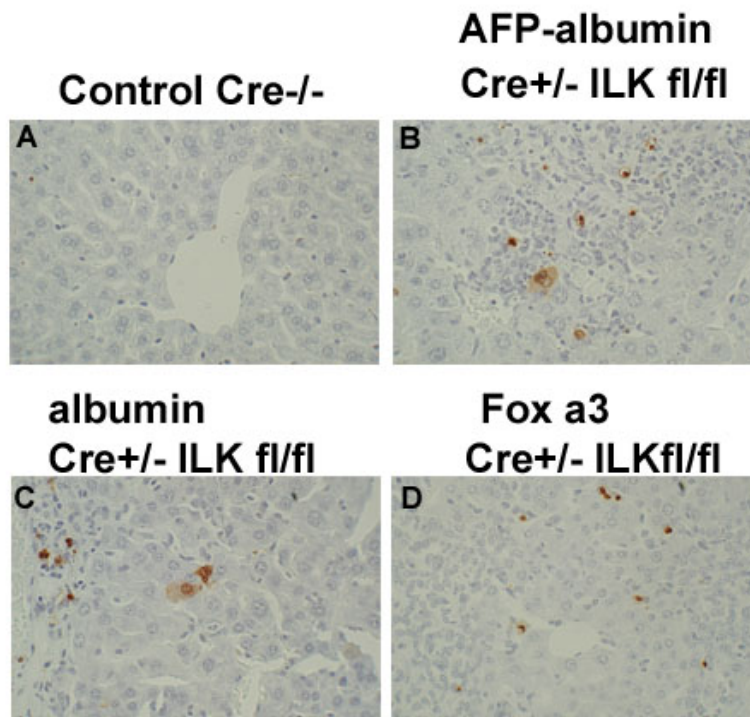
Figure 39: TUNEL staining shows increased apoptosis in the livers of the ILK conditional-knock-out animals. TUNEL staining in liver sections of: A)control WT animal, B) AFP-albumin-Cre-ILK-knock-out animal, C) albumin-Cre-ILK-knock-out animal, D) Foxa3-Cre-ILK-knock-out animal.

Increased proliferation in all the ILK conditional knock-outs in the liver

Cases of increased apoptosis in liver are often associated with increased proliferation, which is a compensatory mechanism associated with liver regeneration(Michalopoulos and DeFrances, 1997). Thus, we also monitored cell proliferation by immunohistochemistry for two cell cycle markers; Proliferating Cell Nuclear Antigen (PCNA), a marker for cells in all stages of cell cycle, and Ki67, a marker for cells in the DNA synthesis phase (Data not shown). As shown in Fig.40, all three types of liver ILK-conditional knock-outs exhibited significantly increased PCNA (Fig.40, compare B, C and D to panel A) and Ki 67 staining (Data not shown), suggesting that hepatocytes are undergoing cell proliferation. Interestingly, the number of actual mitoses is also dramatically increased in the ILK-conditional knock-out animals compared to the controls (Fig.40E).
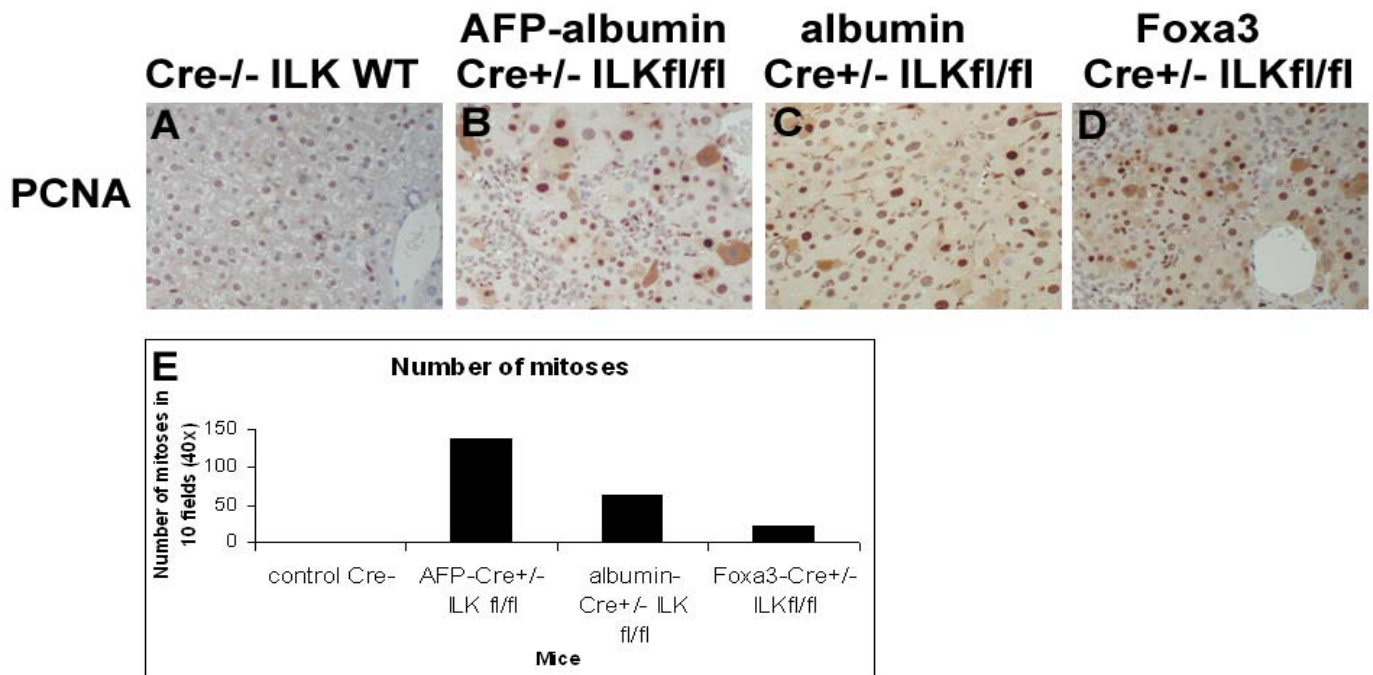
Figure 40: Increased proliferation in the livers of the ILK conditional-knock-out animals. A-D) PCNA staining in livers from control animals (A), AFP-albumin-ILK-knock-out animals (B), albumin-ILK-knock-out animals (C), Foxa3-ILK-knock-out animals (D), E) bar graph showing the number of mitoses in the livers of control and conditional knock-out animals as observed in 10 different fields under the 40x, F-I) Ki 67 staining in livers from control animals (F), AFP-albumin-ILK-knock-out animals (G), albumin-ILK-knock-out animals (H), Foxa3-ILK-knock-out animals (I).

Microarray data analysis

Finally, in order to shed more light upon the mechanism involved in the liver changes observed in the animals that lack ILK from their hepatocytes, we performed a GeneChip Microarray analysis in 8-week old AFP-albumin-ILK-knock-out, albumin-ILK-knock-out and Foxa3-ILK-knock-out animals. The data from the microarray analysis are summarized in separate gene categories in Tables 1-11. In all three types of ILK-conditional knock-outs, the same genes were significantly up- or down-regulated, suggesting that the removal of ILK is responsible for these changes.

In brief, there seems to be an increase in almost all integrin genes (Table 1) possibly in order to compensate for the lost signal from the matrix due to the removal of the ILK. At the same time, there is a significant upregulation in all the types of procollagen genes (Table 2), which explains why there is excessive deposition of collagen in the electron microscopic images (Figure 38C). More striking was the fact that in all three conditional knock-outs, there was an across the board decrease of many differentiation-related markers, especially in the cytochrome P450 family members (Table 3) indicating a decrease in differentiation. Interestingly, increased expression of the mRNA levels of several apoptosis-related genes such as annexins, Bax, Bad, PUMA, TNF (Table 6) supports our previous data showing apoptosis in the livers of the conditional knock-out animals (Figure 39). Furthermore, an interesting change in several growth factors (Table 4), transcription factors (Table 5), signaling proteins (Table 7), several classes of proteases (Table 9), cell adhesion proteins (Table 10) and cell cycle proteins (Table 11), underlines the complexity of the signaling events triggered by the removal of ILK signaling and the importance of that for the normal liver function and homeostasis.

7.4   DISCUSSION

Cell-ECM adhesions are of utmost importance for the normal signal transduction between the environment and the cells within a tissue. Liver is a good example of an organ that is greatly dependent on the ECM, deregulations of which can give rise to serious diseases such as cirrhosis.

In the present study, we utilized the LoxP-Cre system(Kos, 2004) to eliminate ILK from mice at different stages of their development/life by mating the ILK-floxed animals with one of three Cre-expressing strains of mice; AFP-albumin-Cre, albumin-Cre or Foxa3-Cre mice.

Our results show that ILK was indeed removed from the animals and in fact it was specifically removed from hepatocytes and not the non-parenchymal cells of the liver. Although the anti-ILK antibody worked nicely for western blotting analyses, we encountered great difficulties in immunohistochemical studies with all the commercially available anti-ILK antibodies that we tried.

Interestingly, there was never a doubt about the phenotype of the ILK conditional-knock-out animals. All three types of ILK conditional knock-out in the liver had abnormal liver architecture, evident apoptosis, compensatory proliferation and different degrees of biliar malformations with the Foxa3-ILK-knock-out mice having complete absence of bile ducts. Moreover, the abnormally formed or completely absent microvilli in the canaliculi space and the abnormal junctional complexes as seen by electron microscopy further corroborate the idea that ILK is essential for normal liver architecture.

The observed hepatocyte apoptosis is consistent with previous studies where inhibition of ILK results in apoptosis in cancer cell lines(Persad et al., 2000a), or overexpression of ILK inhibits anoikis(Attwell et al., 2000a). In fact, as shown in Chapter 6, elimination of ILK from the ILK-floxed hepatocytes *in vitro* and *in vivo* by adenoviral delivery of Cre-recombinase gives rise to massive apoptosis in cultured cells and fulminant hepatitis in the whole animal. The adenovirus-mediated elimination of ILK from hepatocytes represents a more acute response to the removal of ILK while the genetic elimination of ILK corresponds to a chronic response but with severe architectural abnormalities involved.

Furthermore, the microarray analysis provided us with more insight into the mechanism governing the observed changes following elimination of ILK. ILK removal is accompanied by a dramatic reduction in the mRNA levels of most members of the cytochrome P450 family (Table 1), indicating inhibited differentiation, while at the same time there is an up-regulation of

integrins α4, α5, α6, αL, αX, β1, β2 and β5, suggesting an attempt to compensate for the loss of ILK signaling by elevating the level of integrins and matrix-related genes (Table 3). Overall, the microarray analysis provided us with explanations as to why there is such a phenotype in the mice, although it also generated a lot of questions that need to be addressed in the future regarding the pathways that are being activated or blocked upon ILK elimination.

In conclusion, the dramatic changes seen with ablation of ILK demonstrate the importance of matrix signaling in hepatocytes and in the whole liver, and the important role of ILK for maintaining the normal liver architecture.

Table 1. Changes in the mRNA expression level of <u>integrins</u> in the ILK conditional knock-out animals. The number next to the name of the gene corresponds to the fold increase or decrease of the mRNA expression level of that gene in the ILK-conditional knock-out animal compared to the respective control animal.

Gene	Albumin-Cre+/-ILKfl/fl	AFP-albumin-Cre+/- ILK fl/fl	Foxa3-Cre+/-ILKfl/fl
integrin alpha 5	2.67	1.94	1.78
integrin alpha 6	5.14	9.42	54.19
integrin alpha 8	7.33	2.03	20.02
integrin beta 1	1.89	1.63	1.85
integrin beta 2	3.62	1.90	2.66
integrin beta 5	2.58	1.84	2.46

Table 2. Changes in the mRNA expression level of <u>ECM proteins</u> in the ILK conditional knock-out animals. The number next to the name of the gene corresponds to the fold increase or decrease of the mRNA expression level of that gene in the ILK-conditional knock-out animal compared to the respective control animal.

Gene	Albumin-Cre+/-ILKfl/fl	AFP-albumin-Cre+/-ILKfl/fl	Foxa3-Cre+/-ILKfl/fl
Nidogen 1	15.17	14.69	35.62
procollagen, type I, alpha 1	14.34	9.73	2.86
procollagen, type I, alpha 2	14.97	6.29	12.97
procollagen, type III, alpha 1	17.28	4.16	7.90
procollagen, type IV, alpha 1	5.99	7.67	7.78
procollagen, type IV, alpha 5	2.41	4.24	4.35
procollagen, type V, alpha 1	5.81	2.08	8.01
procollagen, type V, alpha 2	8.63	2.63	5.95
procollagen, type VI, alpha 1	3.11	4.52	3.58
procollagen, type VI, alpha 2	2.49	4.88	21.08
Vimentin	5.53	6.05	7.95

Table 3. Changes in <u>liver-differentiation-related genes</u> in the ILK conditional knock-out animals. The number next to the name of the gene corresponds to the fold increase or decrease of the mRNA expression level of that gene in the ILK-conditional knock-out animal compared to the respective control animal.

Gene	Albumin-Cre+/-ILKfl/fl	AFP-albumin-Cre+/-ILKfl/fl	Foxa3-Cre+/-ILKfl/fl
AFP	8.19	62.98	4.45
cytochromeP450, CYP4F13	0.46	0.89	0.33
cytochrome P450, 17	0.11	0.97	0.10
cytochrome P450, 1a2, aromatic compound inducible	0.38	0.44	0.26
cytochrome P450, 2c39	0.05	0.42	0.13
cytochrome P450, 2c40	0.33	0.26	0.06
cytochrome P450, 2d10	0.60	0.89	0.28
cytochrome P450, 2g1	0.32	0.66	0.18
cytochrome P450, 2j5	0.35	0.28	0.19
cytochrome P450, 46	0.79	0.08	0.66
cytochrome P450, 4a14	0.50	0.16	0.32
cytochrome P450, 51	0.80	0.36	0.54
cytochrome P450, 7b1	0.30	0.18	0.14
cytochrome P450, CYP3A	0.01	0.12	0.02
cytochrome P450, steroid inducible 3a41	0.06	0.24	0.02
cytochrome P450, subfamily IVF, polypeptide 14	0.23	0.81	0.15
H19 fetal liver mRNA	6.56	169.70	11.21
hexokinase 1	1.58	2.39	10.93
hexokinase 2	1.58	3.45	2.90

met proto-oncogene	3.08	0.57	0.97
Serum amyloid A 2	6.42	7.85	1.87
Villin	-	30.3	7.52
Villin 2	1.82	-	-

Table 4. Changes in <u>Growth Factor genes</u> in the ILK conditional knock-out animals. The number next to the name of the gene corresponds to the fold increase or decrease of the mRNA expression level of that gene in the ILK-conditional knock-out animal compared to the respective control animal.

Gene	Albumin-Cre+/- ILKfl/fl	AFP-albumin-Cre+/- ILK fl/fl	Foxa3-Cre+/- ILKfl/fl
BDNF	1.70	0.10	34.18
Bone morphogenetic protein 1	0.79	0.89	0.57
Bone morphogenetic protein 2	0.77	0.47	0.85
Bone morphogenetic protein 7	0.72	0.27	0.86
colony stimulating factor 1 (macrophage)	3.03	2.31	3.36
EGFR	0.70	0.68	0.43
FGF	1.97	1.64	7.94
FGF-1	0.42	0.39	0.19
FGF-4	0.74	1.33	2.75
FGF-receptor 1	2.62	2.44	5.24
FGF-receptor 2	1.89	1.65	2.15
FGF-9	1.32	2.65	0.67
FGF-21	2.43	0.74	2.63
Growth differentiation factor 9	2.03	0.84	0.87
insulin-like growth	15.43	6.43	23.81

factor 2			
insulin-like growth factor 2 receptor	1.99	0.75	3.43
insulin-like growth factor 2, binding protein 3	2.55`	15.54	3.64
insulin-like growth factor binding protein 7	4.06	2.07	3.39
nerve growth factor, beta	5.24	1.60	4.62
PDGF alpha	1.68	3.64	3.21
PDGF, polypeptide C	3.07	2.69	5.32
TGF alpha	1.32	1.62	1.91
TGFb induced, 68 kDa	2.01	1.59	2.90
TGF beta 1	2.60	2.06	3.85
TGF-beta type I receptor	1.36	1.82	2.23
VEGF-A	0.53	0.50	0.23

Table 5. Changes in <u>Transcription Factor genes</u> in the ILK conditional knock-out animals.
The number next to the name of the gene corresponds to the fold increase or decrease of the mRNA expression level of that gene in the ILK-conditional knock-out animal compared to the respective control animal.

Gene	Albumin-Cre+/- ILKfl/fl	AFP-albumin-Cre+/- ILK fl/fl	Foxa3-Cre+/- ILKfl/fl
adaptor protein complex AP-1, beta 1 subunit	2.08	1.33	0.70
E2F transcription factor 1	1.81	1.25	6.58
Foxa3	1.31	1.57	0.85
Foxp1	2.03	2.61	2.38
Gut-enriched Kruppel-like factor GKLF	0.81	0.34	2.16
HIF-1alpha	0.60	0.78	6.86
HNF1beta	28.47	1.66	2.17
HNF-3forkhead homolog-4 (HFH-4)	0.47	0.86	2.52
HNF-4	1.39	0.80	1.20
homeo box C9 (Hoxc9)	3.49	4.67	0.22
Hoxa11	0.33	0.50	0.62
Hoxa13	1.68	1.61	10.35
homeobox transcription factor NKX2-3	0.81	0.61	2.02
Hoxa3	15.60	0.29	5.79
Kruppel-like factor	5.00	1.58	6.10

7			
Kruppel-like factor 15	0.69	0.69	0.64
Kruppel-like factor 9	0.56	0.61	0.38

Table 6. Changes in <u>Apoptosis-related genes</u> in the ILK conditional knock-out animals. The number next to the name of the gene corresponds to the fold increase or decrease of the mRNA expression level of that gene in the ILK-conditional knock-out animal compared to the respective control animal.

Gene	Albumin-Cre+/- ILKfl/fl	AFP-albumin-Cre+/- ILK fl/fl	Foxa3-Cre+/- ILKfl/fl
annexin A1	3.44	2.43	5.28
annexin A2	19.22	16.34	5.30
annexin A4	2.72	1.55	5.09
annexin A6	1.82	1.86	1.82
annexin V	3.44	4.80	5.10
BCL2-antagonistkiller 1 (Bak1)	1.76	1.50	3.50
Bax	1.64	1.33	2.57
Bcl-associated death promoter (Bad)	2.49	0.86	7.12
BH3 interacting domain death agonist (Bid)	0.80	0.41	0.51
caspase 2	1.33	1.67	3.24
caspase 3	1.32	1.32	27.46
caspase 7	0.48	0.70	0.45
caspase 8	0.72	0.84	0.85
caspase 11	2.73	2.42	3.76
caspase 12	6.11	4.52	4.09
cytochrome c oxidase, subunit Va	0.64	0.91	0.43
cytochrome c oxidase, subunit Vb	0.83	0.67	0.41
cytochrome c oxidase,	0.62	0.70	1.97

subunit VI a, polypeptide 2			
cytochrome c oxidase, subunit VIc	0.77	0.74	0.36
cytochrome c oxidase, subunit VIIc	0.83	0.47	0.55
LPS-induced TNF-alpha factor	2.73	3.10	2.12
programmed cell death 4	0.59	0.49	0.24
programmed cell death 6	1.16	0.73	0.75
PUMA	1.74	2.09	0.65
tumor necrosis factor receptor superfamily, member 21	3.01	1.51	2.12
tumor necrosis factor receptor superfamily, member 9	1.09	0.59	0.62
ubiquinol-cytochrome c reductase core protein 1	0.67	1.93	0.56

Table 7. Changes in <u>Signaling pathway-related genes</u> in the ILK conditional knock-out animals. The number next to the name of the gene corresponds to the fold increase or decrease of the mRNA expression level of that gene in the ILK-conditional knock-out animal compared to the respective control animal.

Gene	Albumin-Cre+/- ILKfl/fl	AFP-albumin-Cre+/- ILK fl/fl	Foxa3-Cre+/- ILKfl/fl
adenylate cyclase 7	2.32	8.55	2.82
Cdc42	1.61	1.77	2.52
dedicator of cyto-kinesis 2 (Dock2)	8.25	4.38	5.49
ELK1	2.59	3.13	4.12
ELK3	1.99	1.21	5.18
frizzled homolog 6	1.31	1.43	1.86
frizzled homolog 2	1.22	0.30	3.96
Harvey rat sarcoma oncogene, subgroup R (Rras)	2.50	2.34	2.64
inhibitor of kappaB kinase gamma (Ikbkg)	2.05	1.48	25.20
Jun oncogene	1.61	1.79	5.56
Jun-B oncogene	1.53	1.40	4.87
MAP2K5	0.40	0.64	1.39
MAP2K6	0.60	0.49	0.07
MAP3K5	0.79	0.85	0.69
Map3k4	1.72	2.67	1.95
Map4k4	2.24	2.56	5.41
Map3k14	4.76	0.69	1.28
MAPK3	2.04	1.70	2.40

neuroblastoma ras oncogene (Nras)	1.86	2.31	2.08
N-myc downstream regulated 1	5.95	2.47	33.90
N-myc downstream regulated 3	0.66	0.51	0.53
nuclear factor kappa B subunit p100 (Nfkb2)	8.70	10.34	7.89
p21 (CDKN1A)-activated kinase 1 (Pak1)	3.05	2.10	5.07
protein kinase C, epsilon	0.71	0.66	1.87
ras homolog 9 (RhoC)	5.53	6.49	8.26
Ras suppressor protein 1 (RSU-1)	1.53	1.44	1.73
Rho-associated coiled-coil forming kinase 2 (ROCK2)	1.22	1.96	2.04
Rous sarcoma oncogene	4.04	5.72	20.36
secreted frizzled-related sequence protein 1	1.58	1.56	2.19
spleen tyrosine kinase (Syk)	12.93	20.33	6.50
STAT1	0.63	2.79	0.70
STAT3	1.72	2.14	3.55

STAT5b	0.71	1.60	1.87
STAT6	1.36	1.99	2.60
Wnt10a	1.79	1.30	3.28
Wnt5b	1.55	1.53	0.65

Table 8. Changes in <u>Cytoskeleton-related genes</u> in the ILK conditional knock-out animals. The number next to the name of the gene corresponds to the fold increase or decrease of the mRNA expression level of that gene in the ILK-conditional knock-out animal compared to the respective control animal.

Gene	Albumin-Cre+/- ILKfl/fl	AFP-albumin-Cre+/- ILK fl/fl	Foxa3-Cre+/- ILKfl/fl
actin, beta, cytoplasmic	1.41	1.77	2.66
Gelsolin	2.10	3.28	1.62
Lamin A	3.27	2.11	3.54
Lamin B1	2.96	1.83	2.00
microtubule-associated protein tau	7.46	1.92	16.37
myocyte enhancer factor 2A	0.64	0.70	2.02
myocyte enhancer factor 2B	**0.57**	**0.87**	0.81
Myosin heavy chain IX	1.64	2.50	9.08
myosin IC	4.41	1.44	3.05
myosin IXb	2.65	3.10	1.50
myosin VIIb	6.39	3.19	1.72
myosin X	2.27	2.15	3.57
tropomyosin 1, alpha	4.51	3.24	15.10

tropomyosin 3, gamma	1.59	1.85	3.18
tubulin, alpha 1	2.66	2.69	7.34
tubulin, beta 5	2.19	3.21	4.23
Vimentin	**5.53**	**6.05**	7.95

Table 9. Changes in <u>proteases</u> in the ILK conditional knock-out animals. The number next to the name of the gene corresponds to the fold increase or decrease of the mRNA expression level of that gene in the ILK-conditional knock-out animal compared to the respective control animal.

Adamts: a disintegrin-like and metalloprotease with thrombospondin type 1 motif, **Adam:** a disintegrin and metalloprotease domain.

Gene	Albumin-Cre+/- ILKfl/fl	AFP-albumin-Cre+/- ILK fl/fl	Foxa3-Cre+/- ILKfl/fl
Adam10	5.91	0.56	8.13
Adam17	0.55	0.63	0.60
Adamts5	10.64	32.60	14.46
Adamts8	1.79	0.58	2.04
calpain 1	10.29	2.19	10.06
calpain 6	7.37	2.61	3.72
calpain 7	0.83	0.66	0.61
calpain 12	0.40	2.13	1.86
Cathepsin F	0.69	0.74	0.79
Cathepsin K	1.80	19.80	2.06
Cathepsin S	3.94	4.28	3.95
MMP-2	7.20	109.66	6.58
MMP-7	6.05	2.01	1.35
MMP-14	5.72	3.06	4.27
MMP-15	2.81	3.68	1.87
MMP-19	0.88	0.70	2.70
MMP-23	12.38	1.73	6.46
plasminogen activator, tissue	9.88	11.91	9.06
tissue inhibitor of MMP-3	1.94	3.56	3.57
Trypsin 2	0.78	0.24	0.15
urokinase-type plasminogen activator receptor, type 2	2.03	2.45	2.18

Table 10. Changes in <u>genes encoding adhesion molecules</u> in the ILK conditional knock-out animals. The number next to the name of the gene corresponds to the fold increase or decrease of the mRNA expression level of that gene in the ILK-conditional knock-out animal compared to the respective control animal.

Gene	Albumin-Cre+/- ILKfl/fl	AFP-albumin-Cre+/- ILK fl/fl	Foxa3-Cre+/- ILKfl/fl
Activated leukocyte cell adhesion molecule (ALCAM)	4.11	2.08	8.28
cadherin 1	3.52	16.43	3.75
Cadherin 2	0.77	0.87	0.95
Cadherin 23 (otocadherin)	0.78	0.78	0.48
catenin alpha 1	1.43	2.19	1.80
Catenin beta	2.21	0.87	4.05
CEA-related cell adhesion molecule 1	0.48	0.36	0.46
CEA-related cell adhesion molecule 9	0.71	0.11	2.55
Claudin 1	3.26	3.14	2.03
Claudin 2	2.06	1.91	2.94
Claudin 3	2.02	2.07	2.42
Claudin 6	1.74	0.34	6.86
Claudin 7	1.97	1.52	5.14
Connexin 43	7.14	0.81	2.08
Gamma parvin	2.23	26.47	7.43
Integrin-linked kinase (ILK)	0.50	0.50	0.78
NCAM-1	2.50	2.70	6.27
selectin, platelet (p-selectin) ligand	2.91	2.52	2.23

(Selpl)			
tight junction protein 2	2.26	1.69	3.90
Talin	0.53	1.65	2.29
Vinculin	2.62	2.28	3.12
vascular cell adhesion molecule 1 (Vcam1)	15.06	3.68	2.53

Table 11. Changes in <u>cell-cycle-related genes</u> in the ILK conditional knock-out animals. The number next to the name of the gene corresponds to the fold increase or decrease of the mRNA expression level of that gene in the ILK-conditional knock-out animal compared to the respective control animal.

Gene	Albumin-Cre+/- ILKfl/fl	AFP-albumin-Cre+/- ILK fl/fl	Foxa3-Cre+/- ILKfl/fl
Arrestin, beta 2	1.96	2.02	4.64
Cdc20	2.59	5.46	3.42
Cdc25a	1.42	2.40	7.77
Cdc37	0.61	0.50	0.75
Cdk4	1.39	1.67	1.97
Cdk5	0.54	0.70	2.07
cyclin A2	2.58	2.52	1.88
cyclin B2	2.70	2.24	12.09
cyclin C	1.82	0.79	0.63
cyclin G	0.66	0.67	1.65
cyclin G2	1.47	1.50	2.43
cyclin I	0.73	0.84	0.71
cyclin-dependent kinase inhibitor 1A (P21)	5.59	3.51	10.59
Gadd45b	1.94	0.21	15.97
growth arrest specific 5	0.70	0.29	0.43
growth arrest specific 1	0.76	0.87	0.46
Ki 67	11.67	2.09	2.08

8.0 GENERAL DISCUSSION AND FUTURE DIRECTIONS

In the present Thesis dissertation, I focused on two major areas of research. First, I investigated the cellular and molecular mechanisms that govern cell-matrix and cell-cell adhesions. In that regard, as described in Chapters 2 and 3, I examined the role of novel cell-matrix adhesion proteins in the normal function of the cells.

More sprecifically, in Chapter 2 migfilin is identified not only as a cell-matrix adhesion protein but also as a cell-cell adhesion protein. Moreover, migfilin is shown to be an essential component of cell-cell adhesions in endothelial and epithelial cells since depletion of the protein leads to compromised organization of the adherens junctions and as a result to a weakened cell-cell adhession.

Furthermore, in Chapter 3, the role of RSU-1, a newly identified PINCH-binding protein, was examined in cell-adhesion-related functions. RSU-1 is shown to be important in regulating cell spreading and Rac activity, functions highly relevant to cell adhesion.

In the second part of my Thesis, I investigated the role of one of the cell-matrix adhesion proteins, namely ILK, in the system of hepatocyte differentiation and in liver biology in general. As described in Chapter 5, ILK along with PINCH and parvin play an important role during the matrix-induced hepatocyte differentiation.

Thus, it is not surprising that removal of ILK either from hepatocytes or from the whole liver (Chapters 6 and 7, respectively) has a dramatic effect. Depletion of ILK from cultured hepatocytes *in vitro* leads to massive apoptosis, clearly showing that ILK is absolutely essential for hepatocyte survival. Furthermore, removal of ILK from the whole animal *in vivo*, by

injecting the ILK-floxed animals with Cre-recombinase-expressing adenovirus, results in fulminant hepatitis (Chapter 6). Last but not least, genetic elimination of the ILK gene specifically from the liver by breeding the ILK-floxed animals with AFP-albumin, albumin, or Foxa3-Cre trangenics, results in animals whose livers are completely disorganized, fibrotic, with many cells that undergo apoptosis, with abnormal mitoses and great diffects in the biliar system (Chapter 7).

Taking into account the fact that complete ILK knock-out is embryonic lethal at a stage as early as peri-implantation (Sakai et al., 2003), it is not surprising that ILK is proven to be critical as well, for a specific organ such as the liver. The work presented here, clearly demonstates the significance of ILK for hepatocyte survival and for maintaining normal liver architecture and function, suggesting that liver is greatly dependent upon cell-matrix interactions and the signaling pathways that they activate.

Therefore, the present work emphasizes the significance of cell-matrix adhesion proteins and their interactions in fundamental cellular processes such as survival, differentiation, cell spreading, and cell-cell communication, while it also highlights the importance of such a protein (ILK) in the specific biological system of the liver.

However, there are still a few unanswered questions that need to be addressed in the future in order to complete our understanding of the molecular mechanism by which each of the studied proteins works. For instance, how does the interaction of PINCH and RSU-1 affect different cellular functions? Or, what is the exact mechanism by which ILK exerts its actions in the liver? What is the molecular pathway that gets activated? What is the series of events that leads from the genetic elimination of ILK to the extreme phenotype that we observed?

In conclusion, the present work provides new insight into the role of matrix, cell-matrix adhesion proteins and their interactions both in basic cellular function and in application on a specific organ system and shows a good correlation between *in vitro* and *in vivo* findings.

BIBLIOGRAPHY

Adams, C. L. and Nelson, W. J. (1998). Cytomechanics of cadherin-mediated cell--cell adhesion. *Curr. Opin. Cell Biol.* **10**, 572-577.

Ahmed, N., Oliva, K., Rice, GE., Quinn, MA. (2004). Cell-free 59kDa immunoreactive integrin-linked kinase: a novel marker for ovarian carcinoma. *Clin Cancer Res* **10**, 2415-20.

Ahmed, N., Riley, C., Oliva, K., Stutt, E., Rice, GE., Quinn, MA. (2003). Integrin-linked kinase expression increases with ovarian tumour grade and is sustained by peritoneal tumour fluid. *JPathol* **201**, 229-37.

Akazawa, H., Kudoh, S., Mochizuki, N., Takekoshi, N., Takano, H., Nagai, T. and Komuro, I. (2004). A novel LIM protein Cal promotes cardiac differentiation by association with CSX/NKX2-5. *J Cell Biol* **164**, 395-405.

Attwell, S., Roskelley, C. and Dedhar, S. (2000). The integrin-linked kinase (ILK) suppresses anoikis. *Oncogene* **19**, 3811-5.

Attwell, S., Mills, J., Troussard, A., Wu, C. and Dedhar, S. (2003). Integration of cell attachment, cytoskeletal localization, and signaling by integrin-linked kinase (ILK), CH-ILKBP, and the tumor suppressor PTEN. *Mol Biol Cell* **14**, 4813-25. Epub 2003 Sep 05.

Avizienyte, E., Wyke, A., Jones, R., McLean, G., Westhoff, M., Brunton, V., and Frame, M. (2002). Src-induced de-regulation of E-cadherin in colon cancer cells requires integrin signaling. *Nat Cell Biol* **4**, 632-638.

Bach, I. (2000). The LIM domain: regulation by association. *Mech dev* **91**, 5-17.

Bellanger, J. M., Astier, C., Sardet, C., Ohta, Y., Stossel, T. P. and Debant, A. (2000). The Rac1- and RhoG-specific GEF domain of Trio targets filamin to remodel cytoskeletal actin. *Nat Cell Biol* **2**, 888-92.

Ben-Ze'ev, A. (1999). The dual role of cytoskeletal anchor proteins in cell adhesion and signal transduction. *Ann NY Acad Sci* **886**, 37-47.

Block, G. D., Locker, J., Bowen, W. C., Petersen, B. E., Katyal, S., Strom, S. C., Riley, T., Howard, T. A. and Michalopoulos, G. K. (1996). Population expansion, clonal growth, and specific differentiation patterns in primary cultures of hepatocytes induced by HGF/SF, EGF and TGF alpha in a chemically defined (HGM) medium. *J Cell Biol* **132**, 1133-49.

Braga, V. M. M. (2002). Cell-cell adhesion and signalling. *Curr Opin Cell Biol* **14**, 546-556.

Brakebusch, C. and Fassler, R. (2003). The integrin-actin connection, an eternal love affair. *Embo J* **22**, 2324-33.

Braun, A., Bordoy, R., Stanchi, F., Moser, M., Kostka, G. G., Ehler, E., Brandau, O. and Fassler, R. (2003). PINCH2 is a new five LIM domain protein, homologous to PINCHand localized to focal adhesions. *Exp Cell Res* **284**, 239-50.

Bucher, N. L., Robinson, GS., Farmer, SR. . (1990). Effects of extracellular matrix on hepatocyte growth and gene expression: implications for hepatic regeneration and the repair of liver injury. . *Semin Liver Dis* **10**, 11-19.

Burridge, K. and Chrzanowska-Wodnicka, M. (1996). Focal adhesions, contractility, and signaling. *Annu Rev Cell Dev Biol* **12**, 463-518.

Cairns, R., Khokha, R., Hill, RP. (2003). Molecular mechanisms of tumor invasion and metastasis: an integrated view. *Curr Mol Medicine* **3**, 659-71.

Cavallaro, U., Christofori, G. (2001). Cell adhesion in tumor invasion and metastasis:loss of the glue is not enough. *Biochim et Biophys ACTA* **1552**, 39-45.

Chaney, L. K. and Jacobson, B. S. (1983). Coating cells with colloidal silica for high yield isolation of plasma membrane sheets and identification of transmembrane proteins. *J Biol Chem* **258**, 10062-72.

Chen, Y. T., Stewart, D. B. and Nelson, W. J. (1999). Coupling assembly of the E-cadherin/beta-catenin complex to efficient endoplasmic reticulum exit and basal-lateral membrane targeting of E-cadherin in polarized MDCK cells. *J Cell Biol* **144**, 687-99.

Clark, K. A., McGrail, M. and Beckerle, M. C. (2003). Analysis of PINCH function in Drosophila demonstrates its requirement in integrin-dependent cellular processes. *Development* **130**, 2611-21.

Comerford, K. M., Lawrence, D. W., Synnestvedt, K., Levi, B. P. and Colgan, S. P. (2002). Role of vasodilator-stimulated phosphoprotein in PKA-induced changes in endothelial junctional permeability. *FASEB J.* **16**, 583-5.

Conacci-Sorrell, M., Zhurinsky, J., Ben-Ze'ev, A. (2002). The cadherin-catenin adhesion system in signaling and cancer. *J Clin Invest* **109**, 987-991.

D'Amico, M., Hulit, J., Amanatullah, D. F., Zafonte, B. T., Albanese, C., Bouzahzah, B., Fu, M., Augenlicht, L. H., Donehower, L. A., Takemaru, K. et al. (2000). The integrin-linked kinase regulates the cyclin D1 gene through glycogen synthase kinase 3beta and cAMP-responsive element-binding protein-dependent pathways. *J Biol Chem* **275**, 32649-57.

Dai, D. L., Makretsov, N., Campos, E. I., Huang, C., Zhou, Y., Huntsman, D., Martinka, M. and Li, G. (2003). Increased expression of integrin-linked kinase is correlated with melanoma progression and poor patient survival. *Clin Cancer Res* **9**, 4409-14.

Dawid, I., Breen, JJ., Toyama, R. (1998). LIM domains: multiple roles as adapters and functional modifiers in protein interactions. *Trends Genet* **14**, 156–162.

Dedhar, S. (2000). Cell-substrate interactions and signaling through ILK. *Curr Opin Cell Biol* **12**, 250-256.

Delcommenne, M., Tan, C., Gray, V., Rue, L., Woodgett, J. and Dedhar, S. (1998). Phosphoinositide-3-OH kinase-dependent regulation of glycogen synthase kinase 3 and protein kinase B/AKT by the integrin-linked kinase. *Proc Natl Acad Sci U S A* **95**, 11211-6.

Dougherty, GW., Chopp, T., Qi, S. and Cutler, M. L. (2005). The Ras suppressor Rsu-1 binds to the LIM 5 domain of the adaptor protein PINCH1 and participates in adhesion-related functions. *Exp Cell Res* **306**, 168-79.

Friedrich, E. B., Liu, E., Sinha, S., Cook, S., Milstone, D. S., MacRae, C. A., Mariotti, M., Kuhlencordt, P. J., Force, T., Rosenzweig, A. et al. (2004). Integrin-linked kinase regulates endothelial cell survival and vascular development. *Mol Cell Biol* **24**, 8134-44.

Fukuda, T., Chen, K., Shi, X. and Wu, C. (2003a). PINCH-1 is an obligate partner of integrin-linked kinase (ILK) functioning in cell shape modulation, motility, and survival. *J Biol Chem* **278**, 51324-33.

Fukuda, T., Guo, L., Shi, X. and Wu, C. (2003b). CH-ILKBP regulates cell survival by facilitating the membrane translocation of protein kinase B/Akt. *J Cell Biol* **160**, 1001-8.

Geiger, B., Bershadsky, A., Pankov, R. and Yamada, K. M. (2001). Transmembrane crosstalk between the extracellular matrix--cytoskeleton crosstalk. *Nat Rev Mol Cell Biol* **2**, 793-805.

Graff, J., Deddens, JA., Konicek, BW., Colligan, BM., Hurst, BM., Carter, HW., Carter, JH. (2001). Integrin-linked kinase expression increases with prostate tumor grade. *Clin Cancer Res* **7**, 1987-91.

Graham, F., Prevec, L. (1991) In Methods in Molecular Biology. Humana, Clifton, NJ.

Grashoff, C., Thievessen, I., Lorenz, K., Ussar, S., Fassler, R. (2004). Integrin-linked kinase: integrin's mysterious partner. *Curr Opin Cell Biol* **16**, 565-71.

Grevengoed, E. E., Price, M. H., McCartney, B. M., Hayden, M. A., DeNofrio, J. C. and Peifer, M. (2002). Abelson kinase regulates epithelial morphogenesis in Drosophila. *Dev Biol* **250**, 91-100.

Hajra, K., Fearon, ER. (2002). Cadherin and catenin alterations in human cancer. *Genes, Chromosomes Cancer* **34**, 255-268.

Hanahan, D., Weinberg, RA. (2000). The Hallmarks of Cancer. *Cell* **100**, 57-70.

Hannigan, G., Troussard, A. and Dedhar, S. (2005). Integrin-linked kinase: a cancer therapeutic target unique among its ILK. *Nature Rev Cancer* **5**, 51-63.

Hannigan, G. E., Leung-Hagesteijn, C., Fitz-Gibbon, L., Coppolino, M. G., Radeva, G., Filmus, J., Bell, J. C. and Dedhar, S. (1996). Regulation of cell adhesion and anchorage-dependent growth by a new beta 1-integrin-linked protein kinase. *Nature* **379**, 91-6.

Helwani, F. M., Kovacs, E. M., Paterson, A. D., Verma, S., Ali, R. G., Fanning, A. S., Weed, S. A. and Yap, A. S. (2004). Cortactin is necessary for E-cadherin-mediated contact formation and actin reorganization. *J Cell Biol* **164**, 899-910.

Herrmann, J., Abriss, B.,van de Leur, E., Weiskirchen, S., Gressner, AM., Weskirchen, R. (2004). Comparative analysis of adenoviral transgene delivery via tail vein or portal vein into rat liver. *Arch Virol* **149**, 1611-1617.

Heuser, J. E. and Kirschner, M. W. (1980). Filament organization revealed in platinum replicas of freeze-dried cytoskeletons. *J Cell Biol* **86**, 212-34.

Huang, Y., Li, J., Zhang, Y. and Wu, C. (2000). The roles of integrin-linked kinase in the regulation of myogenic differentiation. *J Cell Biol* **150**, 861-72.

Hynes, R. O. (2002). Integrins: bidirectional, allosteric signaling machines. *Cell* **110**, 673-87.

Jamora, C. and Fuchs, E. (2002). Intercellular adhesion, signalling and the cytoskeleton. *Nat Cell Biol* **4**, E101-8.

Jurata, L. W. and Gill, G. N. (1998). Structure and function of LIM domains. *Curr Top Microbiol Immunol* **228**, 75-113.

Kadrmas, J. L., Smith, M. A., Clark, K. A., Pronovost, S. M., Muster, N., Yates, J. R. r. and Beckerle, M. C. (2004). The integrin effector PINCH regulates JNK activity and epithelial migration in concert with Ras suppressor 1. *J Cell Biol* **167**, 1019-1024.

Kaneko, Y., Kitazato, K. and Basaki, Y. (2004). Integrin-linked kinase regulates vascular morphogenesis induced by vascular endothelial growth factor. *J Cell Sci* **117**, 407-15. Epub 2003 Dec 16.

Kato, K., Shiozawa, T., Mitsushita, J., Toda, A., Horiuchi, A., Nikaido, T., Fujii, S., Konishi, I. (2004). Expression of the Mitogen-Inducible Gene-2 (mig-2) is elevated in human uterine leiomyomas but not in leiomyosarcomas. *Hum Pathol* **35**, 55-60.

Kellendonk, C., Opherk, C., Anlag, K., Schutz, G., Tronche, F. (2000). Hepatocyte-specific expression of Cre recombinase. *Genesis* **26**, 151-153.

Khurana, T., Khurana, B., Noegel, A. (2002). LIM proteins:association with the actin cytoskeleton. *Protoplasma* **219**, 1-12.

Kim, T. H., Bowen, W. C., Stolz, D. B., Runge, D., Mars, W. M. and Michalopoulos, G. K. (1998). Differential expression and distribution of focal adhesion and cell adhesion molecules in rat hepatocyte differentiation. *Exp Cell Res* **244**, 93-104.

Kim, T. H., Mars, W. M., Stolz, D. B. and Michalopoulos, G. K. (2000). Expression and activation of pro-MMP-2 and pro-MMP-9 during rat liver regeneration. *Hepatology* **31**, 75-82.

Kim, T. H., Mars, W. M., Stolz, D. B., Petersen, B. E. and Michalopoulos, G. K. (1997). Extracellular matrix remodeling at the early stages of liver regeneration in the rat.[see comment]. *Hepatology* **26**, 896-904.

Kleinman, H., McGarvey, M L., Hassell, JR., Star, V L., Cannon, F B., Laurie, G W., Martin, GR. (1986). Basement membrane complexes with biological activity. *Biochemistry*

25, 312-318.

Kolls, J., Peppel, K., Silva, M., Beutler, B. (1994). Prolonged and effective blockade of tumor necrosis factor activity through adenovirus-mediated gene transfer. *Proc Natl Acad Sci* **91**, 215-219.

Kos, C. (2004). Cre/loxP System for generating tissue-specific knockout mouse models. *Nutr Rev* **62**, 243-246.

Krause, M., Bear, J. E., Loureiro, J. J. and Gertler, F. B. (2002). The Ena/VASP enigma. *J Cell Sci* **115**, 4721-6.

Krause, M., Dent, E. W., Bear, J. E., Loureiro, J. J. and Gertler, F. B. (2003). Ena/VASP proteins: regulators of the actin cytoskeleton and cell migration *Annu Rev Cell Dev Biol* **19**, 541-64.

Kumar, A. S., Naruszewicz, I., Wang, P., Leung-Hagesteijn, C. and Hannigan, G. E. (2004). ILKAP regulates ILK signaling and inhibits anchorage-independent growth. *Oncogene* **23**, 3454-61.

Kumaran, V., Joseph, B., Benten, D. and Gupta, S. (2005). Integrin and extracellular matrix interactions regulate engraftment of transplanted hepatocytes in the rat liver. *Gastroenterology* **129**, 1643-53.

Larue, L., Ohsugi, M., Hirchenhain, J. and Kemler, R. (1994). E-cadherin null mutant embryos fail to form a trophectoderm epithelium. *Proc Natl Acad Sci U S A* **91**, 8263-7.

Lawrence, D. W., Comerford, K. M. and Colgan, S. P. (2002). Role of VASP in reestablishment of epithelial tight junction assembly after Ca2+ switch. *Am J Phys Cell Phys* **282**, C1235-45.

Lee, C., Friedman, JR., Fulmer, JT., Kaestner, KH. (2005). The initiation of liver development is dependent on Foxa transcription factors. *Nature* **435**, 944-947.

Legate, K. R., Montanez, E., Kudlacek, O. and Fassler, R. (2006). ILK, PINCH and parvin: the tIPP of integrin signalling. *Nat Rev Mol Cell Biol* **7**, 20-31.

Li, F., Zhang, Y. and Wu, C. (1999). Integrin-linked kinase is localized to cell-matrix focal adhesions but not cell-cell adhesion sites and the focal adhesion localization of integrin-linked kinase is regulated by the PINCH-binding ANK repeats. *J Cell Sci* **112**, 4589-99.

Li, Y., Yang, J., Dai, C., Wu, C. and Liu, Y. (2003). Role for integrin-linked kinase in mediating tubular epithelial to mesenchymal transition and renal interstitial

fibrogenesis.[erratum appears in J Clin Invest. 2004 Feb;113(3):491]. *J Clin Invest* **112**, 503-16.

Lin, X., Qadota, H., Moerman, D. G. and Williams, B. D. (2003). C. elegans PAT-6/actopaxin plays a critical role in the assembly of integrin adhesion complexes in vivo. *Curr Biol* **13**, 922-32.

Liu, S., Calderwood, D. A. and Ginsberg, M. H. (2000). Integrin cytoplasmic domain-binding proteins. *J Cell Sci* **113**, 3563-71.

Mackinnon, A. C., Qadota, H., Norman, K. R., Moerman, D. G. and Williams, B. D. (2002). C. elegans PAT-4/ILK Functions as an Adaptor Protein within Integrin Adhesion Complexes. *Curr Biol* **12**, 787-97.

Marotta, A., Parhar, K., Owen, D., Dedhar, S. and Salh, B. (2003). Characterisation of integrin-linked kinase signalling in sporadic human colon cancer. *Br J Cancer* **88**, 1755-62.

Marotta, A., Tan, C., Gray, V., Malik, S., Gallinger, S., Sanghera, J., Dupuis, B., Owen, D., Dedhar, S. and Salh, B. (2001). Dysregulation of integrin-linked kinase (ILK) signaling in colonic polyposis. *Oncogene.* **20**, 6250-7.

Masuelli, L. and Cutler, M. (1996). Increased expression of the Ras suppressor Rsu-1 enhances Erk-2 activation and inhibits Jun kinase activation. *Mol Cell Biol* **16**, 5466-5476.

Mhashilkar, A. M., Stewart, A. L., Sieger, K., Yang, H. Y., Khimani, A. H., Ito, I., Saito, Y., Hunt, K. K., Grimm, E. A., Roth, J. A. et al. (2003). MDA-7 negatively regulates the beta-catenin and PI3K signaling pathways in breast and lung tumor cells. *Molecular Therapy: the Journal of the American Society of Gene Therapy.* **8**, 207-19.

Michalopoulos, G. K., Bowen, W. C., Zajac, V. F., Beer-Stolz, D., Watkins, S., Kostrubsky, V. and Strom, S. C. (1999). Morphogenetic events in mixed cultures of rat hepatocytes

and nonparenchymal cells maintained in biological matrices in the presence of hepatocyte growth factor and epidermal growth factor. *Hepatology* **29**, 90-100.

Michalopoulos, G. K. and DeFrances, M. C. (1997). Liver regeneration. *Science* **276**, 60-6.

Mohammed, F., Khokha, R. (2005). Thinking outside the cell: proteases regulate hepatocyte division. *Trends Cell Biol* **15**, 555-563.

Monga, S., Micsenyi, A., Germinaro, M., Apte, U., Bell, A. (2006). β-catenin regulation during matrigel-induced rat hepatocyte differentiation. *Cell Tissue Res* **323**, 71-79.

Mongroo, P. S., Johnstone, C. N., Naruszewicz, I., Leung-Hagesteijn, C., Sung, R. K., Carnio, L., Rustgi, A. K. and Hannigan, G. E. (2004). beta-parvin inhibits integrin-linked kinase signaling and is downregulated in breast cancerI. *Oncogene* **4**, 4.

Nagafuchi, A., Shirayoshi, Y., Okazaki, K., Yasuda, K. and Takeichi, M. (1987). Transformation of cell adhesion properties by exogenously introduced E-cadherin cDNA. *Nature* **329**, 341-3.

Niederreiter, M., Gimona, M., Streichsbier, F., Celis, JE., Small, JV. (1994). Complex protein composition of isolated focal adhesions: a two-dimensional gel and database analysis. *Electrophoresis* **15**, 511-9.

Nikolopoulos, S., Turner, CE. (2000). Actopaxin, a new focal adhesion protein that binds paxillin LD motifs and actin and regulates cell adhesion. *J Cell Biol* **151**, 1435-1448.

Nikolopoulos, S., Turner, CE. (2001). Integrin-linked kinase (ILK) binding to paxillin LD1 motif regulates ILK localization to focal adhesions. *J Biol Chem* **276**, 23499-23505.

Novak, A. and Dedhar, S. (1999). Signaling through beta-catenin and Lef/Tcf. *Cell Mol Life Sci* **56**, 523-37.

Novak, A., Hsu, S. C., Leung-Hagesteijn, C., Radeva, G., Papkoff, J., Montesano, R., Roskelley, C., Grosschedl, R. and Dedhar, S. (1998). Cell adhesion and the integrin-linked kinase regulate the LEF-1 and beta-catenin signaling pathways. *Proc Natl Acad Scie USA* **95**, 4374-9.

Ohashi, K. and Kay, M. A. (2004). Extracellular matrix component cotransplantation prolongs survival of heterotopically transplanted human hepatocytes in mice. *Transplant Proc* **36**, 2469-70.

Ohta, Y., Suzuki, N., Nakamura, S., Hartwig, J. H. and Stossel, T. P. (1999). The small GTPase RalA targets filamin to induce filopodia. *Proc Natl Acad Sci U S A* **96**, 2122-8.

Otsu, K., Ito, K., Kuzumaki, T. and Iuchi, Y. (2001). Differential regulation of liver-specific and ubiquitously-expressed genes in primary rat hepatocytes by the extracellular matrix. *Cell Phys Biochem* **11**, 33-40.

Perez-Moreno, M., Jamora, C. and Fuchs, E. (2003). Sticky business: orchestrating cellular signals at adherens junctions. *Cell* **112**, 535-548.

Persad, S., Attwell, S., Gray, V., Delcommenne, M., Troussard, A., Sanghera, J. and Dedhar, S. (2000). Inhibition of integrin-linked kinase (ILK) suppresses activation of protein kinase B/Akt and induces cell cycle arrest and apoptosis of PTEN-mutant prostate cancer cells. *Proc Natl Acad Sci U S A* **97**, 3207-12.

Persad, S., Attwell, S., Gray, V., Mawji, N., Deng, J. T., Leung, D., Yan, J., Sanghera, J., Walsh, M. P. and Dedhar, S. (2001). Regulation of protein kinase B/ Akt-serine-473 phosphorylation by integrin linked kinase (ILK): Critical roles for kinase activity and amino acids arginine-211 and serine-343. *J Biol Chem* **19**, 19.

Persad, S. and Dedhar, S. (2003). The role of integrin-linked kinase (ILK) in cancer progression. *Cancer Metast Rev* **22**, 375-84.

Pinkse, G. G. M., Jiawan-Lalai, R., Bruijn, J. A. and de Heer, E. (2005). RGD peptides confer survival to hepatocytes via the beta1-integrin-ILK-pAkt pathway. *J Hepatol* **42**, 87-93.

Pinkse, G. G. M., Voorhoeve, M. P., Noteborn, M., Terpstra, O. T., Bruijn, J. A. and De Heer, E. (2004). Hepatocyte survival depends on beta1-integrin-mediated attachment of hepatocytes to hepatic extracellular matrix. *Liver Int* **24**, 218-26.

Popov, Z., Gil-Diez de Medina, S., Lefrere-Belda, M-A., Hoznek, A., Bastuji-Garin, S., Abbou, C.C., Thiery, JP., Radvanyi, F., Chopin, DK. (2000). Low E-cadherin expression in bladder cancer at the transcriptional and protein level provides prognostic information. *Br J Cancer* **83**, 209 - 214.

Postic, C. and Magnuson, M. A. (2000). DNA excision in liver by an albumin-Cre transgene occurs progressively with age. *Genesis* **26**, 149-50.

Radeva, G., Petrocelli, T., Behrend, E., Leung-Hagesteijn, C., Filmus, J., Slingerland, J. and Dedhar, S. (1997). Overexpression of the integrin-linked kinase promotes anchorage-independent cell cycle progression. *J Biol Chem* **272**, 13937-44.

Rogalski, T. M., Mullen, G. P., Gilbert, M. M., Williams, B. D. and Moerman, D. G. (2000). The UNC-112 gene in Caenorhabditis elegans encodes a novel component of cell-matrix adhesion structures required for integrin localization in the muscle cell membrane. *J Cell Biol* **150**, 253-64.

Rothen-Rutishauser, B., Riesen, F. K., Braun, A., Gunthert, M. and Wunderli-Allenspach, H. (2002). Dynamics of tight and adherens junctions under EGTA treatment. *J Memb Biol* **188**, 151-62.

Sakai, T., Li, S., Docheva, D., Grashoff, C., Sakai, K., Kostka, G., Braun, A., Pfeifer, A., Yurchenco, P. D. and Fassler, R. (2003). Integrin-linked kinase (ILK) is required for polarizing the epiblast, cell adhesion, and controlling actin accumulation. *Genes Dev* **17**, 926-40.

Schmeichel, K. L. and Beckerle, M. C. (1994). The LIM domain is a modular protein-binding interface. *Cell* **79**, 211-9.

Shafiei, M., Rockey, DC. (2006). The role of integrin linked kinase in liver wound healing. *J Biol Chem* **281,** 24863-72.

Shayakhmetov, D., Li, ZY., Ni,S., Lieber A. (2004). Analysis of adenovirus sequestration in the liver, transduction of hepatic cells, and innate toxicity after injection of fiber-modified vectors. *J Virol* **78**, 5368-5381.

Sepulveda, J. L., Gkretsi, V. and Wu, C. (2005). Assembly and signaling of adhesion complexes. *Curr Top Dev Biol* **68**, 183-225.

Stolz, D. B. and Jacobson, B. S. (1992). Examination of transcellular membrane protein polarity of bovine aortic endothelial cells in vitro using the cationic colloidal silica microbead membrane-isolation procedure. *J Cell Sci* **103**, 39-51.

Stossel, T. P., Condeelis, J., Cooley, L., Hartwig, J. H., Noegel, A., Schleicher, M. and Shapiro, S. S. (2001). Filamins as integrators of cell mechanics and signalling. *Nat Rev Mol Cell Biol* **2**, 138-45.

Su, J., Wang, LY., Liang, YL., Zha, XL. (2005). Role of cell adhesion signal molecules in hepatocellular carcinoma cell apoptosis. *World J Gastroenterol* **11**, 4667-4673.

Takafuta, T., Saeki, M., Fujimoto, T. T., Fujimura, K. and Shapiro, S. S. (2003). A new member of the LIM protein family binds to filamin B and localizes at stress fibers. *J Biol Chem* **278**, 12175-81.

Tan, C., Costello, P., Sanghera, J., Dominguez, D., Baulida, J., de Herreros, A. G. and Dedhar, S. (2001). Inhibition of integrin linked kinase (ILK) suppresses beta-catenin-Lef/Tcf-dependent transcription and expression of the E-cadherin repressor, snail, in APC-/- human colon carcinoma cells. *Oncogene* **20**, 133-40.

Tan, C., Cruet-Hennequart, S., Troussard, A., Fazli, L., Costello, P., Sutton, K., Wheeler, J., Gleave, M., Sanghera, J. and Dedhar, S. (2004). Regulation of tumor angiogenesis by integrin-linked kinase (ILK). *Cancer Cell* **5**, 79-90.

Terpstra, L., Prud'homme, J., Arabian, A., Takeda, S., Karsenty, G., Dedhar, S. and St-Arnaud, R. (2003). Reduced chondrocyte proliferation and chondrodysplasia in mice lacking the integrin-linked kinase in chondrocytes. *J Cell Biol* **162**, 139-48.

Tronche, F., Kellendonk, C., Kretz, O., Gass, P., Anlag, K., Orban, PC., Bock, R., Klein, R., Schutz, G. (1999). Disruption of the glucocorticoid receptor gene in the nervous system results in reduced anxiety. *Nat Genet* **23**, 99-103.

Troussard, A., Costello, P., Yoganathan, TN., Kumagai, S., Roskelley, CD., Dedhar, S. (2000). The integrin-linked kinase (ILK) induces an invasive phenotype via AP-1 transcription factor-dependent upregulation of matrix metalloproteinase 9 (MMP-9). *Oncogene* **19**, 5444-5452.

Troussard, A. A., Mawji, N. M., Ong, C., Mui, A., St -Arnaud, R. and Dedhar, S. (2003). Conditional knock-out of integrin-linked kinase demonstrates an essential role in protein kinase B/Akt activation. *J Biol Chem* **278**, 22374-8.

Tu, Y., Huang, Y., Zhang, Z., Hua, Y. and Wu, C. (2001). A new focal adhesion protein that interacts with integrin-linked kinase and regulates cell adhesion and spreading. *J Cell Biol* **153**, 585-598.

Tu, Y., Li, F., Goicoechea, S. and Wu, C. (1999). The LIM-only protein PINCH directly interacts with integrin-linked kinase and is recruited to integrin-rich sites in spreading cells. *Mol Cell Biol* **19**, 2425-34.

Tu, Y., Li, F. and Wu, C. (1998). Nck-2, a novel Src homology2/3-containing adaptor protein that interacts with the LIM-only protein PINCH and components of growth factor receptor kinase signaling pathways. *Mol Biol Cell* **9**, 3367-3382.

Tu, Y., Wu, S., Shi, X., Chen, K. and Wu, C. (2003). Migfilin and Mig-2 link focal adhesions to filamin and the actin cytoskeleton and function in cell shape modulation. *Cell* **113**, 37-47.

Ueda, K., Ohta, Y. and Hosoya, H. (2003). The carboxy-terminal pleckstrin homology domain of ROCK interacts with filamin-A. *Biochem Biophys Res Com* **301**, 886-890.

Vadlamudi, R. K., Li, F., Adam, L., Nguyen, D., Ohta, Y., Stossel, T. P. and Kumar, R. (2002). Filamin is essential in actin cytoskeletal assembly mediated by p21- activated kinase 1. *Nat Cell Biol* **4**, 681-90.

van der Flier, A. and Sonnenberg, A. (2001). Structural and functional aspects of filamins. *Biochim Biophys Acta* **1538**, 99-117.

Vasaturo, F., Dougherty, GW., Cutler, ML. (2000). Ectopic expression of RSU-1 results in elevation of p21CIP and inhibits anchorage-independent growth of MCF-7 breast cancer cells. *Breast Cancer Res Treat* **61**, 69-78.

Vasioukhin, V., Bauer, C., Yin, M. and Fuchs, E. (2000). Directed actin polymerization is the driving force for epithelial cell-cell adhesion. *Curr Opin Cell Biol* **100**, 209-219.

Wang, Y., Krushel, LA., Edelman, GM. (1996). Targeted DNA recombination in vivo using an adenovirus carrying the cre recombinase gene. *Proc Natl Acad Sci U S A* **93**, 3932-3936.

White, D. E., Cardiff, R. D., Dedhar, S. and Muller, W. J. (2001). Mammary epithelial-specific expression of the integrin-linked kinase (ILK) results in the induction of mammary gland hyperplasias and tumors in transgenic mice. *Oncogene* **20**, 7064-72.

Wu, C. (2004). The PINCH-ILK-parvin complexes: assembly, functions and regulation. *Biochim Biophys Acta* **1692**, 55-62.

Wu, C. (2005). PINCH, N(i)ck and the ILK: network wiring at cell-matrix adhesions. *Trends Cell Biol* **15**, 460-6.

Wu, C. and Dedhar, S. (2001). Integrin Linked Kinase (ILK) and Its Interactors: A New Paradigm for the Coupling of Extracellular Matrix to Actin Cytoskeleton and Signaling Complexes. *J Cell Biol* **155**, 505-510.

Wu, C. (2001). ILK interactions. *J Cell Sci* **114**, 2549-2550.

Wu, C., Keightley, S. Y., Leung-Hagesteijn, C., Radeva, G., Coppolino, M., Goicoechea, S., McDonald, J. A. and Dedhar, S. (1998). Integrin-linked protein kinase regulates fibronectin matrix assembly, E-cadherin expression, and tumorigenicity. *J Biol Chem* **273**, 528-36.

Xu, W., Baribault, H. and Adamson, E. D. (1998). Vinculin knockout results in heart and brain defects during embryonic development. *Development* **125**, 327-37.

Yamaji, S., Suzuki, A., Kanamori, H., Mishima, W., Takabayashi, M., Fujimaki, K, Tomita, N., Fujisawa, S., Ohno, S., Ishigatsubo Y. (2002). Possible role of ILK-affixin complex in integrin-cytoskeleton linkage during platelet aggregation. *Biochem Biophys Res Commun* **297**, 1324-31.

Yap, A. S., Brieher, W. M. and Gumbiner, B. M. (1997). Molecular and functional analysis of cadherin-based adherens junctions. *Annu Rev Cell Dev Biol* **13**, 119-46.

Yoganathan, N., Yee, A., Zhang, Z., Leung, D., Yan, J., Fazli, L., Kojic, D. L., Costello, P. C., Jabali, M., Dedhar, S. et al. (2002). Integrin-linked kinase, a promising cancer therapeutic target: biochemical and biological properties. *Pharmacol Therap* **93**, 233-42.

Yoganathan, T. N., Costello, P., Chen, X., Jabali, M., Yan, J., Leung, D., Zhang, Z., Yee, A., Dedhar, S. and Sanghera, J. (2000). Integrin-linked kinase (ILK): a "hot" therapeutic target. *Biochem Pharmacol* **60**, 1115-9.

Zamir, E. and Geiger, B. (2001). Molecular complexity and dynamics of cell-matrix adhesions. *J Cell Sci* **114**, 3583-90.

Zervas, C. G. and Brown, N. H. (2002). Integrin adhesion: when is a kinase a kinase? *Curr Biol* **12**, R350-1.

Zervas, C. G., Gregory, S.L., Brown, N.H. (2001). *Drosophila* integrin-linked kinase is required at sites of integrin adhesion to link the cytoskeleton to the plasma membrane. *J Cell Biol* **152**, 1007-1018.

Zhang, Y., Chen, K., Tu, Y., Velyvis, A., Yang, Y., Qin, J. and Wu, C. (2002). Assembly of the PINCH-ILK-CH-ILKBP complex precedes and is essential for localization of each component to cell-matrix adhesion sites. *J Cell Sci* **115**, 4777-86.

Zhang, Y., Chen, K., Guo, L. and Wu, C. (2002a). Characterization of PINCH-2, a new focal adhesion protein that regulates the PINCH-1-ILK interaction, cell spreading, and migration. *J Biol Chem* **277**, 38328-38.

Zhang, Y., Guo, L., Chen, K. and Wu, C. (2002b). A critical role of the PINCH-integrin-linked kinase interaction in the regulation of cell shape change and migration. *J Biol Chem* **277**, 318-26.

Zhang Y., Tu Y., Gkretsi V., Wu C. (2006). Migfilin interacts with VASP and regulates VASP localization to cell-matrix adhesions and migration. *J Biol Chem* **281,** 12397-12407.